

CHARACTERIZATION OF THE REGULATION OF  
FORMIN PROTEIN Bni1p IN *SACCHAROMYCES*  
*CEREVISIAE*

A Dissertation

Presented to the Faculty of the Graduate School

of Cornell University

In Partial Fulfillment of the Requirements for the Degree of

Doctor of Philosophy

by

Wenyu Liu

August 2011

© 2011[Wenyu Liu]

# CHARACTERIZATION OF THE REGULATION OF FORMIN PROTEIN Bni1p IN *SACCHAROMYCES* *CEREVISIAE*

Wenyu Liu, Ph. D.

Cornell University 2011

Formins are a family of conserved proteins that assemble unbranched actin filaments. In budding yeast, *Saccharomyces cerevisiae*, the formin isoforms Bni1p and Bnr1p are vital for nucleating and elongating the essential actin cables to guide polarized growth. Here I demonstrate that there are three localization regions in the N-terminal domain of Bni1p: one in the N-terminal 333 amino acids which requires dimerization, one in the region encompassed by amino acids 334-834 which covers the DID-DD-CC domains, and the third in the Spa2p binding domain. The three localization regions can each localize to the bud cortex and bud neck independently of endogenous Bni1p at the right stage of the cell cycle. Bni1p truncations with internal regions of the N-terminal half deleted confirm that the N-terminal domain is important for localization. Cells with delocalized Bni1p truncations have misoriented cables, defects in nuclear movement and spindle orientation, with the extent of these phenotypes varying in accordance with how much of the N-terminal region is truncated. Defects in nuclear movement and spindle orientation are due to the Bni1p truncations assembling actin cables at the wrong place. Thus, although the N-terminal localization regions of Bni1p are not needed for the viability of cells, they are needed for proper functions of formins.

## BIOGRAPHICAL SKETCH

The author, Wenyu Liu, was born in Wuhu, Anhui of China in September, 1982. Her hometown is a small but beautiful city by the Yangtze River. Her father worked as a firefighter to investigate and prevent fire. Her mother works in a college as a science teacher. Wenyu grew up in a happy and caring family and benefited tremendously from it. After graduating from the No. 1 Middle School of Wuhu in 2000, Wenyu was admitted the University of Science and Technology of China, one of the best universities in China, majored in Biosciences. She came to Cornell University in the summer of 2004 to continue her study in the Field of Genetics and Development as a graduate student. After three lab rotations, she joined the lab of Dr. Anthony Bretscher in 2005 and worked on formins along her rotation.

## ACKNOWLEDGMENTS

I would like first to express my extreme thanks to my advisor Anthony Bretscher for his patience, encouragement, enthusiasm, and immense knowledge. I have learned a lot and am still learning from him on how to plan and design experiments, how to analyze data and how to present results, and most importantly to think logically. It is never enough to state my gratitude to him for being always supportive during my PhD life.

I would also like to thank everyone in the Bretscher lab, present and past. They have made the lab a friendly and home-like place to stay. The stimulating discussions we had every day in the lab added fun to the research life. In particular, I would like to thank Dave Pruyne, who taught me doing yeast genetics since my rotation. He gave me many suggestions with his comprehensive knowledge and showed me how to be a careful scientist. I want to express thanks to my bench mate David Hokanson, who offered me a lot of help during my thesis and paper writing and beared with my Chinese English along with Jess Wayt.

I want to thank all my family and friends, especially my husband Qing He whose patient love enabled me to complete this work.

## TABLE OF CONTENTS

Biographical sketch	iii
Acknowledgements	iv
Table of contents	v
List of figures	viii
List of tables	x
List of abbreviations	xi
Chapter 1 General introduction	1
Polarity in <i>Saccharomyces cerevisiae</i>	1
Yeast actin cytoskeleton	8
Polarized transport by Myosins	12
Formin proteins	16
Formins in <i>Saccharomyces cerevisiae</i>	23
Chapter 2 N-terminus of Bni1p contains multiple localization signals	32
Abstract	32
Introduction	32
Materials and methods	33
Yeast strains and molecular biology techniques	33
Yeast two hybrid screen	33
Microscopy	36
Results	37
The N-terminal domain of Bni1p contains more than one localization region	37
The GBD domain of Bni1p localizes to the bud cortex and bud neck	

when dimerized	40
The N-terminal half of Bni1p contains three localization regions	42
The role of microtubules in Bni1p localization	42
The effects of small GTPases on the localization of Bni1p	45
Yeast two hybrid screen for peptides that binds the N-terminal region of Bni1p	47
Discussion and future directions	51
Three localization domains in the Bni1p N-terminal region	51
The role of small GTPases on the localization of Bni1p	53
Yeast Two hybrid screen	54
 Chapter 3 Bni1p constructs lacking the N-terminal localization domains compromise growth and spindle orientation	56
Abstract	56
Introduction	57
Material and methods	58
Yeast strains and molecular biology techniques	58
Microscopy	63
Protein extracts and immunoblotting	63
Results	64
The C-terminal domain of Bni1p contains a fourth localization domain	64
Spa2p has an additional function in addition to binding the SBD	67
The N-terminal region of Bni1p is essential for spindle orientation	72
Actin assembly activity is essential for Bni1p class II phenotypes	80
Discussion and future direction	80

Chapter 4	Discussion and future direction	86
Appendix I	Identification of Boi1/2p in <i>Saccharomyces cerevisiae</i>	89
	Abstract	89
	Introduction	89
	Materials and methods	90
	Yeast strains and molecular biology techniques	90
	Yeast two hybrid assay	90
	Isolation of conditional <i>boi1Δboi2-ts</i> mutants	94
	Microscopy and Imaging	95
	Results	95
	Yeast two hybrid showed weak interaction between Boi1/2p with N-terminal region of Bni1p	95
	Isolation of temperature sensitive strains of <i>boi1Δ boi2ts</i>	95
	Cell polarity is affected in <i>boi2ts</i> cells	99
	Discussion and future directions	101
	The interaction between Boi1/2p and formins	101
	The role of boi1/2p in polarized growth	103
References		104

## LIST OF FIGURES

Figure 1.1	Yeast polarized growth	3
Figure 1.2	Transport of organelles and secretory vesicles by Myo2p on actin cables	14
Figure 1.3	Domain organizations of mammalian formins	17
Figure 1.4	Structure of FH2 dimer and its role on actin filament barbed ends	19
Figure 1.5	Formins in budding yeast <i>Saccharomyces cerevisiae</i>	24
Figure 2.1	Scheme of Bni1p N-terminal overexpression constructs	38
Figure 2.2	Selected GFP images of overexpressed Bni1p N-terminal constructs during budding	39
Figure 2.3	Selected GFP images of overexpression Bni1p N-terminal constructs in <i>bni1Δ</i> cells	41
Figure 2.4	The role of microtubules in Bni1p localization	44
Figure 2.5	Selected images of Bni1p overexpression constructs in Rho family mutants	46
Figure 3.1	Scheme of constructs	62
Figure 3.2	Two classes of Bni1p N-terminal truncations	65
Figure 3.3	Phalloidin staining and live GFP image of <i>bni1ΔNp-3GFP</i> strains	68
Figure 3.4	Phenotypes of <i>bni1ΔN</i> in <i>spa2Δ</i> background	71
Figure 3.5	Growth assay of <i>bni1ΔNp</i> in an <i>arp1Δ</i> background with or without <i>ARPI</i> on a <i>CEN-URA3</i> plasmid	74
Figure 3.6	Phenotypes of Class I Bni1p truncations regarding spindle and nuclei orientation	78
Figure 3.7	Phenotypes of Class II Bni1p truncations	79
Figure 3.8	The phenotypes of <i>bni1ΔNp</i> mutants are due to its actin assembly	

	ability	81
Figure 3.9	Tagging <i>bni1ΔN</i> with CRIB domain rescues the cold sensitivity and actin disruption in <i>bni1Δ79-988p</i>	82
Figure 5.1	Domain organizations of Boi2p and construct scheme	91
Figure 5.2	Growth assay of the yeast two hybrid assays between formins and Boi1/2p	96
Figure 5.3	Growth assays of <i>boi1Δ boi2ts</i> at 26 °C, 30 °C, 32 °C, 35 °C, and 37 °C	97
Figure 5.4	Phenotypes of polarity marker Sec4p and Myo2p in Boi2ts strains at restrictive temperature	100
Figure 5.5	Localization of Bni1p is affected in Boi2ts strains at restrictive temperature	102

## LIST OF TABLES

Table 2.1	Yeast strains used in Chapter 2	34
Table 2.2	Plasmids used in Chapter 2	35
Table 2.3	localization of Bni1p N-terminal constructs	43
Table 2.4	Yeast two hybrid candidates with Bni1 1-724aa	48
Table 3.1	Yeast strains used in Chapter 3	59
Table 3.2	Plasmids used in Chapter 3	61
Table 3.3	Phenotypes of Bni1p truncations in different backgrounds	75
Table 5.1	Yeast strains used in Appendix I	92
Table 5.2	Plasmids used in Appendix I	93
Table 5.3	Summary of the yeast two hybrid assay between formins and Boi1/2p	96
Table 5.4	Nucleotide and amino acid change in <i>boi1Δboi2ts</i> mutant alleles	98

## LIST OF ABBREVIATIONS

aa: amino acid

CC: coiled coil

CRIB: Cdc42-Rac interactive binding domain

CWI: Cell wall integrity

DAAM: Dishevelled-associated activator of morphogenesis

DAD: Diaphanous autoregulatory domain

DD: Dimerization domain

Dia: Diaphanous

DID: Diaphanous inhibitory domain

DRL: Diaphanous related

FH1: Formin Homology 1

FH2: Formin Homology 2

FH3: formin homology domain 3

FHOD: Formin homology domain-containing protein

FMN: Formin

FRAP: Fluorescence Recovery after Photobleaching

FRL: Formin-related gene in leukocytes

GAP: GTPase Activating protein

GBD: GTPase binding domain

GDI: GDP dissociation inhibitor

GDP: Guanosine diphosphate

GEF: Guanine nucleotide Exchange Factor

GPCR: G-protein coupled Receptors

GTP: Guanosine 5'-triphosphate

INF: Inverted formin

MAPK: Mitogen-Activated Protein Kinase

NPF: nucleation promoting factor

PAK: p21 Activated kinase

PH: pleckstrin homology

SAM: sterile alpha motif

SBD: Spa2p Binding Domains

SH3: Src homology 3

SILAC: Stable isotope labeling by amino acids in cell culture

SPB: spindle pole body

TGN: trans-Golgi network

WASP: Wiskott-Aldrich syndrome protein

y2h: yeast 2 hybrid

## CHAPTER 1

### General Introduction

#### **Polarity in *Saccharomyces cerevisiae***

Cell polarity underlies many functions that are fundamental to cell development and processes such as differentiation, activation of the immune response, directed migration, and cytokinesis. Budding yeast, *Saccharomyces cerevisiae*, also known as baker's yeast or brewer's yeast, is a great model organism to study polarity due to its small genome and powerful genetics methods. And because of the small size of yeast cells, the actin cytoskeleton is the primary component for regulating polarized growth and for segregation of most intracellular structures (Fagarasanu and Rachubinski, 2007). Studies have shown that yeast cell polarity is analogous to higher organisms (Drubin and Nelson, 1996). In budding yeast, cells undergo polarized growth in two instances: budding during vegetative growth and mating between haploid cells (Figure 1.1).

There are three types of yeast cells determined by their different mating type: MAT<sub>a</sub> and MAT<sub>α</sub> cells, which are haploid cells containing one set of chromosomes, and MAT *a/α* cells, which is a diploid cell type containing two sets of chromosomes. All three cell types are able to initiate budding when cells reach a critical cell size in the late G1 phase of the cell cycle. The budding site is first selected. Then the actin cytoskeleton composed mainly of actin cables and actin patches becomes polarized to establish an axis for secretion and organelles to be targeted to the bud site (actin cytoskeleton will be discussed later in this introduction). The bud thus continues to

grow with the directed transport of secretory vesicles and the segregation of organelles (Pruyne et al., 2004b). Cytokinesis occurs when the bud grows to a critical size, usually smaller than the mother cell, and the nuclei have been segregated (Figure 1.1). The other polarized growth, mating, initiates when a haploid yeast cell receives a pheromone signal from the opposite mating type. Haploid cells are then arrested in G1 phase and polarized axes are reoriented to form a mating projection called a “shmoo” in the direction of a potential mate. Finally, plasma membrane as well as nuclei are fused with the mating partner to form a diploid cell (Bardwell, 2004).

Both budding and mating processes require the establishment of a polarized cytoskeleton through the small GTPase Cdc42p. Cdc42p, which is highly conserved through all eukaryotes, is a member of the Rho subfamily of Ras GTPases. As with other GTPases, Cdc42p can bind to Guanosine diphosphate (GDP) and Guanosine 5'-triphosphate (GTP), with the GTP bound form being the active state. Cdc24p is the only known Guanine nucleotide Exchange Factor (GEF) for Cdc42p which induces the transition from GDP-Cdc42p to GTP-Cdc42p, turning on Cdc42p. There are four potential GTPase Activating proteins (GAP) for Cdc42p: Bem2p, Bem3p, Rga1p and Rga2p. GAPs promote the hydrolysis of GTP-Cdc42p to GDP-Cdc42p, turning off Cdc42p. The Rho GDP dissociation inhibitor (GDI) Gdi1p can regulate Cdc42p by inhibiting the dissociation of GDP from Cdc42p as well as by inhibiting its GTPase activity and by extracting Cdc42p from membranes into the cytosol (Perez and Rincon, 2010).

Though both budding and mating processes establish polarized growth through Cdc42p, they differ in specific signaling pathways. During budding in wildtype cells,

### **Figure 1.1 Yeast polarized growth**

At the beginning of a budding cycle (G1 phase), a bud site is first selected by cortical cues. Actin patches are clustered at the future bud site, actin cables are formed from this site while aligning along the cell cortex. Septins are recruited and form a ring structure.

As the bud emerges (S phase), actin patches concentrate towards the small bud tip. Actin cables extend from the small bud tip and the bud neck towards the mother cell. The septin ring stays at the bud neck and expands into a wider structure. The nucleus and spindle pole bodies are replicated. The bud cell grows apically (from the tip).

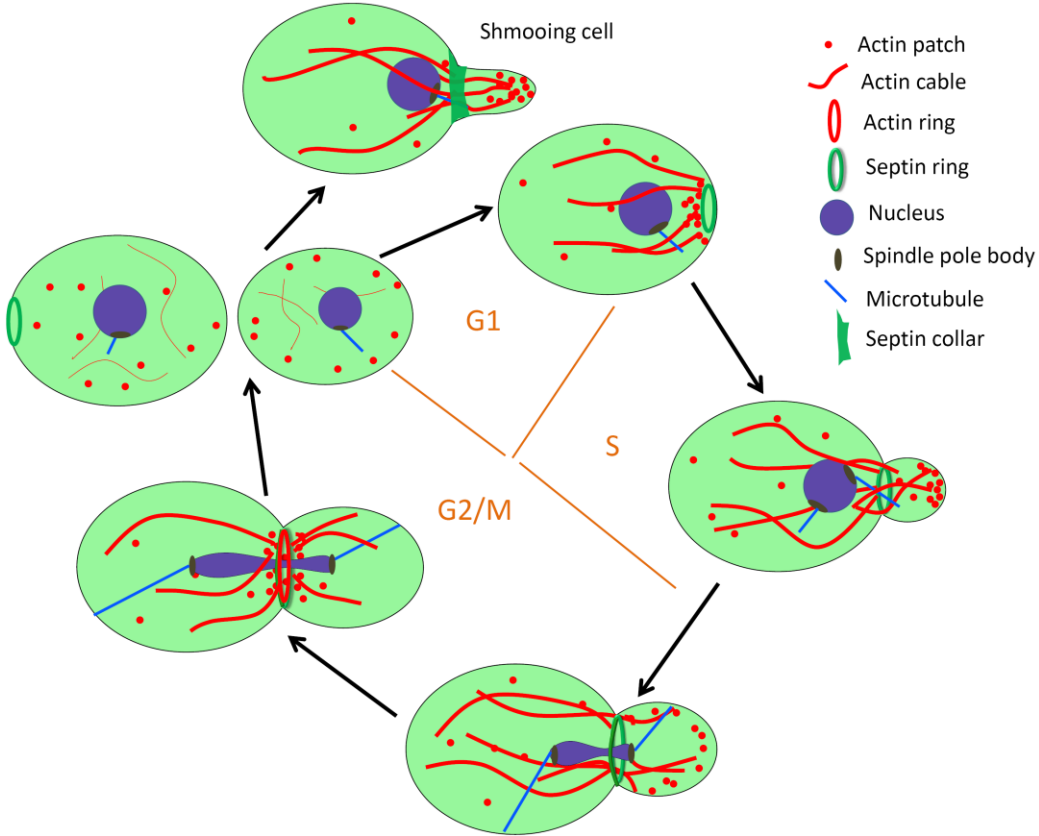
As the bud grows bigger (G2 phase), actin patches distributed near the bud cortex instead of at the concentrated bud tip area. Actin cables also grow from bud cortex and bud neck to the mother cell. The bud grows isotropically into an ellipsoid shape. Septins still localizes at the bud neck. The newly assembled spindle pole body migrates to the other side of the nucleus, setting up a spindle between the two spindle pole bodies. The spindles are elongated and one of the nuclei is transported near the bud neck area.

At the end of bud growth (M phase), the actin patches and cables are redistributed towards the bud neck. An actin ring called the actomyosin ring assembles in between the widened septin ring barrier. The cytoplasmic microtubules emanating from the two spindle poles associate closely with the mother or bud cortex, and as the spindle elongates, one nucleus is moved into the bud and transported towards the bud cortex while one nucleus stays in the mother cell. After chromosome separation, the spindle

breaks down, and the nucleus undergoes fission. The actomyosin ring contracts at the bud neck and the septum forms, thus completing mitosis.

After the bud is separated from the mother cell, mother cell directly goes into the next cell cycle while the bud needs to grow to the size of the mother before it can initiate budding itself.

During the G1 phase, if a haploid yeast cell receives pheromone signal for opposite mating type, budding cycle will be inhibited and instead a mating projection call “shmoo” is formed. Actin patches and cables are formed towards the shmoo tip. The two shmoo cells fuse and nucleus then fuse and form a diploid cell.



the bud sites are selected according to their ploidy. Diploid cells bud bipolarly, meaning that budding occurs from either pole of the elongated mother cell. Haploid cells bud axially with future bud sites adjacent to previous ones. These two budding patterns have different cortical markers, but they both deliver the bud site selection signal to the Ras related GTPase Rsr1p. Rsr1p directly interacts with Cdc42p and this interaction is enhanced by the presence of Cdc24p (Kozminski et al., 2003). Cdc24p, which is sequestered by Far1p in the nucleus during early G1 phase, is released from the nucleus to the cytoplasm when G1 cyclin activated Cdc28p phosphorylates Far1p to be degraded (Shimada et al., 2000). Cdc24p binds Rsr1p and the scaffolding protein Bem1p, which also interacts with Cdc42p and its downstream effectors p21 Activated kinases (PAK) Cla4p, Ste20p, Boi1p and Boi2p. The binding of Cdc24p with Rsr1p and Bem1 might trigger its release from autoinhibition, leading to the activation of Cdc42p (Shimada et al., 2004b). Together, Cdc42p, Cdc24p and Bem1p form a positive feedback loop that regulates the recruitment of Cdc42 to the future bud site (Butty et al., 2002; Howell et al., 2009; Wedlich-Soldner et al., 2004).

After Cdc42p has been recruited to the presumptive bud site, its localization at the growth site is highly dynamic (Wedlich-Soldner et al., 2004). Several mechanisms are proposed for the dynamics and maintenance of Cdc42p polarization. First, the Bem1p mediated protein complex has been proposed to constitute a positive feedback loop to maintain Cdc42p polarization (Irazoqui et al., 2003). Second, septins are thought to act as a barrier between the cortex of the bud and the mother, maintaining the asymmetric distributions of cortical proteins including Cdc42p (Barral et al., 2000). Third, actin structures are suggested to have opposing roles in maintaining Cdc42p at

the bud tip. Actin patches are responsible for the dispersal of Cdc42p through endocytosis while actin cables are required to counteract the dispersal and maintain Cdc42p polarity (Irazoqui et al., 2005; Marco et al., 2007). Finally, Rdi1p mediates a fast recycling pathway of Cdc42p (Slaughter et al., 2009).

In *rsr1Δ* cells which lack the bud site selection pathway, Cdc42p polarization can still occur at a single site, though at a random location. The symmetry breaking here could be explained by an amplification mechanism in which a stochastic initial gathering of polarity markers including Cdc42p, Bem1p, and Cdc24p develop into a concentrated cluster of polarity factors (Howell et al., 2009; Kozubowski et al., 2008).

On the other hand, during mating, peptide pheromones secreted by haploid MATa cells and MAT $\alpha$  cells (a factor and  $\alpha$  factor, respectively) bind to GPCRs (G-protein coupled Receptors) on the opposite cell type, which activates a heterotrimeric G protein-coupled Mitogen-Activated Protein Kinase (MAPK) cascade. The pheromone bound GPCR dissociates the heterotrimeric G protein into a G $\alpha$  monomer (Gpa1) and a G $\beta\gamma$  heterodimer. The free G $\beta\gamma$  dimer binds to multiple targets including PAK Ste20p, and a MAPK cascade scaffold protein Ste5p. Ste20p phosphorylates Ste11p (a MAPK kinase kinase), which phosphorylates Ste7p (a MAPK kinase), which phosphorylates and activates the MAPK Fus3p and Kss1p (Dohlman, 2002). Activated Fus3p also phosphorylates Far1p (Elion et al., 1993), which acts as a cell cycle inhibitor to arrest the cell in G1 phase as mentioned above during the budding process. In response to mating pheromones, the Far1p-Cdc24p complex is exported from the nucleus and, instead of being targeted to the bud site, interacts with G $\beta\gamma$  and is targeted to the shmoo tip. Far1p also recruits Cdc42p and Bem1p directly, as well as

through Cdc24p (Butty et al., 1998).

Once the polarization of Cdc42p is established during budding or mating, it organizes the actin cytoskeleton, septins, polarized secretion and cell wall synthesis and thus orchestrates the growth of the bud and shmoo formation. Cdc42p performs these functions by regulating a variety of downstream effectors such as: PAK kinases Ste20p, Cla4p and Skm1p; Cdc42-Rac interactive binding domain (CRIB) containing proteins Gic1p and Gic2p, formin protein Bni1p, exocyst subunit Sec3p, and Boi1/2p, which will be discussed in Appendix I. PAKs are serine/threonine kinases that are involved in multiple cellular processes. They can phosphorylate type I myosin Myo3p and Myo5p which are nucleation promoting factors (NPF) of the Arp2/3 complex, which functions in endocytosis (Wu et al., 1996; Wu et al., 1997). Ste20p regulates multiple MAPK pathways that control mating, filamentous growth, and osmotic stress response, and is also involved in exit from mitosis and hydrogen peroxide-induced apoptosis (Chen and Thorner, 2007). Cla4p has been implicated in the phosphorylation and assembly of the septin ring, which plays a fundamental role in cytokinesis and cell compartmentalization (Versele and Thorner, 2004). In addition, Cla4p regulates mitotic entry and exit (Hofmann et al., 2004). Very little is known about Skm1p, and no clear function has been attributed to this PAK (Martin et al., 1997). The CRIB domain containing proteins Gic1p and Gic2p are suggested to have a role in the recruitment of septins to the bud site (Iwase et al., 2006). The formin protein Bni1p is an actin cable nucleator and has been shown to interact with Cdc42p. Its regulation and function will be discussed later in this introduction. Sec3p is an exocyst subunit that is on the plasma membrane instead of on the secretory vesicles (Finger et al.,

1998). Its interaction with Cdc42p could lead to its polarized localization (Zhang et al., 2001).

Unlike mating, the budding process finishes with cytokinesis, dividing the bud from the mother. In budding yeast, two complementary mechanisms contribute to the process of cytokinesis: contraction of the actomyosin ring and septum formation, both of which need septin rings. Septin rings are ring-like structures composed of GTP binding proteins Cdc3p, Cdc10p, Cdc11p, Cdc12p, and the nonessential component Shs1p. They are recruited to the future bud site early in the cell cycle, before bud emergence. Septins play essential roles in cytokinesis, not only as a scaffold for the formation of the actomyosin ring and septum, but also as barriers to restrict the movement of cytokinetic component outside of bud neck area (Dobbelaere and Barral, 2004) as well as diffusion between mother and bud cell (Barral et al., 2000; Takizawa et al., 2000).

### **Yeast actin cytoskeleton**

Actin structures in vivo are composed of actin filaments, also called F-actin, which are assembled from actin monomers. An actin monomer, also called G-actin, is a small globular protein. It polymerizes to form double stranded helical filament structure, F-actin, which participates in many important cellular processes. Actin monomers are also asymmetric and they follow the same orientation in a single actin filament, forming two structurally and functionally different ends. The slow growing end is called the minus or pointed end and the fast growing end is called plus or barbed end. The rate limiting step in *de novo* actin polymerization is the formation of dimers and trimers since actin dimers are highly unstable. Once actin trimers or tetramers are

formed, they are stable seeds for polymerization (Sept and McCammon, 2001).

The actin monomer contains a nucleotide-binding site that can bind ATP or ADP. The conformation of actin is different between ATP and ADP bound actin. ATP bound actin has a higher affinity for adjacent subunits than ADP bound actin, leading to the fact that ATP-actin favors filaments polymerization while ADP-actin favors depolymerization (Alberts, 2002).

*In vitro* the assembly of an actin filament is largely dependent on the concentration of the G-actin pool. A balance is eventually reached between polymerization and depolymerization, and the filaments enter a steady-state phase called “treadmilling”. In this state, there is a constant polymerization and depolymerization of the filaments. The filaments polymerize at their barbed ends and depolymerize at their pointed ends. The concentration of G-actin in this state is called “critical concentration”. If the G-actin concentration is lower than critical concentration, depolymerization occurs. On the contrary, if the G-actin concentration is higher than critical concentration, polymerization happens (Alberts, 2002).

Actin polymerization *in vivo* is much more complicated than *in vitro*. Many actin binding proteins participate in different aspects of actin filament dynamics. Profilin is one example. Profilin is a small, abundant, and an almost essential G-actin binding protein. It is highly conserved and critical for actin organization and cell morphology. In budding yeast, there is only one profilin homolog, Pfy1p. It is estimated that most of the G-actin *in vivo* exists bound to profilin due to its abundance (Pollard et al., 2000). Thus, profilin binding could inhibit spontaneous actin assembly by preventing interactions between actin monomers. It also restricts actin monomer addition to

filament barbed ends, blocking addition to pointed ends. However, it can promote actin assembly caused by formin proteins, a family of actin nucleator which I will talk more in this introduction later. In addition, profilin stimulates the nucleotide exchange on G-actin (Goldschmidt-Clermont et al., 1991; Korenbaum et al., 1998; Selden et al., 1999).

As shown in Figure 1.1, the actin cytoskeleton in yeast consists of three structures: actin patches, cables and an actomyosin ring, which are involved in endocytosis, polarized growth and cytokinesis respectively.

Actin patches contain branched actin structures. They are motile with a life time of approximately 10~20s. The actin filaments in patches are nucleated by the conserved actin nucleator Arp2/3 complex, which is composed of seven proteins: Arp2p, Arp3p, Arc15p, Arc18p, Arc19p, Arc40p, and Arc35p (Winter et al., 1997). The Arp2/3 complex is activated by five NPFs *in vivo*: the yeast homolog of Wiskott-Aldrich syndrome protein (WASP) Las17p, Pan1p, type I myosins Myo3p, Myo5p and Abp1p (Duncan et al., 2001; Goode et al., 2001; Lee et al., 2000; Winter et al., 1999). When activated, the Arp2p and Arp3p subunits form a structure that mimics the barbed end of an actin filament. Actin monomers then polymerize at this barbed end while the Arp2/3 complex remains bound to the pointed end (Pollard and Beltzner, 2002). The complex binds to the sides of a preexisting actin filament to nucleate formation of a new filament at a 70 ° angle (Higgs and Pollard, 2001).

Actin patches mainly function in endocytosis. A working model of actin patch development has three stages: the first is early recruitment, which is a nonmotile phase. It begins with the cytosolic regions of membrane receptors or static complexes

residing at the cell cortex. Clathrin, multiple scaffolding proteins and clathrin adaptors are recruited to these early complexes, which in turn recruit additional patch components that promote actin assembly, including Las17p, Pan1p and End3p. The second stage is the intermediate stage with slow motility. Actin can be detected at this stage along with the Arp2/3 complex and membrane invagination. Patches undergo slow, nondirectional movements within the plane of the cortex. The third stage is scission and rapid transport of patches. Patches/vesicles begin to move inward rapidly from the cell cortex while shedding off many of the early patch components such as Las17p, Pan1p, Myo3p, and Myo5p. Serine/threonine kinase Prk1p and Ark1p are suggested to trigger the transition from slow movement to fast movement by negatively regulating the actin assembly-stimulating activity of proteins such as Pan1p (Moseley and Goode, 2006). This fast movement has been suggested to be traveling along actin cables with a rate similar to actin cable flow (Huckaba et al., 2004).

In budding yeast, actin cable filaments can be distinguished from Arp2/3 complex-dependent filaments by their association with the F-actin binding proteins tropomyosins: Tpm1p and Tpm2p (Evangelista et al., 2002; Liu and Bretscher, 1989; Pruyne et al., 1998). They are required for polarized secretion and organelle inheritance. Actin cables are bundles of relatively short actin filaments that are aligned along the cell cortex from the bud site/tip and bud neck into the mother cell. Besides the actin cable specific stabilizing proteins Tpm1p and Tpm2p, actin cables are also decorated with F-actin bundling proteins Sac6p and Abp140p. During polarized growth, the actin cables are oriented with their barbed ends towards the growth sites (Figure 1.1). Myosin V motor proteins, Myo2p and Myo4p, walk along these cables

towards the growth site carrying cargos such as organelles, secretory vesicles, and mRNAs. Formin proteins are responsible and essential for the nucleation and assembly of actin cables at the bud tip and bud neck. Actin cables are dynamic structures. For a typical actin cable during budding, the barbed ends of the filaments associate with the bud tip/cortex or bud neck, where it is anchored and continuously assembled by formin proteins, while the pointed ends move away from the assembly site with a rate of around  $0.3\mu\text{m/s}$  (Yang and Pon, 2002). The speed of the actin cable movement coincides with the speed of the actin polymerization rate, suggesting that actin polymerization drives the actin cable away from the growth site.

The actomyosin ring is composed of many proteins including the Class II Myosin Myo1p, actin, tropomyosins, and IQGAP Iqg1p. Myo1p is recruited to the presumptive bud site shortly before bud emergence to form a ring. This recruitment is dependent on septins. The Myo1p ring remains at the mother-bud neck until the end of anaphase, when it's joined by a ring of F-actin. This actin ring formation is dependent on formin proteins (Tolliday et al., 2002). The actomyosin ring then contracts to a point and disappears. Although the formation of the Myo1p ring is not dependent on actin, its contraction is actin dependent. During ring contraction, cortical actin patches congregate at the mother-bud neck, and actin cables are oriented towards the neck from both mother and bud, and the septum forms. Thus cell separation happens (Bi et al., 1998).

### **Polarized transport by Myosins**

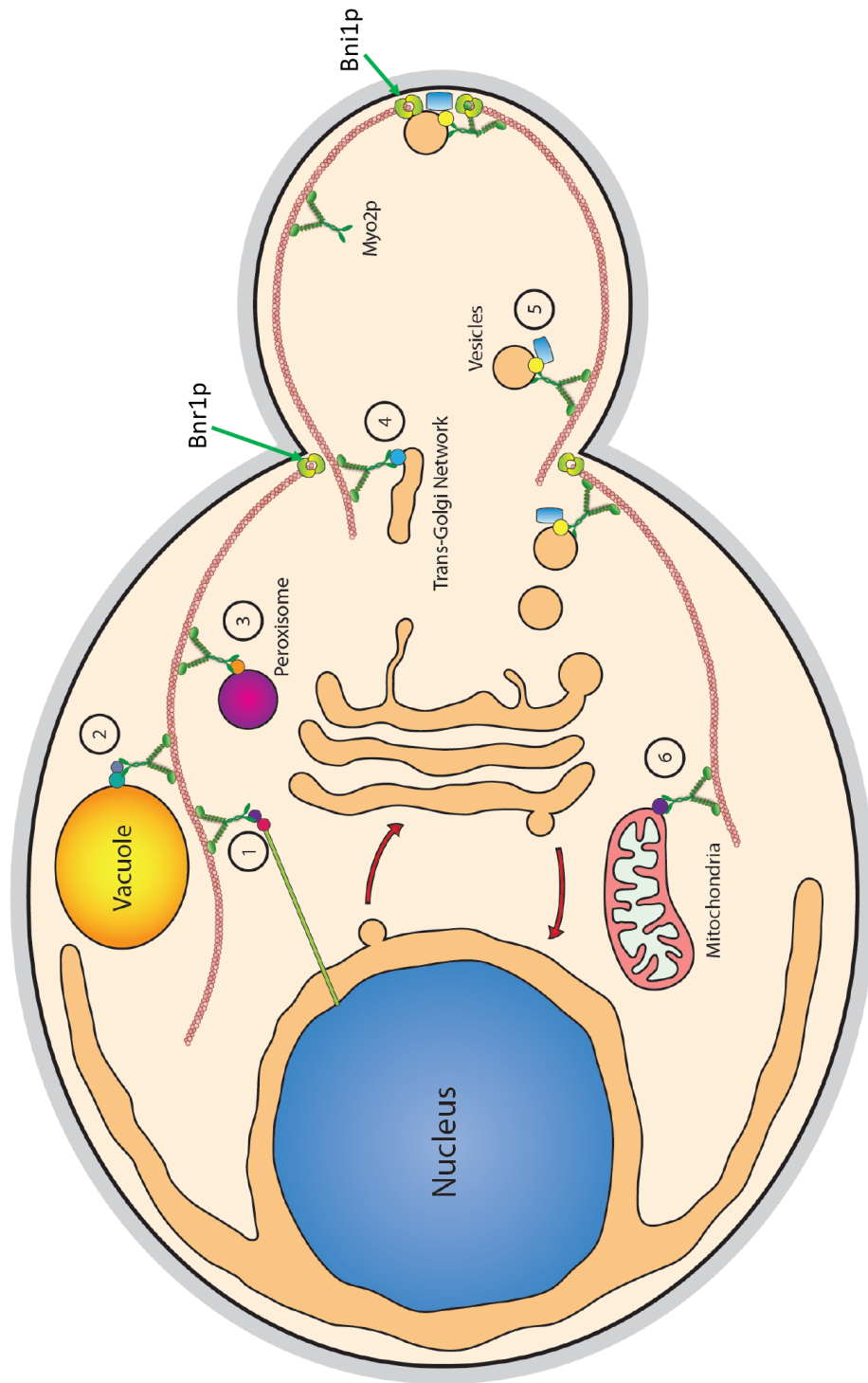
The major function of actin cables is to serve as the tracks for type V myosins to carry cargos such as secretory vesicles, organelles and mRNAs to the polarized sites

(Figure 1.2). There are two type V myosins in budding yeast, with heavy chains encoded by *MYO2* and *MYO4*. Myo2p is essential and responsible for the transport of secretory vesicles, which are the essential cargo of Myo2p (Pruyne et al., 2004b; Pruynne et al., 1998), as well as the orientation of the nucleus (Beach et al., 2000; Hwang et al., 2003; Yin et al., 2000), and segregation of vacuoles (Weisman, 2003), mitochondria (Altmann et al., 2008; Simon et al., 1995), peroxisomes (Fagarasanu et al., 2006; Hoepfner et al., 2001), and trans-Golgi network (TGN) (Arai et al., 2008). The non-essential Myo4p transports mRNAs of *ASH1* and *IST2* (Takizawa et al., 1997; Takizawa and Vale, 2000), as well as cortical endoplasmic reticulum (Schmid et al., 2006).

Myo2p transports different cargos by binding to cargo specific receptors. PI4P and Rab proteins, specifically Ypt31/32p for TGN and Sec4p for secretory vesicles, collaborate in the association of secretory compartments with Myo2p (Santiago-Tirado et al., 2011). Vac17p on vacuoles (Ishikawa et al., 2003), Inp2p on peroxisomes (Fagarasanu et al., 2006) mediate the cargo interaction with Myo2p respectively. Nuclear orientation depends on forces acting on cytoplasmic microtubule radiating from the spindle pole body (SPB), a plaque-like structure embedded in the nuclear envelope equivalent to the centrosome of higher organisms. For nuclear orientation, Myo2p guides the cytoplasmic microtubule by transporting Kar9p which in turn binds to microtubule plus ends localizing protein Bim1p (Hwang et al., 2003; Yin et al., 2000). Unlike other organelle transport, the movement of the nucleus is relayed to the microtubule motor protein Dyn1p and associated dynactin complex later during anaphase (Li et al., 1993; Muhua et al., 1994). Thus, nuclear segregation involves two

**Figure 1.2 Transport of organelles and secretory vesicles by Myo2p on actin cables**

Actin cables are nucleated and assembled by the formin Bni1p from the bud tip and Bnr1p from the bud neck to serve as tracks for Myo2p transport. Myo2p transports microtubule plus ends through Bim1p (red) and Kar9 (purple) for orientation of the nucleus (1); the vacuole through Vac17p (teal) and Vac8p (green) (2); peroxisome through Inp2p (3); trans-Golgi network through Ypt31/32p (4); post-Golgi secretory vesicles through Sec4p (5); and mitochondria possibly through Mmr1p (6). Adapted from an image made by Kirk Donovan.



pathways: one through Myo2p and the other through the dynein/dynactin pathway. Failure of either pathway is not lethal and simply results in a low frequency of abnormal nuclear segregation. However, loss of both pathways is lethal (Fujiwara et al., 1999; Miller et al., 1999; Tong et al., 2001).

### **Formin proteins**

Formin proteins are large (120-220 kDa), multidomain proteins. They were first named after a knockout mouse that exhibited “limb deformity” in 1990 (Mass et al., 1990; Woychik et al., 1990). This family of proteins is highly conserved and characterized by the presence of Formin Homology domain 1 and 2 (FH1 and FH2) domains. Formins exist in all eukaryotes examined, with most species possessing many isoforms. Phylogenetic analysis of formins was performed using the FH2 domain (Higgs and Peterson, 2005), thus categorizing the metazoan formins into seven subgroups: Diaphanous (Dia); Formin-related gene in leukocytes (FRL); Dishevelled-associated activator of morphogenesis (DAAM); Formin homology domain-containing protein (FHOD); Formin (FMN); Delphilin and Inverted formin (INF) (Figure 1.3). Four of these subfamilies Dia, FRL, DAAM and FHOD possess similarities outside of the FH2 domain, and have been termed DRF (Diaphanous related formin).

Formin proteins assemble unbranched actin filaments. They have been implicated in the formation of multiple cellular structures such as stress fibers, filopodia, cell-cell junctions, phagocytic cups and contractile rings. These structures are essential to migration, cell division, polarized growth, phagocytosis, and more (Campellone and Welch, 2010). The major role of formins, which is conserved among eukaryotes, is their actin assembly ability. Formins are able to both nucleate and elongate actin

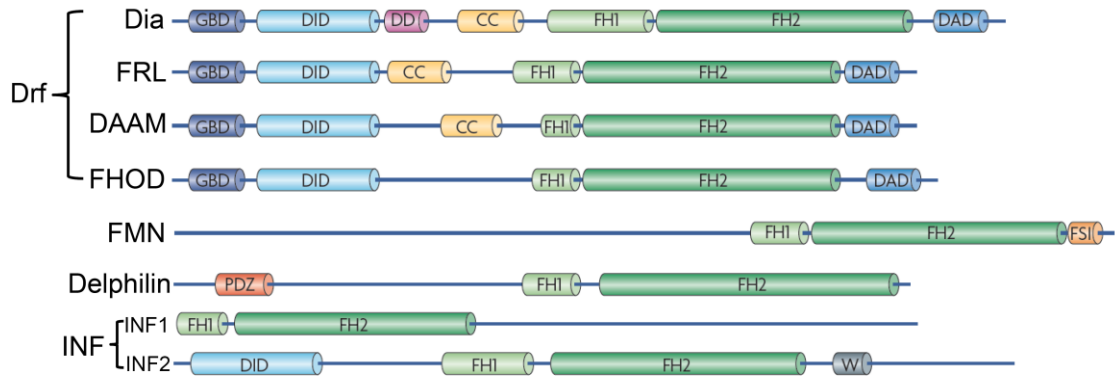


**Figure 1.3 Domain organizations of mammalian formins.**

CC, coiled coil; DAAM, Dishevelled-associated activator of morphogenesis; DAD, Diaphanous-autoinhibitory-domain; DD, Dimerization domain; Dia, Diaphanous; DID, Diaphanous inhibitory domain; FH1, Formin homology domain 1; FH2, Formin homology domain 2; FHOD, Formin homology domain-containing protein; FMN, formin; FRL, formin-related in leukocytes; FSI, formin–Spire interaction domain; GBD, GTPase binding domain; INF, inverted formin; PDZ, Postsynaptic density protein, Discs large, Zona occludens 1 domain; W, WASP homology 2 domain. Adapted, with permission, from the © 2010 Macmillan Publishers Limited. All rights reserved 238 | APRIL 2010 | volume 11 (Campellone and Welch, 2010)

filaments. Besides assembling actin filaments, Bnr1p, Frl1, Frl2, Frl3 and mDia2 also have the ability to bundle actin filaments *in vitro* (Esue et al., 2008; Li and Higgs, 2005; Moseley and Goode, 2005). Also, Frl1 and Inf2 were shown to sever and/or depolymerize actin filaments (Chhabra and Higgs, 2006; Harris et al., 2004). In addition to their roles in actin structure formation, many mammalian formins have also been shown to bind to microtubules and proteins that interact with microtubule plus ends to promote microtubule stability (Bartolini et al., 2008; Lewkowicz et al., 2008; Wen et al., 2004). This suggests that formins could function in the crosstalk between the actin and microtubule cytoskeleton (Chesarone et al., 2010).

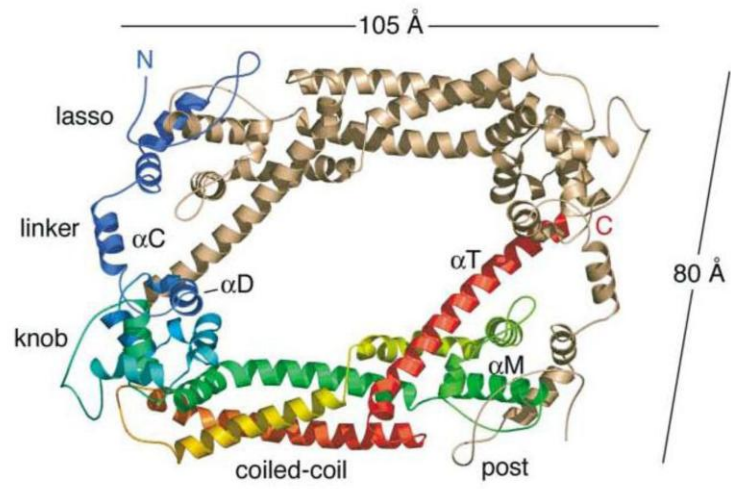
Studies suggest that diverse formins assemble filaments using similar mechanisms, but the rates of particular assembly steps vary (Kovar et al., 2006). Generally, the C-terminal region of formin proteins contains the FH1 and FH2 functional domains while the N-terminal half typically governs localization and activity of the C-terminal functional region. *In vitro*, the FH2 domains of most formin proteins are required and sufficient to nucleate unbranched actin filaments and enable processive elongation at the barbed ends (Copeland et al., 2004; Harris et al., 2004; Harris et al., 2006; Kovar et al., 2003; Kovar and Pollard, 2004; Li and Higgs, 2003; Pruyne et al., 2002; Romero et al., 2004). Both biochemical and structural studies on several formins suggest that the FH2 domain needs to form homodimers to perform its actin nucleation activity (Harris et al., 2004; Harris et al., 2006; Lu et al., 2007; Moseley et al., 2004; Shimada et al., 2004a; Xu et al., 2004). In the dimer, a loop of amino acids called the “lasso” from one FH2 domain encircles another loop, the “post”, from the other FH2 domain and forms a highly stable and flexible interaction. A “knob” region between

**Figure 1.4 Structure of FH2 dimer and its role on actin filament barbed ends**

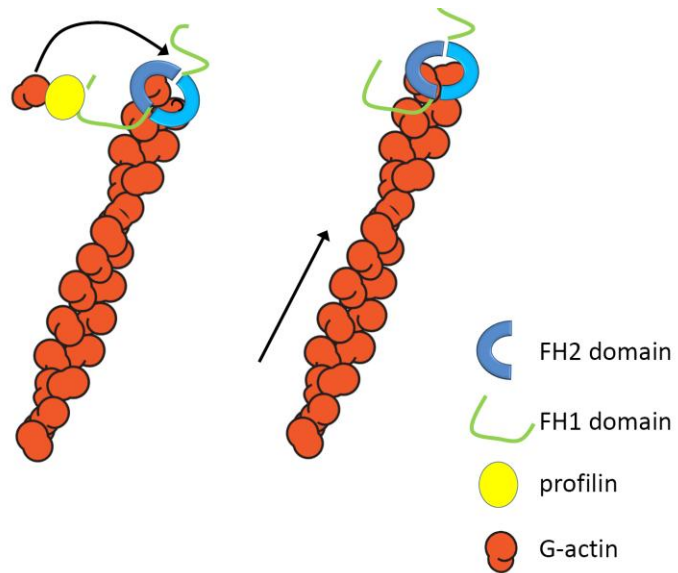
(A) Ribbon diagram showing the overall architecture of the FH2 dimer. One molecule is colored using the visible spectrum (from blue at the N terminus to red at the C terminus), the second molecule is colored tan. The lasso, linker, knob, coiled-coil, and post subdomains are labeled, and the approximate dimensions of the dimer are indicated. The N and C termini and selected  $\alpha$  helices of one molecule are labeled. Note the manner in which the lasso region of each molecule encircles a portion of the post subdomain of the other molecule in the dimer. Adapted, with permission, from the Cell 2004 by Cell Press 711 | March 2004 | Volume 116 (Xu et al., 2004)

(B) Processive barbed end elongation by Formin FH1-FH2. A FH2 dimer associates with the barbed end of an actin filament, while the FH1 domains recruit profilin-actin. The FH1 domain delivers profilin-actin to the barbed end, and the FH2 upward the barbed end to interact with the newly added actin monomer while rotating along with the actin filament.

(A)



(B)



the “lasso” and the “post” on each monomer projects above the plane of the lasso and post interface, giving the dimer a doughnut shape (Figure 1.4a). Moreover, a co-crystal structure of a Bni1p FH2 dimer with tetramethylrhodamine–actin revealed that each FH2 dimer bridges two actin subunits in a configuration that resembles the short-pitch actin dimer of a filament (Otomo et al., 2005b). As mentioned earlier, the actin dimers are unstable and energetically unfavorable. The FH2 domain dimers can thus stabilize spontaneously formed actin dimers and trimers to overcome the kinetic barriers (Chesarone et al., 2010; Pring et al., 2003). To elongate an actin filament, the FH2 dimer remains bound to the barbed end while moving processively during the rapid addition of actin subunits, protecting the barbed end from capping proteins. The structure of the FH2 dimer with actin also suggests a model, in which the FH2 dimer alternates between two bound states. In one state, both FH2 monomers bind the two terminal actin subunits at the barbed end of filament. In the other state, a third actin subunit is incorporated with the structural change of the flexible linker connecting the two FH2 dimers (Otomo et al., 2005b) (Figure 1.4b). In this model, the formin is predicted and has been shown to rotate along the axis of the double helical F-actin structure (Mizuno et al., 2011).

N-terminal to the FH2 domain is a proline-rich region called the FH1 domain, which binds profilin. As described above, profilin is an essential small actin binding protein that’s associated with actin monomers, and profilin-actin comprises the major pool of monomeric actin *in vivo* (previous introduction). The FH1 domains of different formins vary in length, proline content and number of potential profilin binding sites (Higgs, 2005). Profilin stimulates formin-induced actin assembly *in vitro* most likely

through increasing the local concentration of G-actin at the barbed end by interacting with the formin FH1 domain and with actin monomers (Kovar et al., 2003; Moseley and Goode, 2005; Pring et al., 2003; Sagot et al., 2002b). The importance of profilin is more obvious for the fission yeast formin Cdc12p. Cdc12p alone acts as a standard barbed end capping protein, limiting filament growth to the pointed end. Addition of profilin gates Cdc12p's actin assembly ability at the barbed end (Kovar et al., 2003).

The N-terminal region of formin proteins is generally considered to be the regulatory region. One mechanism suggested for the regulatory function of the N-terminal domain in DRF proteins is through autoinhibition by binding of the N-terminal Diaphanous inhibitory domain (DID) to the C-terminal Diaphanous autoregulatory domain (DAD) (Alberts, 2001; Li and Higgs, 2003; Li and Higgs, 2005) (Figure 1.3). Both biochemical and structural evidence suggest that autoinhibition is relieved by binding of Rho GTPases to the GTPase binding domain (GBD), which partially overlaps with the DID (Lammers et al., 2005; Li and Higgs, 2003; Li and Higgs, 2005; Nezami et al., 2006; Otomo et al., 2005a; Rose et al., 2005; Seth et al., 2006).

It has also been shown that the N-terminal region of formin proteins can homodimerize through a Dimerization Domain (DD) (Li and Higgs, 2005; Otomo et al., 2005a). It is worth noting that relieving autoinhibition by GTPases is incomplete, raising the possibility that additional regulatory factors exist for full activation (Li and Higgs, 2005; Seth et al., 2006). Also, there might be a feedback loop between formin proteins and Rho activators, indicated by Dia1 stimulating Rho-GEF (LARG) (Kitzing et al., 2007).

In addition to functioning in formin autoinhibition, the DAD domain has been suggested in a recent paper to have a direct role in actin nucleation (Gould et al., 2011). In addition to binding to the DID domain in the N-terminal region to mask the function of the FH2 domain, a dimerized DAD domain from mDia1 is sufficient to nucleate actin assembly. This property of the DAD domain may be common among other DRF family proteins which contain DAD domains. Consistent with this model, the FH1-FH2-COOH domains, which includes the DAD from Bni1p, Bnr1p, and Daam1p all have significantly higher actin assembly activities than their FH1-FH2ΔDAD counterparts (Gould et al., 2011).

### **Formins in *Saccharomyces cerevisiae***

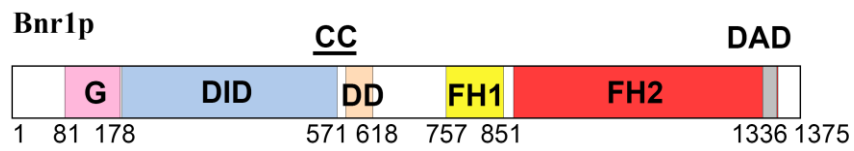
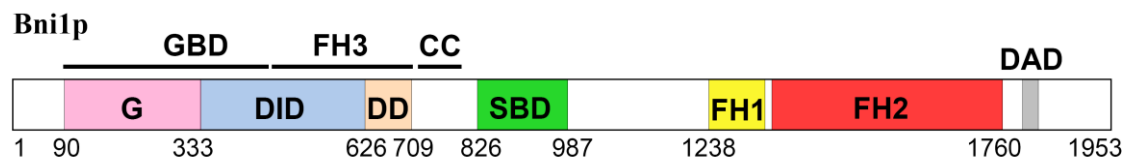
Two formin isoforms exist in the budding yeast *Saccharomyces cerevisiae*: Bni1p and Bnr1p. Although *bni1Δ* or *bnr1Δ* single deletions are not lethal, deleting both of them is lethal (Ozaki-Kuroda et al., 2001; Vallen et al., 2000). They both belong to the DRF family, and similar to other formin proteins in the DRF family, they contain FH1, FH2 and DAD domains at the C-terminus, as well as GBD and DID domains at the N-terminus. Bni1p also contains a Formin homology domain 3 (FH3), which is implicated in subcellular localization and formin regulation (Kato et al., 2001; Petersen et al., 1998) and a Spa2p Binding Domain (SBD) which binds to polarisome scaffolding protein Spa2 and has been suggested to localize Bni1p (Fujiwara et al., 1998) (Figure 1.5a). The role of formin proteins functioning in actin cable assembly was first established in studies of Bni1p (Evangelista et al., 2002; Pruyne et al., 2002; Sagot et al., 2002a; Sagot et al., 2002b). Since *bni1Δ bnr1Δ* is lethal, *bnr1Δ bni1ts* cells were used and actin cables as well as actin rings were diminished within minutes

**Figure 1.5 Formins in budding yeast *Saccharomyces cerevisiae***

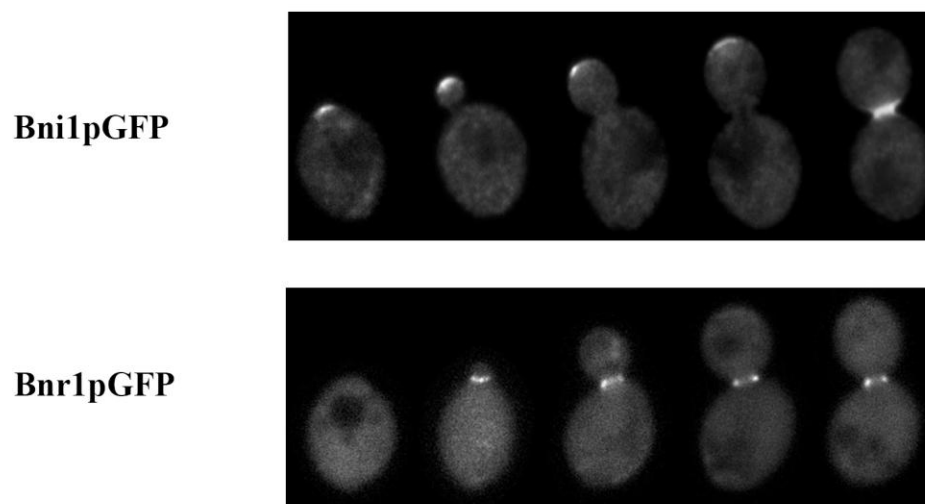
(A) Domain organization of formins in budding yeast, Bni1p and Bnr1p. CC, coiled coil; DAD, Diaphanous-autoinhibitory-domain; DD, Dimerization domain; Dia, Diaphanous; DID, Diaphanous inhibitory domain; FH1, Formin homology domain 1; FH2, Formin homology domain 2; FH3, Formin homology domain 3; GBD, GTPase binding domain; SBD, Spa2p binding domain.

(B) Distribution of Bni1p and Bnr1p in selected cell. Bni1pGFP from a high-copy plasmid. Bnr1pGFP fluorescence is shown in endogenous labeled cells. Adapted with permission from David W Pruyne

(A)



(B)



after shifting cells to the restrictive temperature without disrupting actin patch integrity (Evangelista et al., 2002; Sagot et al., 2002a). Subsequent biochemical assays demonstrated that the FH2 domain of Bni1p directly nucleates the assembly of actin cables (Pruyne et al., 2002; Sagot et al., 2002b).

The two formin proteins Bni1p and Bnr1p partially overlap in their localization (Figure 1.5b). During polarized growth, Bni1p localizes to the future budding site in unbudded cells, to the tip of small buds, at the cortex of medium buds, and to the bud neck during anaphase. On the other hand, Bnr1p localizes to the neck of cells with buds of all sizes and disappears before the constriction of actomyosin ring (Buttery et al., 2007; Fujiwara et al., 1998; Gao et al., 2010; Kamei et al., 1998; Pruyne et al., 2004a). In pheromone stimulated cells, Bni1p localizes to the shmoo tip (Evangelista et al., 1997), while Bnr1p localizes to the septin collar at the shmoo base (Gao et al., 2010).

Bni1p and Bnr1p share similar but distinct functions. Bni1p and Bnr1p maintain distinct sets of actin cables. In unbudded cells, *bni1Δ* cells display a higher incidence of unorganized actin cables and reduced proportion of Myo2p at the nascent bud site, while *bnr1Δ* cells show a similar actin distribution as wild type yeast. In small to medium budded cells, actin cables in *bni1Δ* cells are reduced in the bud with Myo2p and Sec4p, a Rab protein on secretory vesicles, concentrated at the bud neck and also diffusely at the bud cortex. In small to medium-budded *bnr1Δ* cells, actin cables in the mother are reduced with Myo2p and Sec4p distributed similarly to wildtype cells. In large budded cells, the actin cable structure in both *bni1Δ* and *bnr1Δ* cells are similar to wildtype cells, although *bni1Δ* cells have more disorganized cables (Pruyne et al.,

2004a). A comparative study of their biochemical activities showed that Bnr1p could bundle actin filaments and is 10-15 fold more potent than Bni1p in actin assembly activity *in vitro* (Moseley and Goode, 2005; Wen and Rubenstein, 2009). Bni1p is phosphorylated *in vivo*, but Bnr1p hasn't been shown to be phosphorylated (Moseley and Goode, 2005). Live cell imaging of Bni1p tagged with 3GFP displayed linear, retrograde movements with a rate of  $0.48 \pm 0.22 \mu\text{m/s}$ , similar to that of actin cable growth. This retrograde movement of Bni1p is dependent on actin cables and its actin assembly ability. It is proposed that Bni1p nucleates actin assembly at the cell cortex, then releases from the cortex and is carried with the assembling cable before falling off, while Bnr1p showed relative static and confined localization at the bud neck before actomyosin ring contraction. Fluorescence Recovery After Photobleaching (FRAP) experiments confirmed the dynamic properties of Bni1p between polarized sites and the cytoplasm with  $t_{1/2} < 8\text{s}$ . On the other hand, FRAP of the entire bud neck, where Bnr1p is localized, resulted in little or no recovery of Bnr1p. FRAP of half of the bud neck showed that Bnr1p has a  $t_{1/2}$  of recovery around 60s, suggesting a slow exchange rate of Bnr1p even within the bud neck region (Buttery et al., 2007). The above differences in localizations and functions between Bni1p and Bnr1p suggested that the two formin isoforms are regulated differently.

As a DRF, Bni1p has been suggested to be regulated by autoinhibition similarly to its mammalian homolog mDia1. Indeed, overexpression of Bni1FH1-COOH or Bni1p $\Delta$ DAD, but not overexpression of full length Bni1p, induced excessive actin filaments (Evangelista et al., 1997; Sagot et al., 2002a). Direct evidence came from an *in vitro* pyrene actin assembly assay showing that an N-terminal piece of Bni1p could

inhibit the acceleration phase of actin polymerization by the Bni1FH1-COOH region (Wang et al., 2009).

Autoinhibition could be released by binding of small GTPases to the N-terminal GBD domain. Both Bni1p and Bnr1p have been shown to bind to small Rho GTPases. Besides Cdc42p, there are five other Rho proteins in budding yeast, Rho1p-5p. Cdc42p is the critical director of polarized growth including actin polarization, septin assembly and exocytosis (see previous introduction). Rho1p is involved in the Pkc1p-dependent cell wall integrity (CWI) pathway and cell polarity establishment. Rho2p may share some common function with Rho1p (Park and Bi, 2007). Rho3 and Rho4 share a function in cell polarity with Rho3p being the major one. Rho5p was suggested to play a role in CWI pathway also (Schmitz et al., 2002). Among these six Rho proteins, Rho1p and Cdc42p are essential. Bni1p has been shown using yeast two hybrid assays to interact with Cdc42p (Evangelista et al., 1997; Richman et al., 1999; Richman et al., 2004), Rho1p (Kohno et al., 1996) and Rho3p (Robinson et al., 1999), all preferably binding the active GTPases. Cdc42p and Rho1p have been shown to bind to Bni1p *in vitro* (Evangelista et al., 1997; Kohno et al., 1996). On the other hand, only Rho4p binds to Bnr1p by yeast two hybrid and *in vitro* pull down assays (Imamura et al., 1997). Cdc42p is required for recruitment of Bni1p to the nascent bud site (Jaquenoud and Peter, 2000; Ozaki-Kuroda et al., 2001). *cdc42ts* mutants have less polarized cables in unbudded cells (Dong et al., 2003). Bni1p is delocalized in *rho1-ts* strains during mating (Qi and Elion, 2005), and formin nucleated actin cables and rings are also lost in *rho1-ts* strains (Dong et al., 2003; Finger et al., 1998; Guo et al., 2001; Tolliday et al., 2002). *rho3Δ rho4Δ* double disruption is lethal but can be

rescued by the expression of Bni1p  $\Delta$ GBD or Bnr1p $\Delta$ GBD to restore normal actin staining, suggesting that Rho3p and Rho4p's main function may be to activate formins by binding to the GBDs and relieving the autoinhibitory state formed between the GBD and the DAD region (Dong et al., 2003).

In addition to the general autoinhibitory mechanism among DRFs, the yeast formins Bni1p and Bnr1p possess their own regulatory pathways. Bud6p has been suggested to differentially regulate Bni1p and Bnr1p (Moseley and Goode, 2005). Bud6p is a component of the 12S polarisome complex composed of Spa2p, Pea2p, and Bud6p (Sheu et al., 1998). Bud6p was first identified as an actin binding protein using yeast two hybrid (Amberg et al., 1995). Bud6p-GFP expressed at endogenous levels showed that its localization overlaps with both Bni1p and Bnr1p (Delgehyr et al., 2008). Bud6-GFP first associates with the bud tip after bud emergence, and then accumulates at the bud neck coincident with initiation of spindle assembly. Bni1p and Bud6p colocalize at the bud cortex in small budded cells, but association of Bud6p with the bud neck in medium budded cells is not accompanied by Bni1p. On the other hand, Bnr1p is recruited at the bud neck following bud emergence before Bud6p. Both proteins then colocalize until Bnr1p disappears prior to cytokinesis, when Bni1p colocalizes with Bud6p during cytokinesis. Although yeast two hybrid assays suggested that Bud6p interacts with the C-terminal region of both Bni1p and Bnr1p (Kamei et al., 1998), an *in vitro* pull down assay showed that only the Bni1p C-terminal region could interact with Bud6p. Bud6p can also stimulate the actin assembly activity of Bni1 FH1-COOH (Moseley and Goode, 2005; Moseley et al., 2004).

Bni1p also functions intimately with another component of polarisome, Spa2p. Spa2p has been suggested to bind specifically to Bni1p to regulate its localization (Fujiwara et al., 1998; Sheu et al., 1998). Spa2p serves as the scaffolding protein of the polarisome complex and interacts with all the other known components as well as MAP kinase Mpk1p and GAP proteins, Msb3p and Msb4p (Tcheperegine et al., 2005; van Drogen and Peter, 2002). Bni1p 826-987aa binds directly to the C-terminal, SHD-V region of Spa2p (Fujiwara et al., 1998), thus Bni1p 826-987aa is defined as the Spa2 binding domain (SBD). In *spa2Δ* or *bni1Δ822-987* cells, the localization of Bni1p at the small bud tip was significantly reduced (Ozaki-Kuroda et al., 2001).

On the other hand, Bud14p, a protein that interacts with Glc7p, the catalytic subunit of type 1 protein phosphatase, to control dynein-dependent microtubule sliding at the bud cortex and facilitates nuclear migration (Knaus et al., 2005), has been suggested to specifically regulate Bnr1p's actin assembly activity (Chesarone et al., 2009). Bud14p inhibits Bnr1p by displacing Bnr1p from growing barbed ends, controlling the duration of Bnr1p-mediated actin assembly and promoting Bnr1p cycling between the active and inactive state.

Phosphorylation is suggested to play an important role in Bni1p's regulation. The MAPK Fus3p was shown to regulate Bni1p during mating (Matheos et al., 2004), and phosphorylation of Bni1p was greatly reduced in *fus3Δ* cells. Bni1p-GFP also failed to localize to the shmoo tip in *fus3Δ* cells. The fact that Bni1p was less phosphorylated in *ste20Δ* cells further suggested that disrupting mating MAPK pathway affects the phosphorylation of Bni1p (Goehring et al., 2003). The phosphorylation of Bni1p by Fus3p could activate and recruit Bni1p to the shmoo tip during mating. A feedback

loop might exist in this signaling pathway since Fus3p-GFP and the MAPK scaffolding protein GFP-Ste5p were not localized to the shmoo tip after pheromone treatment in *bni1Δ* cells (Qi and Elion, 2005). The actin cable motor protein Myo2p has also been suggested to transport Ste5p to the shmooing tip, which might function in the feedback loop (Qi and Elion, 2005).

Another interesting observation made by Wang *et al* is that Bni1p is phosphorylated by Prk1p (Wang *et al.*, 2009), a serine/threonine kinase that regulates actin-coupled endocytosis (Toshima *et al.*, 2005). They were able to show that Bni1p was phosphorylated directly by Prk1p *in vitro* at three sites, one in the GBD domain, one in the FH1 domain and one at the C-terminal end. Deletion of the *PRK1* gene reduces the phosphorylated Bni1p to about 50%, while deleting both *PRK1* and *ARK1*, which encodes a homolog of Prk1p, reduces the phosphorylated state further (Wang *et al.*, 2009). Using actin assembly assays, it was shown that the autoinhibitory effect of Bni1p N-terminal region on the actin assembly of Bni1p FH1-COOH can be released with the addition of Prk1p. It would be interesting to know how Prk1p/Ark1p coordinates its function on activation of formin proteins and endocytosis by the Arp2/3 complex.

Although those previous studies provide a general picture of how the formins are regulated, exactly how formins are regulated spatially and temporally is not clearly known. Thus I set out to study the regulation of the formin protein Bni1p.

## CHAPTER 2

### **N-terminus of Bni1p contains multiple localization signals**

#### *Abstract*

Formin proteins are critical regulators of actin structure, which nucleate and elongate unbranched actin filaments in all eukaryotes. Budding yeast, *Saccharomyces cerevisiae*, has two formin isoforms, Bni1p and Bnr1p, which have similar but distinct functions and localization, organizing different sets of actin cables during bud growth. Here I examine the N-terminal region of Bni1p responsible for bud cortex and bud neck localization. I found three non-overlapping regions: one in the N-terminal 333 amino acids which requires dimerization, one in the 334-834 amino acids which covers DID-DD-CC domains and the third in the Spa2p binding domain. The three regions can each localize to the bud cortex and bud neck at the right cell cycle stage independently of endogenous Bni1p.

#### *Introduction*

As described in the Chapter 1 general introduction, the formin protein Bni1p has a critical role in organizing the actin cytoskeleton. During budding, in small to medium budded cells, Bni1p assembles actin cables from the bud tip/cortex. Later during cytokinesis, Bni1p shifts localization and assembles actin cables from the bud neck. How Bni1p is regulated to assemble actin cables spatially and temporally has always been of great interests to me. It has been shown that the N-terminal half of Bni1p, 1-1240aa is sufficient for its localization (Ozaki-Kuroda et al., 2001). In this chapter, a series of GFP-tagged constructs encompassing different regions of the N-terminal domains were made and characterized to define localization determinants. Three

different localization domains before the FH1 domain were identified in the N-terminal region. They all localize to the bud cortex and bud neck during the right cell cycle stage independent of endogenous Bni1p.

### ***Materials and methods***

#### **Yeast strains and molecular biology techniques**

Strains used in this study are listed in Table 2.1. All strains were generated in the S288C strain background coming from the deletion consortium (Brachmann et al., 1998). Standard media and techniques for growing and transforming yeast were used (Sherman, 1991). Plasmids used in this study are listed in Table 2.2. Bni1p overexpression plasmids were made using template pHL012 (Liu et al., 1992), and inserting different Bni1p regions using BamHI and MluI restriction sites. GFP was inserted using MluI and NotI. To express the different regions of Bni1p, the relevant strains were grown overnight in 5 ml Sraff-URA media to an OD<sub>600</sub> of 0.4 and then 0.5 ml 20% galactose was added to the media for 3-4 hrs.

#### **Yeast two hybrid screen**

Bait plasmids containing Gal4p binding domain (BD) were transformed into PJ69-4 $\alpha$  strains. I used a prey library from the Fields lab (Uetz et al., 2000). The library was constructed using PJ69-4 $\alpha$  strains with prey plasmids containing Gal4p activating domain (AD). Each prey plasmid contains one of the *S. cerevisiae* open reading frames and was transformed into PJ69-4 $\alpha$  cells individually to construct the yeast library. The library contains all the predicted yeast genes. PJ69-4 $\alpha$  cells with bait plasmid were grown overnight in 5 ml SC-Trp media until the OD reached 0.8~1.0. 1ml of the prey library in PJ69-4 $\alpha$  cells was added to the PJ69-4 $\alpha$  cells. 45 ml of

**Table 2.1 Yeast strains used in Chapter 2**

Strain	Genotype	Source
ABY1848	MATa/ $\alpha$ <i>his3<math>\Delta</math>1/ his3<math>\Delta</math>1 leu2<math>\Delta</math>0/ leu2<math>\Delta</math>0 ura3<math>\Delta</math>0/ ura3<math>\Delta</math>0 met15<math>\Delta</math>0/MET15 lys2<math>\Delta</math>0/LYS2</i>	(Evangelista et al., 2002)
pJ69-4a	MATa <i>trp1-901 leu2-3,112 ura3-52 his3-200 gal4<math>\Delta</math> gal80<math>\Delta</math> LYS2::GAL1-HIS3 GAL2-ADE2 met2::GAL7-lacZ</i>	(James et al., 1996)
pJ69-4a	MATa <i>trp1-901 leu2-3,112 ura3-52 his3-200 gal4<math>\Delta</math> gal80<math>\Delta</math> LYS2::GAL1-HIS3 GAL2-ADE2 met2::GAL7-lacZ</i>	(James et al., 1996)
ABY2838	MATa/ $\alpha$ <i>his3<math>\Delta</math>1/ his3<math>\Delta</math>1 leu2<math>\Delta</math>0/ leu2<math>\Delta</math>0 ura3<math>\Delta</math>0/ ura3<math>\Delta</math>0 met15<math>\Delta</math>0/met15<math>\Delta</math>0 bni1<math>\Delta</math>::KanR/ bni1<math>\Delta</math>::KanR</i>	This study
ABY3280	MATa <i>his3<math>\Delta</math>1 leu2<math>\Delta</math>0 ura3<math>\Delta</math>0 met15<math>\Delta</math>0 spa2<math>\Delta</math>::Kan<sup>R</sup></i>	Invitrogen
ABY1854	MATa <i>his3<math>\Delta</math>1 leu2<math>\Delta</math>0 ura3<math>\Delta</math>0 lys2<math>\Delta</math>0 rho2<math>\Delta</math>::Kan<sup>R</sup></i>	(Dong et al., 2003)
ABY1590	MATa <i>ade2-101 his3<math>\Delta</math>200 leu2-3, 112 ura3-52 lys2-801 rho3<math>\Delta</math>::Kan<sup>R</sup></i>	(Dong et al., 2003)
ABY1849	MATa <i>his3<math>\Delta</math>1 leu2<math>\Delta</math>0 lys2<math>\Delta</math>0 ura3<math>\Delta</math>0 rho4<math>\Delta</math>::KanR</i>	(Dong et al., 2003)
ABY1862	MATa <i>his3<math>\Delta</math>1 leu2<math>\Delta</math>0 lys2<math>\Delta</math>0 ura3<math>\Delta</math>0 rho5<math>\Delta</math>::KanR</i>	(Dong et al., 2003)
ABY1589	MATa <i>ade2 his3 leu2 lys2 trp1 rho1::HIS3 ade3::rho1-2 LEU2</i>	(Dong et al., 2003)
KKY404	MATa <i>his3-<math>\Delta</math>200 leu2-3,112 lys2-801am ura3-52 cdc42-101::LEU2</i>	(Kozminski et al., 2000)

**Table 2.2 Plasmids used in Chapter 2**

Plasmid	Backbone	Genotype
pWL062	pRS316	$P_{GALI-10}$ - <i>BNII</i> (1-1953)-GFP
pWL150	pRS316	$P_{GALI-10}$ - <i>BNII</i> (1-333)-GFP
pWL151	pRS316	$P_{GALI-10}$ - <i>BNII</i> (1-333)-Leucine zipper-GFP
pWL054	pRS316	$P_{GALI-10}$ - <i>BNII</i> (1-596)-GFP
pWL071	pRS316	$P_{GALI-10}$ - <i>BNII</i> (1-596)-Leucine zipper-GFP
pWL060	pRS316	$P_{GALI-10}$ - <i>BNII</i> (1-717)-GFP
pWL055	pRS316	$P_{GALI-10}$ - <i>BNII</i> (1-834)-GFP
pWL148	pRS316	$P_{GALI-10}$ - <i>BNII</i> (334-834)-GFP
pWL099	pRS316	$P_{GALI-10}$ - <i>BNII</i> (1-834 $\Delta$ 596-717)-GFP
pWL067	pRS316	$P_{GALI-10}$ - <i>BNII</i> (1-1239)-GFP
pWL117	pRS316	$P_{GALI-10}$ - <i>BNII</i> (501-717)-GFP
pWL084	pRS316	$P_{GALI-10}$ -GFP- <i>BNII</i> (1-1239)-GFP
pWL108	pRS316	$P_{GALI-10}$ - <i>BNII</i> (592-834)-GFP
pWL107	pRS316	$P_{GALI-10}$ - <i>BNII</i> (987-1239)-GFP
pWL088	pGBKT7	<i>BNII</i> 1-724
pWL053	pRS316	$P_{GALI-10}$ - <i>BNII</i> (1-347)-GFP
pWL070	pRS316	$P_{GALI-10}$ - <i>BNII</i> (1-347)-Leucine zipper-GFP

2xYPDA/Kan was added to the mixture. The mixture was incubated at 30 °C for 20~24 hrs with gentle shaking at 30~50 rpm. Cells were checked by light microscope to determine whether mating had occurred. Mated cells either were spun down and plated on SC-Leu-Trp-His or SC-Leu-Trp-His-Ade to select for the yeast two hybrid candidates, or the cells were diluted and plated on SC-Leu, SC-Trp and SC-Leu-Trp to calculate the mating efficiency. A total of 408,000 diploids, made by mating the prey strains with the bait library, were screened and 189 candidates were confirmed after restreaking. Sequencing of the candidates revealed 46 different genes. Ten candidates were chosen arbitrarily and retransformed and dilution assays were performed to verify the interactions.

### **Microscopy**

Live cells were placed under 2% agarose in synthetic medium containing appropriate amino acids. Images were acquired with a spinning disc confocal microscopy system (3I Corp) using a DMI 6000B microscope (Leica) and a digital camera (QuantEM; Photometrics). Images were further analyzed and adjusted using Slidebook 5. To disrupt microtubule structures, cells were treated with 120 µg/ml benomyl in DMSO for 10 min. Tub1p-GFP was used to verify the disruption of microtubules. To disrupt actin structures, cells were treated with 200 µM Latruculin A for 10 min. Phalloidin staining was used to verify the disruption of F-actin structures: Cells were fixed with 3.7% formaldehyde for 30 min to 1 hr, then washed three times with PBS and treated with 0.2% Triton X-100 for 15 min. The cells were washed and incubated with 100 µl PBS + 3 µl Alexa568-phalloidin for 1 hr. After final washes, the cells were examined by microscopy. When washing the cells, the centrifugation

speed should be kept low to keep the intact actin structures. I used a tabletop centrifuge at 5000 rpm for 1 min.

## ***Results***

### **The N-terminal domain of Bni1p contains more than one localization region**

Full length Bni1p-GFP localizes at the bud site, concentrates at the tip of small budded cells, more broadly as a cap in medium budded cells, and then disappears from the bud cortex of large budded cells and re-appears at the bud neck prior to cytokinesis (Figure 2.2A and (Ozaki-Kuroda et al., 2001; Pruyne et al., 2004a)). To study the localization determinants, constructs encompassing different regions of Bni1p were inserted behind the *GALI* promoter and C-terminally tagged with GFP in a low copy plasmid (Figure 2.1). Cells transformed with these plasmids were induced in galactose for 3-4 hrs. A summary of the live-cell imaging of different GFP tagged Bni1p constructs is shown in Table 2.3. Bni1p-1-1239-GFP, encompassing the entire N-terminal region up to the FH1 domain, showed a broader localization than Bni1p-GFP at the bud cortex of small and medium sized buds, and localized to the bud neck in large budded cells (Figure 2.2B). The shortest N-terminal region that still strongly localized to the bud cortex was Bni1p-1-717-GFP (Figure 2.2C). Constructs shorter than Bni1p-1-717-GFP localized very weakly, with barely detectable localization to the bud cortex and neck. Since the Spa2p binding region lies outside this construct, and Spa2p has been suggested to regulate Bni1p's localization (Fujiwara et al., 1998; Sheu et al., 1998), these results identified an additional localization domain. The localization of Bni1p-822-992-GFP covering the Spa2p binding region was also studied and this construct localizes mostly to the nucleus but also weakly to the bud

**Figure 2.1 Scheme of Bni1p N-terminal overexpression constructs**

Constructs that are localized at the bud cortex and bud neck during the right cell stages are in green, constructs that are not localized at the bud cortex or bud neck are in red.

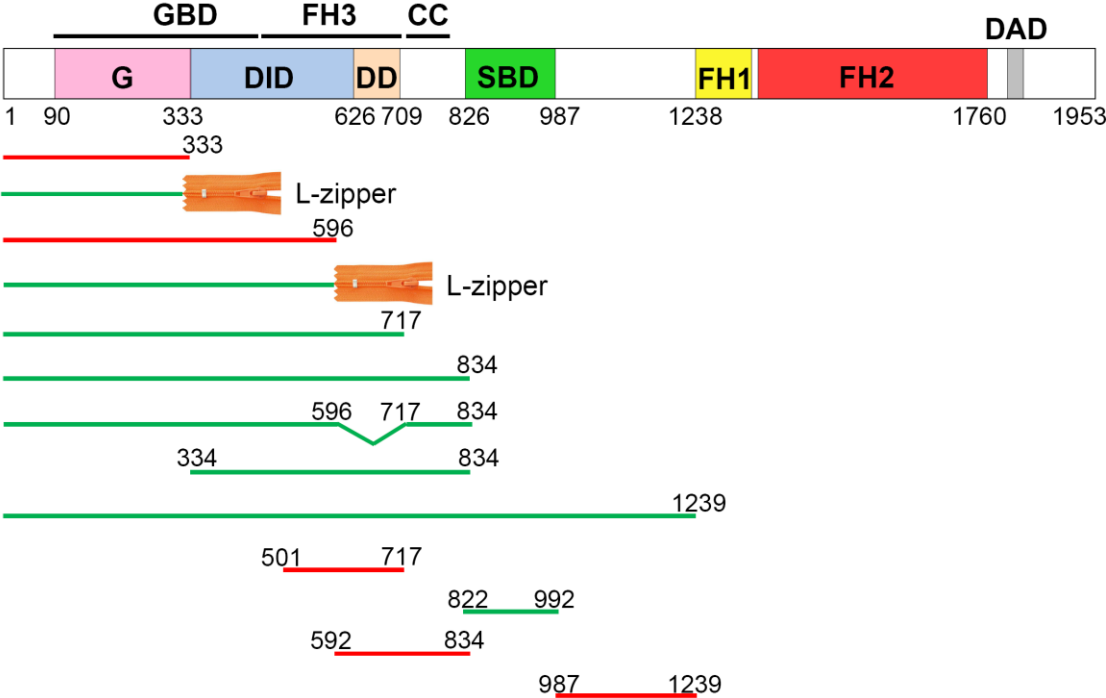
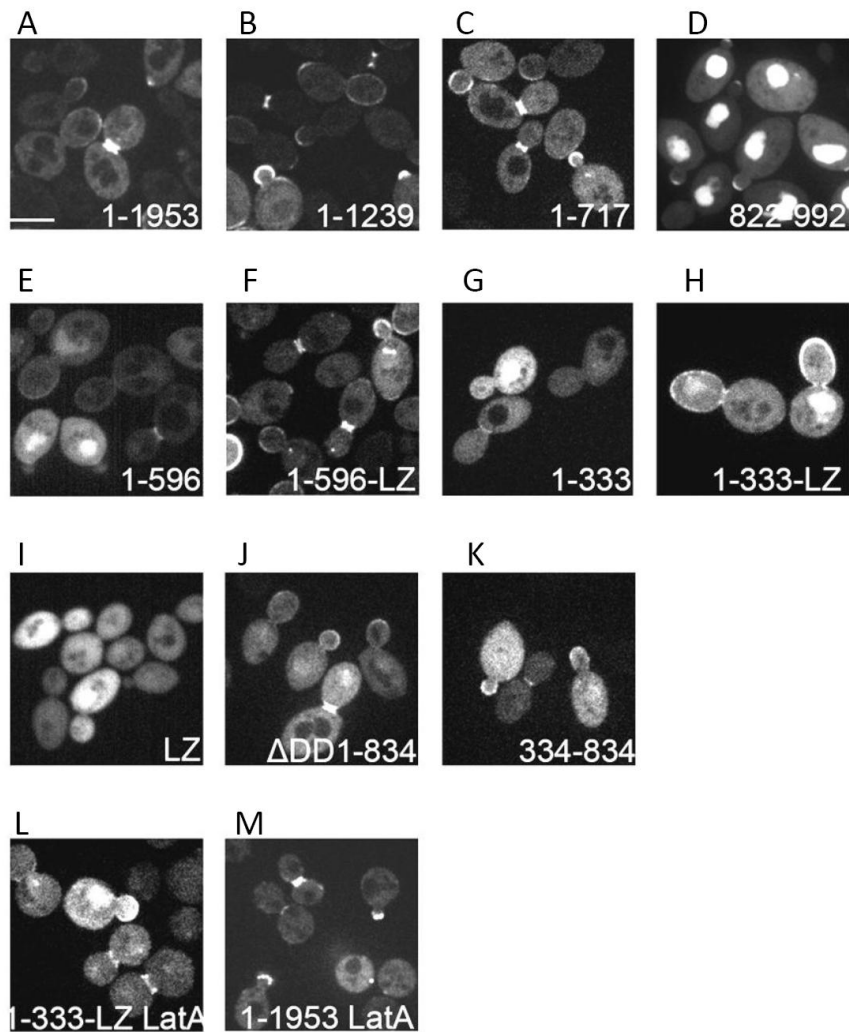


**Figure 2.2 Selected GFP images of overexpressed Bni1p N-terminal constructs during budding**

(A-K) GFP images of overexpressed Bni1p N-terminal regions in a *BNI1* background. (L, M) GFP images of overexpressed Bni1p N-terminal regions in a *bni1Δ* background after treated with 200  $\mu$ M latrunculinA for 10 min. Bni1p constructs were expressed behind the *GALI* promoter and tagged with GFP at the C-terminus, induced with galactose for 3 to 4 hr. Scale bar: 5  $\mu$ m.



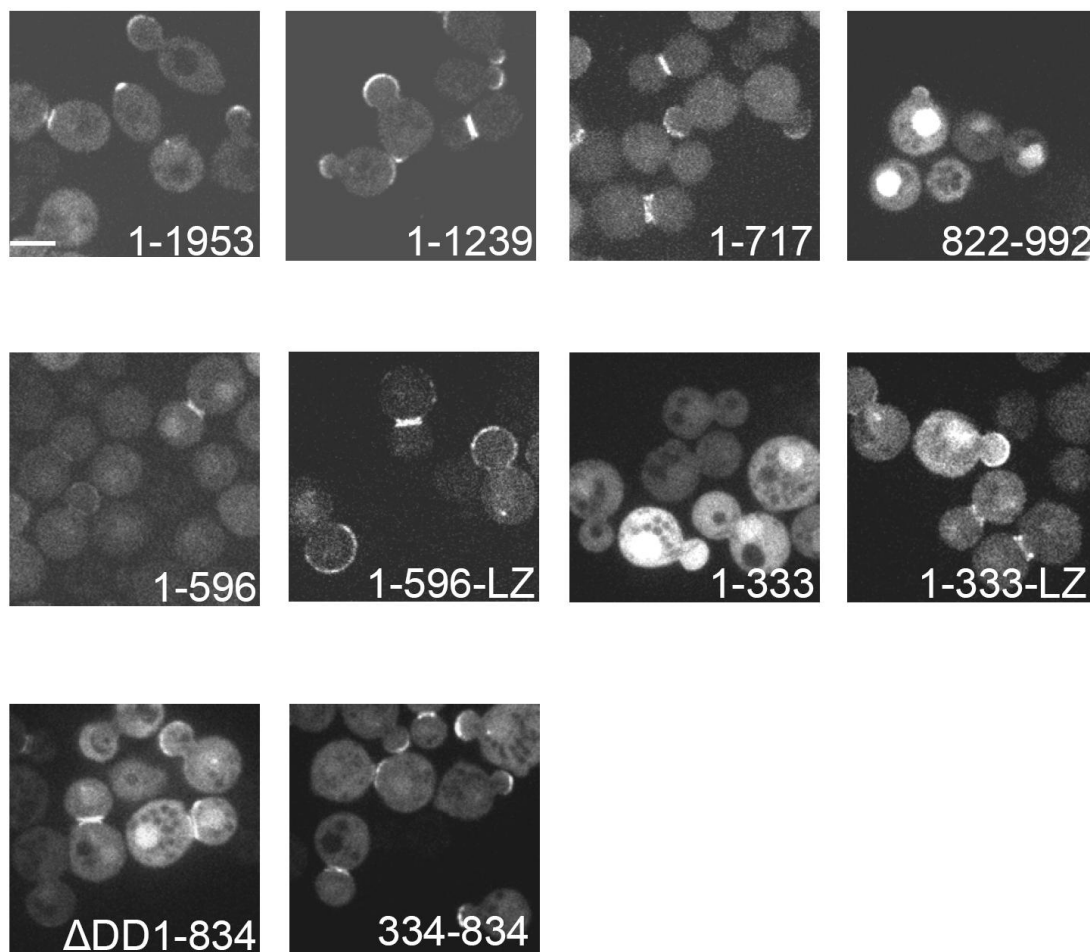
cortex and bud neck (Figure 2.2D). However, Bni1p822-992aa-GFP is no longer localized at the bud cortex and neck in *spa2Δ* cells (Figure 2.5G), suggesting that this localization is Spa2p dependent. Thus Bni1p has at least two localization domains in its N-terminal 1-1239 amino acid region.

### **The GBD domain of Bni1p localizes to the bud cortex and bud neck when dimerized**

As indicated above, Bni1p-1-717-GFP localizes to the bud cortex and the bud neck, yet shorter constructs like Bni1p-1-596-GFP do so very weakly (Figure 2.2E). The difference between these two constructs is the region proposed to be a dimerization domain (DD) (Figure 2.1). Since the DD region of mDia1 has been shown to facilitate dimerization (Li and Higgs, 2005), I asked whether dimerization might be important for localization. I therefore explored whether artificially dimerizing the Bni1p-1-596 construct might allow it to localize appropriately. To do this, I appended a leucine zipper from human CREB which functions as a dimerization domain (Schumacher et al., 2000). Bni1p-1-596-L-Zipper construct localized robustly to the cell cortex and neck (Figure 2.2F). With this result in hand, I explored how much of the N-terminal domain, when dimerized, is necessary for this localization. Accordingly, I found that Bni1p-1-333-GFP does not localize to the bud cortex, whereas Bni1-1-333-L-Zipper localizes to both the bud cortex and the bud neck (Figure 2.2G and H). Expression of just the leucine zipper fused to GFP is cytoplasmic (Figure 2.2I). Additionally, the Bni1p N-terminal construct with the DD deleted could also localize at the bud cortex and neck, suggesting that the coil-coil following the DD might be contributing to the dimerization of N-terminus of Bni1p (Figure 2.2J).

**Figure 2.3 Selected GFP images of overexpression Bni1p N-terminal constructs in *bni1Δ* cells**

Bni1p constructs are expressed under *GALI* promoter and tagged with GFP at the C-terminus, induced with galactose for three to four hours. Scale bar: 2  $\mu$ m.



### **The N-terminal half of Bni1p contains three localization regions**

The above results suggested that the N-terminal region of Bni1p contains more than one localization domain. To determine whether additional N-terminal regions contribute to the localization of Bni1p, the localization of the remaining domains were also studied using GFP tagged constructs. To our surprise, Bni1p-334-834-GFP which covers the DID, DD and the following predicted coiled coil (CC) region before the SBD domain was also able to localize to the bud cortex and bud neck (Figure 2.2K), similarly to Bni1p-1-1239-GFP. Thus, Bni1p is localized at the bud cortex by three localization regions, one residing in the N-terminal 333 amino acids that requires dimerization, one in the region encompassed by 334-834 amino acids which covers the DID-DD-CC domains and the third lies in the region of the Spa2p binding domain. However, additional features of Bni1p are necessary to restrict the full-length protein to the tip of the bud cortex of small budded cells.

To test if the localization regions were dependent on endogenous Bni1p, all constructs were examined in *bni1Δ* cells. All the localizations were not changed in either *bni1Δ* cells (Figure 2.3) or *bnr1Δ* cells, indicating that they are not dimerizing with endogenous Bni1p to localize, but must be binding a cortically localized determinant in the bud and later at the neck. Moreover, the localization of Bni1p-1-333-L-Zipper, or Bni1-GFP, to the bud cortex is independent of the actin cytoskeleton as the localization was unchanged by treating cells for 10 mins with 200 μM of the actin depolymerizing drug Latrunculin A (Figure 2.2L and M).

### **The role of microtubules in Bni1p localization**

In addition to localizing to the bud cortex and bud neck, several of the Bni1p

**Table 2.3 Localization of Bni1p N-terminal constructs**

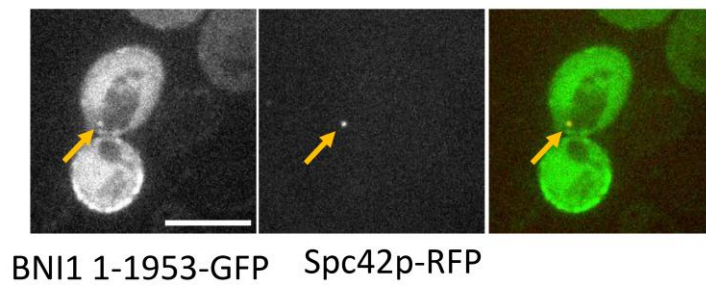
Numbers indicate Bni1p amino acid residues in constructs. “+” or “-” indicates whether the construct was detected by live imaging at the indicated place. The number of “+” indicates how strong the localization is in terms of percentage of cells was observed with the localization. \* both spindle and spindle pole body localizations

Bni1p-GFP construct	Bud tip localization	Bud cortex localization	Bud neck localization	Spindle pole body localization	Mother cortex localization	Expression checked by Western
<b>Bni1p 1-333</b>	+++	+	+++	+/-	-	Yes
<b>1-333-LZ</b>	-	-	+	-	-	NA
<b>1-333-LZ</b>	+++	+++++	+++	+++ *	-	Yes
<b>1-596</b>	+	+	+	+	-	Yes
<b>1-596-LZ</b>	+++	+++++	+++	+++ *	-	Yes
<b>1-717</b>	+++	+++++	+++	+/-	+	Yes
<b>1-834</b>	+++	+++++	+++	++	+	Yes
<b>822-992</b>	+	+	+	-	+	Yes
<b>1-1239</b>	+++	++++++	+++	+	++	Yes
<b>ΔΔΔ 1-834</b>	+++	+++	+++	++	-	Yes
<b>ΔFH3 1-834</b>	-	-	+	+	-	Yes
<b>ΔΔΔ 1-1239</b>	+++	+++	+++	++	+/-	Yes
<b>ΔFH3 1-1239</b>	+	+	+	-	-	Yes
<b>592-834</b>	-	-	-	-	-	Yes
<b>592-717</b>	-	-	-	-	-	Yes
<b>987-1239</b>	-	-	-	-	-	Yes
<b>334-717</b>	-	+/-	+/-	-	-	NA
<b>343-717</b>	-	-	-	-	-	NA
<b>334-834</b>	+++	+++	+++	+	-	Yes
<b>343-834</b>	-	-	-	++	-	NA
<b>1-347</b>	-	-	-	-	-	Yes
<b>1-347-LZ</b>	+++	+++++	+++	+++ *	-	Yes
<b>501-717</b>	-	-	-	-	-	Yes

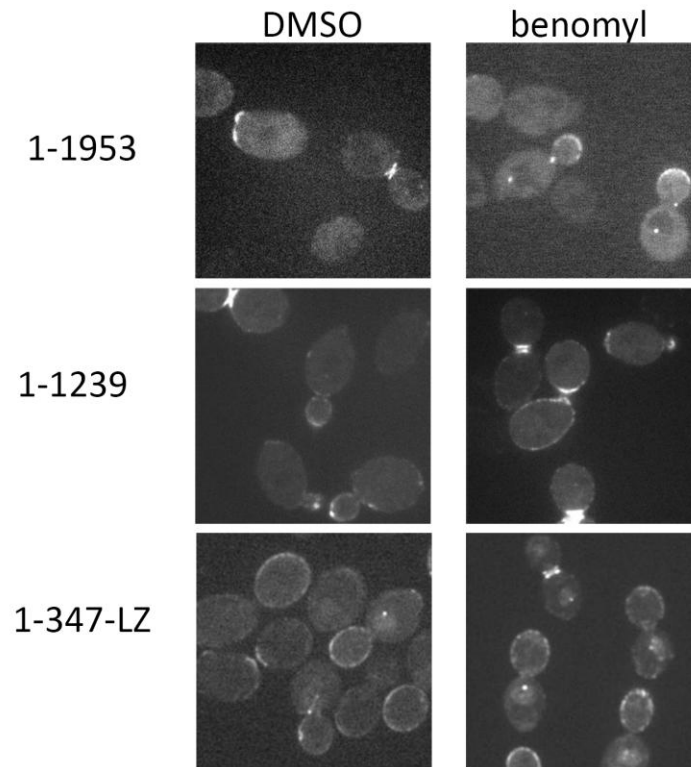
**Figure 2.4 The role of microtubules in Bni1p localization**

(A) Colocalization of Bni1p with SPB. SPB was labeled with Spc42p-RFP and observed in the same cell expressing full length Bni1p-GFP. (B) GFP images of cells with Bni1p overexpression constructs treated with DMSO or 120  $\mu\text{g/ml}$  benomyl for 10 mins. Scale bar: 5  $\mu\text{m}$ .

(A)



(B)



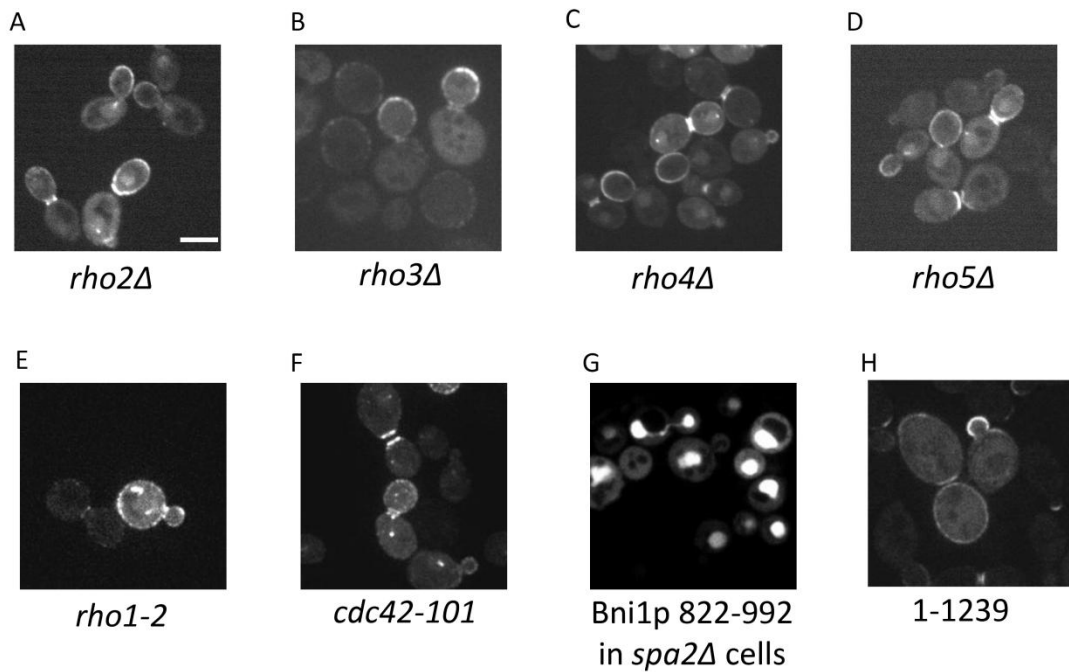
constructs were shown to also have a cytoplasmic spindle pole body (SPB) and spindle localization (Figure 2.2, Figure 2.4A and Table 2.3). This phenotype is most obvious in cells overexpressing constructs tagged with the leucine-zipper. In those cells, strong SPB and sometimes spindle staining could be observed. Since even full length Bni1p colocalizes with the SPB (Figure 2.4A), I wanted to know whether microtubules have any role in the regulation of Bni1p localization. One hypothesis would be that Bni1p is transported to the bud cortex and bud neck from the SPB through cytoplasmic microtubules. To test this, cells were treated with benomyl to disrupt microtubule structure. Tub1p-GFP was used to verify the disruption of microtubules. The disruption of microtubules did not affect Bni1p's bud cortex and neck localization (Figure 2.4B), indicating that microtubule transport is not the main mechanism to transport Bni1p to the growth site during budding. The localization of Bni1p on the SPB might suggest that Bni1p could be functioning inside or from the nucleus. This function may exist in a cell stage other than bud growth, such as sporulation, as indicated by formin *AgBnr2p* in *Ashbya gossypii* (Kemper et al., 2011). Since the Bni1p constructs used in this study were overexpressed, they may go to places where they do not normally localize during budding.

### **The effects of small GTPases on the localization of Bni1p**

Since the dimerized G domain of Bni1p could be localized to the bud cortex and bud neck, and small GTPases are the only known binding partners of the G domain, it is natural to think that small GTPases might have a role in the localization of Bni1p G domain. However, in *rho2Δ*, *rho3Δ*, *rho4Δ*, and *rho5Δ* cells, dimerized G domain localized to the bud cortex and the bud neck similarly to wildtype cells, suggesting

**Figure 2.5 Selected images of Bni1p overexpression constructs**

(A-F) The localization of GFP tagged Bni1p 1-347-LZ in different small GTPases mutant. (G) The localization of GFP tagged Bni1p 822-992 in *spa2Δ* cells. (H) The mother cortex localization of GFP tagged Bni1p 1-1239 in WT cells. Bni1p constructs are expressed under *GALI* promoter and induced with galactose for three to four hours. Scale bar: 2  $\mu$ m.



that either none of these non-essential small GTPases function in the G domain localization or that multiple small GTPases are sharing the localizing function (Figure 2.5A-D). For the two essential small GTPases Rho1p and Cdc42p, temperature sensitive strains were used and shifted to the restrictive temperature for 1 hr. In the *cdc42-101ts* mutant, the G domain localized to the bud cortex and bud neck, though the bud cortex localization was more diffuse (Figure 2.5F). In *rho1-2ts* cells, which have been suggested to have defects in the actin cytoskeleton (Helliwell et al., 1998), the bud neck localization was not affected; however, the bud cortex localization in small to medium budded cells was diminished, though not completely, and was sometimes observed on the mother cortex (Figure 2.5E).

### **Yeast two hybrid screen for peptides that binds the N-terminal region of Bni1p**

To identify proteins that interact with the N-terminal region of Bni1p and possibly function in localizing Bni1p, I performed a yeast two hybrid screen. Bni1 1-724aa, which covers the GBD-DID-DD domain, was used as the bait. A total of 408,000 diploids containing both bait and prey plasmids were screened and 189 candidates were discovered after restreaking. Sequencing of the candidates revealed 46 different genes. Proteins that showed yeast two hybrid interactions with Bni1p 1-724aa occur at a frequency of 1:2200. The candidates are shown in Table 2.4. Small GTPases which have shown yeast two hybrid interactions with Bni1p GBD in previous literature, such as Cdc42p, Rho1p and Rho3p (Evangelista et al., 1997; Kohno et al., 1996; Robinson et al., 1999), were not recovered in this screen. This could be explained by the fact that small GTPases are prenylated and bind to the membrane, which stops the proteins

**Table 2.4 Yeast two hybrid candidates with Bni1 1-724aa**

\* Yeast two hybrid (y2h) interactions were checked on SC-Leu-Trp-His, SC-Leu-Trp-His-Ade plates using growth assays. The number of “+” indicates how well the cells grew. “-” means no growth was observed. “/” means the dilution assay as not been performed

Candidate proteins	Times recovered from the screen	Related function	*Y2h with Bni1 1-724aa	*Y2h with Bni1 1-1239aa	*Y2h with Bnr1 1-758aa
Nip100p	2	component of dynactin complex	++	-	-
Sec15p	6	Exocyst component	+	-	-
Exo84p	1	Exocyst component	+	+	-
YAP1801p	8	Clathrin adaptor	++	+	-
Bzz1p	4	Actin patch component	+++	-	-
Atg17p	9	Scaffold for phagophore assembly site	+++	+	-
Nap1p	4	Binds cyclin and functions in budding, histone transport	+++	+	-
Sfh1	25	Chromatin remodel complex	+++	+	-
Mca1p	2	Homolog of caspase, may function in cell cycle progression	++	-	-
Slx5p	4	Subunit of the Slx5-Slx8 SUMO-targeted ubiquitin ligase complex	+++	++	-
Far7p	1	Functions in pheromone cell cycle release	/	/	/
Rsc8p	1	Chromatin remodel complex	/	/	/
Rrp9p	10	RNA splicing	/	/	/
Spp382p	9	RNA splicing	/	/	/
Prp19p	1	RNA splicing	/	/	/
Dsn1p	21	MIND kinetochore complex	/	/	/
Nsl1p	3	MIND kinetochore complex	/	/	/
Spc24p	1	MIND kinetochore complex	/	/	/
Spc25p	1	MIND kinetochore complex	/	/	/
YDR532Cp	7	Subunit of kinetochore-MT binding	/	/	/
Mcm16p	4	Kinetochore-MT mediated chromosome segregation	/	/	/
Bbp1p	1	SPB duplication	/	/	/
Rim20p	13	PH response	/	/	/
Ubp12p	1	ubiquitin hydrolase	/	/	/
Cdc23p	3	APC/C subunit, ubiquitin ligase	/	/	/

**Table 2.4 continued**

Candidate proteins (continued)	Times recovered from the screen	Related function	Y2h with Bni1 1-724aa	Y2h with Bni1 1-1239aa	Y2h with Bnr1 1-758aa
Oxr1p	1	oxidative damage resistance	/	/	/
Cyc8p	2	General transcriptional co-repressor	/	/	/
Hap5p	2	transcriptional activator	/	/	/
Ada2p	3	Transcription coactivator	/	/	/
Rrn6p	1	rDNA transcription factor complex	/	/	/
Skn7p	4	Nuclear response regulator and transcription factor	/	/	/
Ady3p	1	spore wall formation	/	/	/
Slx4p	3	endonuclease	/	/	/
Ade2p	2	Phosphoribosylaminoimidazole carboxylase	/	/	/
Pat1p	9	mRNA-decapping factor	/	/	/
Trm3p	1	methyltransferase	/	/	/
Sds3p	4	component of deacetylase complex	/	/	/
Iki3p	1	elongator component	/	/	/
Bfr2p	2	90s preribosome	/	/	/
Bfr1p	1	mRNP complex	/	/	/
Pex5p	1	peroxisomal	/	/	/
Mrp4p	1	mitochondria ribosomal protein	/	/	/
Rpb3p	1	RNA polymerase II	/	/	/
Ydr357p	1	unknown	/	/	/
Gds1p	1	unknown	/	/	/
retrotransposon	5		/	/	/

from going into the nucleus to induce the yeast two hybrid interactions.

Among the candidates identified, several of them are related to polarity, such as the dynactin component Nip100p, actin patch component Bzz1p and clathrin adaptor YAP1801p (Table 2.4). One category is of great interest: the exocyst components Sec15p and Exo84p. The exocyst is an eight-subunit protein complex required for efficient vesicle fusion with the plasma membrane (Guo et al., 1999a; TerBush et al., 1996). It is composed of Sec3p, Sec5p, Sec6p, Sec8p, Sec10p, Sec15p, Exo70p, and Exo84p. The exocyst docks vesicles at the plasma membrane before fusion (Guo et al., 1999b). Two of the exocyst subunits, Sec3p and some Exo70p, localize to the plasma membrane by interacting with Rho family GTPases (Guo et al., 2001; Wu et al., 2010; Zhang et al., 2001). The remaining exocyst subunits are associated with secretory vesicles transported by Myo2p along actin cables to growth sites, with the Rab GTPase Sec4p (Guo et al., 1999b). Assembly of the complete exocyst by interaction of the plasma membrane-associated and vesicle-associated subunits tethers the vesicle to the plasma membrane and is necessary for subsequent vesicle fusion (Guo et al., 1999b; TerBush et al., 1996). The fact that two of the exocyst components were recovered from the yeast two hybrid screen suggests the interaction between the exocyst and Bni1p.

### *Discussion and future directions*

#### **Three localization domains in the Bni1p N-terminal region**

Formins are essential proteins that regulate actin dynamics. How formin proteins nucleate and elongate actin cables has been well studied (see general introduction). However, how exactly formins are regulated to assemble actin cables at the right time

and right place is largely unknown. In this study, I expressed different N-terminal regions and used live cell imaging to study the localization signals of the budding yeast formin Bni1p. Previously, our lab found that the other budding yeast formin Bnr1p, which stays at the bud neck, has two independent localization domains, L1 (1-466aa) and L2 (466-733aa) (Gao et al., 2010). Here, three localization domains were identified in the N-terminal region of Bni1p that lie before the functional FH1 and FH2 domains. The first is the 1-333aa region which is part of GBD that does not overlap with DID, also called the G domain. This region by itself does not localize to the bud cortex and has very weak bud neck localization. However, when a leucine-zipper from human CREB is added to artificially dimerize the G domain, the G domain then localized to the bud cortex and bud neck clearly and at the right cell cycle stage. This localization is most likely through binding to small GTPases. The second localization region is 334-834aa, which covers the DID-DD-CC domain. How this region is localized is of great interest. No clear binding partners have been identified for this region except Bni1p C-terminal DAD region, but 334-834aa still localizes well in *bni1Δ* cells indicating its localization is not through binding to endogenous Bni1p. The third localization region is 822-992aa, which is the SBD. This region binds to Spa2p and Spa2p has been implicated in localizing Bni1p previously (Fujiwara et al., 1998; Sheu et al., 1998). Indeed, 822-992aa is no longer localized at the bud cortex and neck in *spa2Δ* cells (Figure 2.5G).

The fact that Bni1p 1-333aa needs to be dimerized to be localized to the correct place fits into the autoinhibition model of Bni1p. When the N-terminal DID domain binds to the C-terminal DAD domain, Bni1p exists in the inactive autoinhibited state.

When the interaction between DAD and DID is disrupted, both C-terminal and N-terminal regions are released, thus activating both ends of the protein. The C-terminal FH2 domain needs to homodimerize to assemble actin cables, while the N-terminal region need to dimerize to localize to the right place in the cell. It would be interesting to know exactly what protein(s) release the autoinhibition and bind(s) to Bni1p N-terminal region to localize it.

When some of the GFP tagged Bni1p constructs were overexpressed, GFP was observed at the mother cortex as well, *eg.* Bni1p 1-1239aa, Bni1p 1-834aa (Table 2.3, Figure 2.5H), which was never seen for the full length Bni1p. The mother cortex localization only happens in large budded cells. This again suggests that additional factors are needed to restrict Bni1p to the tip of bud, and there might be diffusion barriers between mother and cortex, *e.g.* septins, to restrict the polarized growth only in the buds.

### **The role of small GTPases on the localization of Bni1p**

It has been suggested that small GTPases functions in the regulation of formin proteins in budding yeast (see introduction). The localization of the dimerized G-domain, which is the presumptive GTPases binding domain, was thus examined in Rho GTPases mutants. Surprisingly, none of the small GTPases mutants had defects in the localization of the dimerized G-domain at the bud neck, suggesting that the localization of Bni1p to the bud neck could be through binding to other factors. Single deletion of the non-essential Rho proteins did not affect the bud cortex localization. The temperature sensitive mutants of Rho1p and Cdc42p on the other hand had a diffuse distribution of the G-domain at the bud cortex, with *rho1-2* even having

mother cortex localization. This suggests that Rho1p and Cdc42p are playing some role in the localization of dimerized G-domain. However, since both Rho1p and Cdc42p had been suggested to function in multiple aspects of cell polarity, this disruption on the Bni1p could be indirect.

### **Yeast Two hybrid screen**

With the identification of three localization domains in the N-terminal region of Bni1p, the next question would be to explore how these domains are localized individually. To address this, a yeast two hybrid screen was carried out. An interesting category of candidates are the exocyst components. One hypothesis for the interactions between Bni1p and exocyst is that Bni1p could interact with exocyst at the growth site, where the exocyst mediates the fusion of secretory vesicles with the plasma membrane. Since secretory vesicles are transported by actin cables to the bud growth site which is nucleated by Bni1p, the interaction of Bni1p with the exocyst might help with the docking of secretory vesicles before the associated exocyst components interact with membrane-bound components. To test this hypothesis, interactions between the exocyst components and Bni1p need to be confirmed with biochemical assays such as pull downs and immunoprecipitations. This step could be difficult due to the possible transient interaction between Bni1p with exocyst components. Specific Bni1p mutants that only disrupt the interactions with exocyst complex would need to be isolated. Phenotypes of exocytosis and exocyst components would need to be observed to study whether disrupting the interaction between the exocyst and Bni1p would have any effect on exocyst function.

Another hypothesis would be that the exocyst functions in a feedback loop of

Bni1p, helping carry Bni1p back to the bud tip/cortex. Retrograde transport of Bni1p has been observed along actin cables (Buttery et al., 2007), however the movement of Bni1p towards the bud tip/cortex has not been directly observed. This hypothesis could be easily tested by observing Bni1p-3GFP or Bni1p 1-717-3GFP in an exocyst component temperature-sensitive mutant at the restrictive temperature.

Future experiments will be needed to test the interactions between the exocyst components and Bni1p, and how their interactions are regulated.

## CHAPTER 3

### **Bni1p constructs lacking the N-terminal localization domains compromise growth and spindle orientation**

#### *Abstract*

In Chapter 2, I have shown that the N-terminal region of Bni1p has multiple localization regions. Here I explore the phenotypes of cells in which endogenous *BNII* has been replaced to express five different N-terminal Bni1p truncations. Based on their growth phenotypes, I divided them into two classes: Class I truncations have deletions from amino acid residue 79 up to 821, and class II truncations have deletions from residue 79 up to 1230. Class I mutants have little effects on growth or the actin cytoskeleton, or in combination with *arp1Δ*. However, Class II deletions grow slower than *bni1Δ* cells, have a defect in nuclear segregation at low temperature, and are synthetically lethal with *arp1Δ* indicating a defect in spindle orientation, and have a dominant phenotype. All the effects of Class II mutants can be abrogated by an additional mutation eliminating their actin nucleating activity. Moreover, a class II mutant can be suppressed by appending a CRIB domain to restore its polarized distribution. Thus, Class II mutants cause a dominant effect by mislocalized assembly of actin filaments. Since Class I mutants, but not Class II mutants, contain Bni1p's Spa2p Binding Domain (SBD), it is likely that loss of binding to Spa2p is responsible for the different properties of Class I and Class II mutants. Class I cells grew more poorly when combined with *spa2Δ*, and surprisingly, Class II mutants were lethal in combination with *spa2Δ*. Thus, Spa2p appears to play a role in localizing Bni1p, but *spa2Δ*'s lethality with Class II mutants reveals it has an additional function

independent of its ability to bind the SBD of Bni1p.

### ***Introduction***

Since the N-terminal region of Bni1p has been suggested to be important for the regulation and localization of Bni1p, I chose to study the phenotypes of Bni1p truncations that lack defined regions of the N-terminal domain. Around this time, a PhD student in our lab, Lina Gao, found that yeast cells lacking localized formins are still viable. To study the regulation of formin localization, I sought to find a situation in which the localized formin is needed for viability.

In budding yeast, Bni1p has been suggested to function in nuclear movement and spindle orientation. Unlike mammalian cells, the nuclear envelope in budding yeast does not break down during mitosis. Microtubule organizing centers, called spindle pole bodies, are embedded in the nuclear envelope and the spindles form inside the nucleus while cytoplasmic microtubules radiate from SPBs (Figure 1.1). Nuclear positioning is ensured by two redundant pathways. The Kar9p/Myo2p/actin pathway acts early during bud formation. Myo2p guides the cytoplasmic microtubule orientation by transporting Kar9p which in turn binds to the microtubule plus ends localizing protein Bim1p (Beach et al., 2000; Hwang et al., 2003; Segal and Bloom, 2001; Yin et al., 2000). The asymmetric distribution of Kar9p ensures that one spindle pole body is positioned to the bud neck and aligns the spindle along the mother–bud axis (Kusch et al., 2002; Liakopoulos et al., 2003; Moore and Miller, 2007). This step is actin and Bni1p dependent as Myo2p walks along actin cables and *bni1* mutants, but not *bnr1* mutants, have been shown to have nuclear movement and microtubule orientation defects (Fujiwara et al., 1999; Kusch et al., 2002; Lee et al., 1999;

Theesfeld et al., 1999). The second pathway functions later in the cell cycle, upon the onset of anaphase, and depends on the function of the minus end directed microtubule motor dynein protein and dynactin complex (Adames and Cooper, 2000; Yeh et al., 2000). These dynein/dynactin dependent movements are mediated by microtubule sliding along the bud (Adames and Cooper, 2000). Although disruption of either the Kar9p/Myo2p/actin or the dynein pathway is viable, disruption of both pathways is lethal (Fujiwara et al., 1999; Miller et al., 1999; Tong et al., 2001).

In this chapter, I describe studies on a series of Bni1p N-terminal truncations which all retain the FH1 domain to the C-terminus. I found that these Bni1p truncations are mislocalized and result in misoriented actin cables, which leads to defects in nuclear movements. The implications of these results are discussed below.

### ***Materials and methods***

#### **Yeast strains and molecular biology techniques**

Strains used in this study are listed in Table 3.1. All strains were generated in the S288C strain background coming from the deletion consortium (Brachmann et al., 1998). Standard media and techniques for growing and transforming yeast were used (Sherman, 1991). To make benomyl plates, benomyl stock need to be added to the boiling and sterilized yeast media before it gets cooled down. Plasmids used in this study are listed in Table 3.2. Figure 3.1A shows the scheme for the integration plasmid used to make the Bni1p truncation mutants. Figure 3.1B shows the scheme for the integration plasmids used to label endogenous Bni1p with 3GFP. Growth assays were performed using 1:10 dilutions.

**Table 3.1 Yeast strains used in Chapter 3**

Strain	Genotype	Source
ABY1848	MATa/α <i>his3Δ1/his3Δ1 leu2Δ0/leu2Δ0 ura3Δ0/ura3Δ0 met15Δ0/MET15 lys2Δ0/LYS2</i>	(Evangelista et al., 2002)
ABY1801	MAT a/α <i>his3Δ1/his3Δ1 leu2Δ0/leu2Δ0 met15<sup>?</sup>/met15<sup>?</sup> lys2<sup>?</sup>/lys2<sup>?</sup> ura3Δ0/ura3Δ0 bnr1Δ::KanR/ bnr1Δ::KanR</i>	(Gao et al., 2010)
ABY2856	MATa <i>his3Δ1 leu2Δ0 ura3Δ0 met15Δ0 bni1Δ79-343::LEU2</i>	This study
ABY2857	MATa <i>his3Δ1 leu2Δ0 ura3Δ0 met15Δ0 bni1Δ79-574::LEU2</i>	This study
ABY2858	MATa <i>his3Δ1 leu2Δ0 ura3Δ0 met15Δ0 bni1Δ79-821::LEU2</i>	This study
ABY2859	MATa <i>his3Δ1 leu2Δ0 ura3Δ0 met15Δ0 bni1Δ79-988::LEU2</i>	This study
ABY2854	MATa <i>his3Δ1 leu2Δ0 ura3Δ0 met15Δ0 bni1Δ79-1230::LEU2</i>	This study
ABY2887	MATa <i>his3Δ1 leu2Δ0 ura3Δ0 met15<sup>?</sup> lys2<sup>?</sup> bnr1Δ::Kan<sup>R</sup> bni1Δ79-343::LEU2</i>	This study
ABY2888	MATa <i>his3Δ1 leu2Δ0 ura3Δ0 met15<sup>?</sup> lys2<sup>?</sup> bnr1Δ::Kan<sup>R</sup> bni1Δ79-574::LEU2</i>	This study
ABY2889	MATa <i>his3Δ1 leu2Δ0 ura3Δ0 met15<sup>?</sup> lys2<sup>?</sup> bnr1Δ::Kan<sup>R</sup> bni1Δ79-821::LEU2</i>	This study
ABY2890	MATa <i>his3Δ1 leu2Δ0 ura3Δ0 met15<sup>?</sup> lys2<sup>?</sup> bnr1Δ::Kan<sup>R</sup> bni1Δ79-988::LEU2</i>	This study
ABY2891	MATa <i>his3Δ1 leu2Δ0 ura3Δ0 met15<sup>?</sup> lys2<sup>?</sup> bnr1Δ::Kan<sup>R</sup> bni1Δ79-1230::LEU2</i>	This study
ABY3090	MATa/α <i>his3Δ1/his3Δ1 leu2Δ0/leu2Δ0 ura3Δ0/ura3Δ0 met15Δ0/MET15 lys2Δ0/LYS2 BNI1/BNI1-3GFP</i>	This study
ABY3092	MAT a/α <i>his3Δ1/his3Δ1 leu2Δ0/leu2Δ0 met15<sup>?</sup>/met15<sup>?</sup> lys2<sup>?</sup>/lys2<sup>?</sup> ura3Δ0/ura3Δ0 bni1Δ79-343::LEU2/ bni1Δ79-343-3GFP::LEU2, URA3</i>	This study
ABY3093	MAT a/α <i>his3Δ1/his3Δ1 leu2Δ0/leu2Δ0 met15<sup>?</sup>/met15<sup>?</sup> lys2<sup>?</sup>/lys2<sup>?</sup> ura3Δ0/ura3Δ0 bni1Δ79-574::LEU2/ bni1Δ79-574-3GFP::LEU2, URA3</i>	This study
ABY3094	MAT a/α <i>his3Δ1/his3Δ1 leu2Δ0/leu2Δ0 met15<sup>?</sup>/met15<sup>?</sup> lys2<sup>?</sup>/lys2<sup>?</sup> ura3Δ0/ura3Δ0 bni1Δ79-821::LEU2/ bni1Δ79-821-3GFP::LEU2, URA3</i>	This study

**Table 3.1 continued**

Strain (cont'd)	Genotype	Source
ABY3095	MAT a/α <i>his3Δ1/his3Δ1 leu2Δ0/leu2Δ0 met15?/met15? lys2?/lys2? ura3Δ0/ura3Δ0 bni1Δ79-988::LEU2/bni1Δ79-988-3GFP::LEU2, URA3</i>	This study
ABY3096	MAT a/α <i>his3Δ1/his3Δ1 leu2Δ0/leu2Δ0 met15?/met15? lys2?/lys2? ura3Δ0/ura3Δ0 bni1Δ79-1230::LEU2/bni1Δ79-1230-3GFP::LEU2, URA3</i>	This study
ABY3283	MATa <i>his3Δ1 leu2Δ0 ura3Δ0 met15? lys2? spa2Δ::KanR bni1Δ79-343-3GFP::LEU2,URA3</i>	This study
ABY3284	MATa <i>his3Δ1 leu2Δ0 ura3Δ0 met15? lys2? spa2Δ::KanR bni1Δ79-574-3GFP::LEU2,URA3</i>	This study
ABY3285	MATa <i>his3Δ1 leu2Δ0 ura3Δ0 met15? lys2? spa2Δ::KanR bni1Δ79-821-3GFP::LEU2,URA3</i>	This study
ABY2851	MATa/α <i>his3Δ1/his3Δ1 leu2Δ0/leu2Δ0 ura3Δ0/ura3Δ0 met15Δ0/met15Δ0 arp1Δ::Kan<sup>R</sup>/arp1Δ::Kan<sup>R</sup> BNI1/bni1Δ79-988::LEU2</i>	This study
ABY2852	MATa/α <i>his3Δ1/his3Δ1 leu2Δ0/leu2Δ0 ura3Δ0/ura3Δ0 met15Δ0/met15Δ0 arp1Δ::Kan<sup>R</sup>/arp1Δ::Kan<sup>R</sup> BNI1/bni1Δ79-1230::LEU2</i>	This study
ABY2860	MAT? <i>his3Δ1 leu2Δ0 ura3Δ0 met15Δ0 arp1Δ::Kan<sup>R</sup> bni1Δ79-343::LEU2</i>	This study
ABY2861	MAT? <i>his3Δ1 leu2Δ0 ura3Δ0 met15Δ0 arp1Δ::Kan<sup>R</sup> bni1Δ79-574::LEU2</i>	This study
ABY2862	MAT? <i>his3Δ1 leu2Δ0 ura3Δ0 met15Δ0 arp1Δ::Kan<sup>R</sup> bni1Δ79-821::LEU2</i>	This study
ABY2881	MATa/α <i>his3Δ1/his3Δ1 leu2Δ0/leu2Δ0 ura3Δ0/ura3Δ0 met15Δ0/met15Δ0 arp1Δ::Kan<sup>R</sup>/arp1Δ::Kan<sup>R</sup> BNI1/bni1Δ79-988 I1431A::LEU2</i>	This study
ABY3007	MATa/α <i>his3Δ1/his3Δ1 leu2Δ0/leu2Δ0 ura3Δ0/ura3Δ0 met15Δ0/met15Δ0 CRIB-bni1Δ79-988::LEU2/CRIB-bni1Δ79-988::LEU2</i>	This study
ABY2897	MATa/α <i>his3Δ1/his3Δ1 leu2Δ0/leu2Δ0 ura3Δ0/ura3Δ0 met15Δ0/met15Δ0 bni1Δ79-988::LEU2/bni1Δ79-988::LEU2</i>	This study

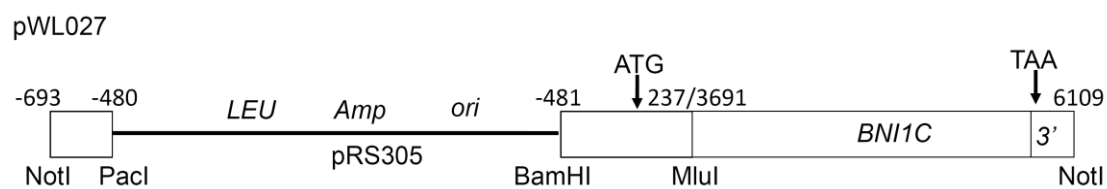
**Table 3.2 Plasmids used in Chapter 3**

Plasmid	Backbone	Genotype
pWL031	pRS305	$P_{BNI1}$ - <i>BNI1</i> (1-79)- <i>BNI1</i> (344-1953)
pWL032	pRS305	$P_{BNI1}$ - <i>BNI1</i> (1-79)- <i>BNI1</i> (575-1953)
pWL033	pRS305	$P_{BNI1}$ - <i>BNI1</i> (1-79)- <i>BNI1</i> (822-1953)
pWL034	pRS305	$P_{BNI1}$ - <i>BNI1</i> (1-79)- <i>BNI1</i> (989-1953)
pWL027	pRS305	$P_{BNI1}$ - <i>BNI1</i> (1-79)- <i>BNI1</i> (1231-1953)
pWL085	pRS306	<i>BNI1C-3GFP-BNI13'</i>
pWL046	pRS305	$P_{BNI1}$ - <i>BNI1</i> (1-79)- <i>BNI1</i> (989-1953 II431A)
pWL069	pRS305	$P_{BNI1}$ - <i>BNI1</i> (1-79)- <i>CRIB-BNI1</i> (989-1953)

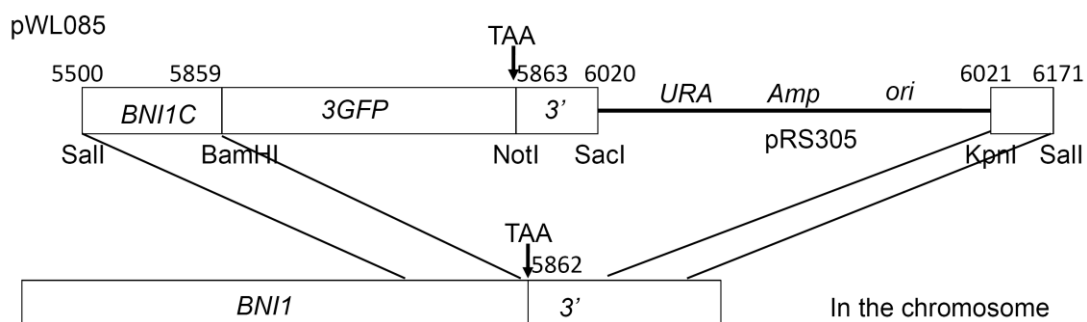
**Figure 3.1 Scheme of constructs**

(A) Map of *BNI1* truncation integration plasmid pWL027. All the *BNI1* truncation integration plasmids follow the same scheme. (B) Map of plasmid pWL085 and its integration site to label endogenous *Bni1p* with 3GFP. Schemes of constructs are numbered in nucleotides.

(A)



(B)



## **Microscopy**

Live cells were placed under 2% agarose in synthetic medium, with appropriate amino acid. Images were acquired with a spinning disc confocal microscopy system (3I Corp) using a DMI 6000B microscope (Leica) and a digital camera (QuantEM; Photometrics). Images were then further analyzed and adjusted using Slidebook 5.

The following protocol was followed for visualization of actin structure: 5 ml of cells were grown to mid-log phase and formaldehyde was added to 3.7% final concentration for fixation for 30 min ~1 hr. Cells were washed three times with PBS and treated with 0.2% Triton X-100 for 15 min. The cells were washed and incubated with 100  $\mu$ l PBS + 3  $\mu$ l Alexa568-phalloidin for 1 hr. After final washes, the cells were ready to be looked at under the microscope. When washing the cells, the centrifugation speed should be kept low to keep the actin structures intact. I used a tabletop centrifuge at 5000 rpm for 1 min. To disrupt actin structures, cells were treated with 200  $\mu$ M Latrunculin A for 10 min. Phalloidin staining was used to verify the disruption of actin structures.

## **Protein extracts and immunoblotting**

Cells were grown to log phase and chilled on ice, washed with ice-cold water and then resuspended in 200  $\mu$ L protein extraction buffer containing 20 mM Tris-HCl pH 7.4, 0.2 mM EDTA, 0.1 M NaCl, 1 mM DTT, and 5% yeast protease inhibitors cocktail in DMSO (Sigma). Roughly 100 $\mu$ L of glass beads (Sigma) were added and the tubes were vortexed for 1 min 3 times with 1 min incubation on ice between each vortex. The samples were centrifuged for 5 min at max speed to remove the cell wall and other membranes. Samples were resolved by SDS-PAGE, transferred into a PVDF

membrane (Immobilon, MILLIPORE), and the relevant protein detected by ECL Western blotting using antibodies against GFP (Santa Cruz) at 1:200.

### ***Results***

#### **The C-terminal domain of Bni1p contains a fourth localization domain**

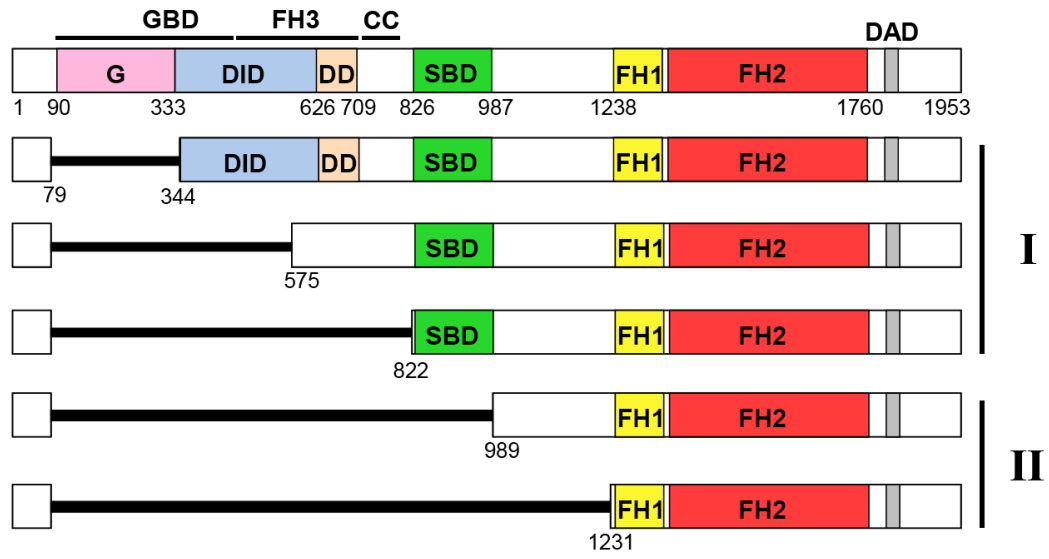
To explore how important the localization domains are for growth, I made a series of constructs deleting progressively larger internal regions of Bni1p from residue 79aa up to the FH1 domain (Figure 3.2A). These constructs were targeted to the chromosomal locus so that the proteins were expressed from the endogenous *BNII* promoter and their expression was examined as in Figure 3.2C. All the constructs were viable and were not affected by the simultaneous deletion of *BNRI* (Figure 3.2B); thereby, confirming our lab's previous result that expression of just the FH1-FH2-COOH region of either formin is sufficient for viability (Gao and Bretscher, 2009). For ease of description, I have grouped the internal deletion series into two classes according to their growth: Class I deletions have no effect on the growth of cells, whereas Class II comprise the two largest internal deletions, *bni1Δ79-988-3GFP* and *bni1Δ79-1230-3GFP*, which grew less well and were both cold-sensitive and temperature sensitive in both *BNRI* and *bnr1Δ* backgrounds (Figure 3.8 and Table 3.3). In fact, Class II internal deletions grew less well than *bni1Δ* cells, a point I will discuss later.

I next examined the actin cytoskeleton and the localization of the Bni1p-derived constructs tagged with 3GFP in cells. Phalloidin staining of Class I *BNII* deletion mutants have a modest disruption of their actin cytoskeleton, which becomes more noticeable with increasing size of the internal deletion. In *bni1-Δ79-821-3GFP* cells,

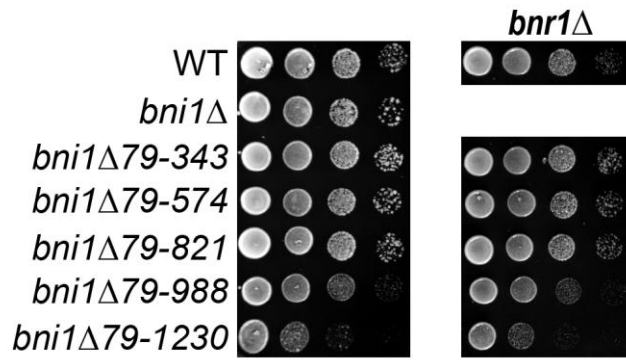
**Figure 3.2 Two classes of Bni1p N-terminal truncations**

(A) Schemes of *BNI1* truncation constructs regarding to full length *BNI1*. Numbers indicate nucleotides. (B) Growth assays of *bni1* truncations in *BNR1* and *bnr1Δ* at 26 °C on YPD plates. (C) Western blot with antibodies against GFP to show expression of the indicated Bni1p constructs.

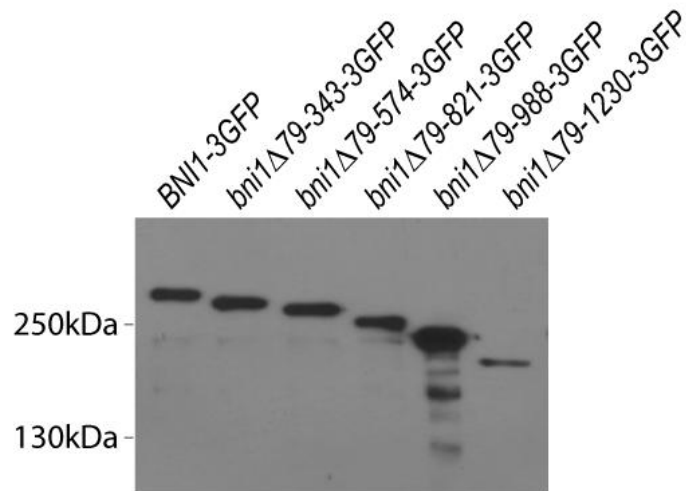
(A)



(B)



(C)



although the actin patches are somewhat polarized, more disoriented actin cables are observed, especially in the mother cells. In contrast, in the Class II *BNI1* mutants, actin cables were obviously shorter and disoriented, and actin patches were depolarized. Class I *BNI1* mutants localized very similarly to wild type Bni1p-3GFP, concentrating at the nascent bud site, tips of small buds, a crescent over the cortex of medium buds, and at the septal planes between dividing cells (Figure 3.3). Despite this general similarity, the localization of *bni1Δ79-821-3GFP* was less robust than the other Class I mutants. The localization of the Class II *BNI1* mutants was much weaker, only being seen in a polarized manner in unbudded and tiny budded cells. This suggests that a fourth localization domain exists in the C-terminal region of Bni1p, which might only function in the early stage of the cell cycle.

Since the constructs expressing just the FH1-FH2-C-terminus of Bni1p are localized at the beginning of the cell cycle, a localization determinant must exist in this region. Thus, in addition to the three N-terminal localization regions described in Chapter 2, Bni1p has a fourth F-actin-independent localization region in the FH1-FH2-C-terminal part of Bni1p.

### **Spa2p has an additional function in addition to binding the SBD of Bni1p**

The major difference between the Class I and Class II internal deletion series of Bni1p is the presence of the Spa2p binding domain (SBD). If Spa2p is a major determinant of Bni1p localization, one would predict that combining *spa2Δ* with Class I *BNI1* mutants should phenocopy a Class II mutant. Indeed, combining Class I mutants with *spa2Δ* compromised the growth of the cells in a progressive manner with the larger deletions being more affected (Figure 3.4A). To explore the basis for these

**Figure 3.3 Phalloidin staining and live GFP image of *bni1ΔNp-3GFP* strains**

Experiments were performed at room temperature as in Methods and Material. Scale bar: 5  $\mu\text{m}$ .

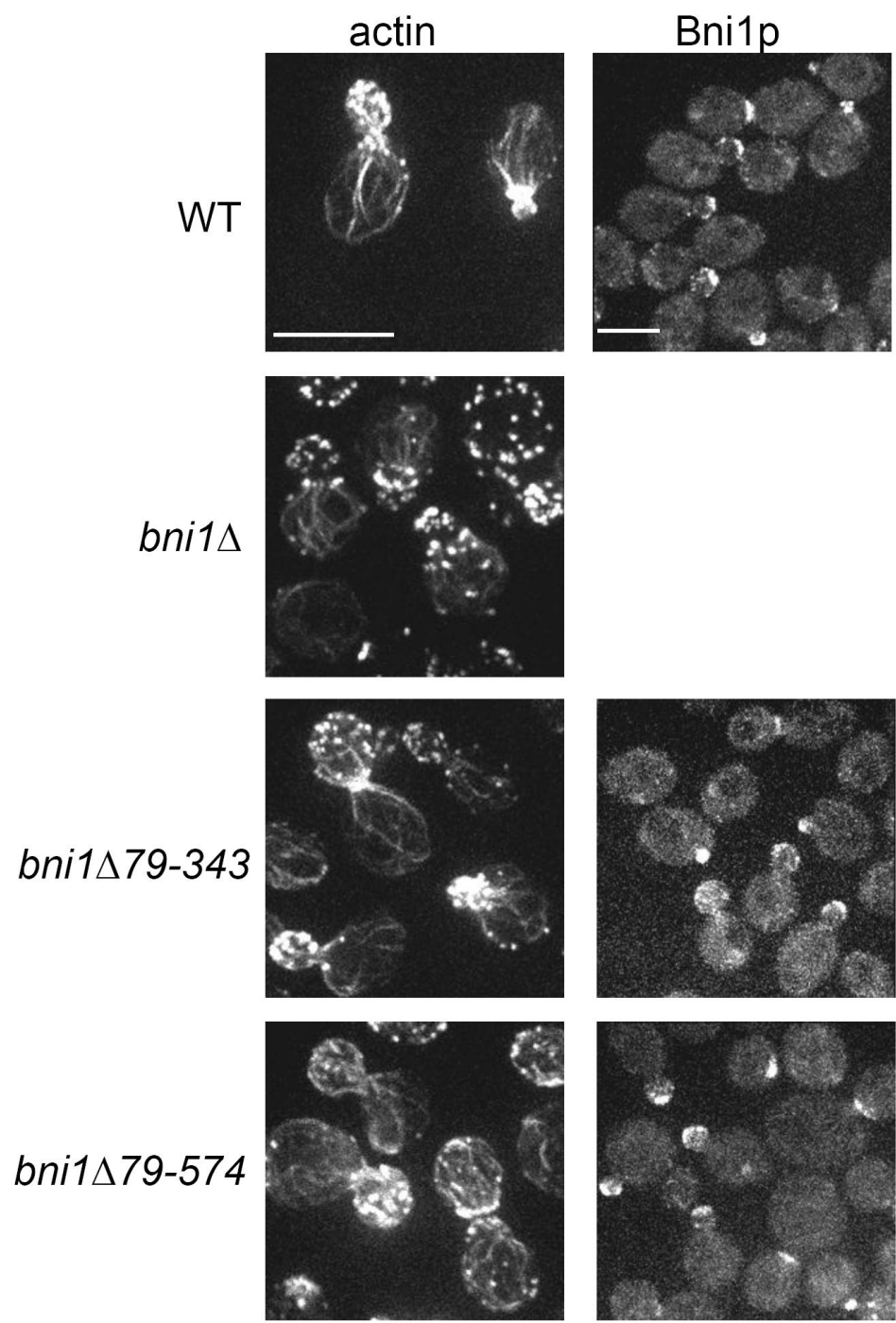


**Figure 3.3 Phalloidin staining and live GFP image of *bni1*ΔNp-3GFP strains**

**(continued)**

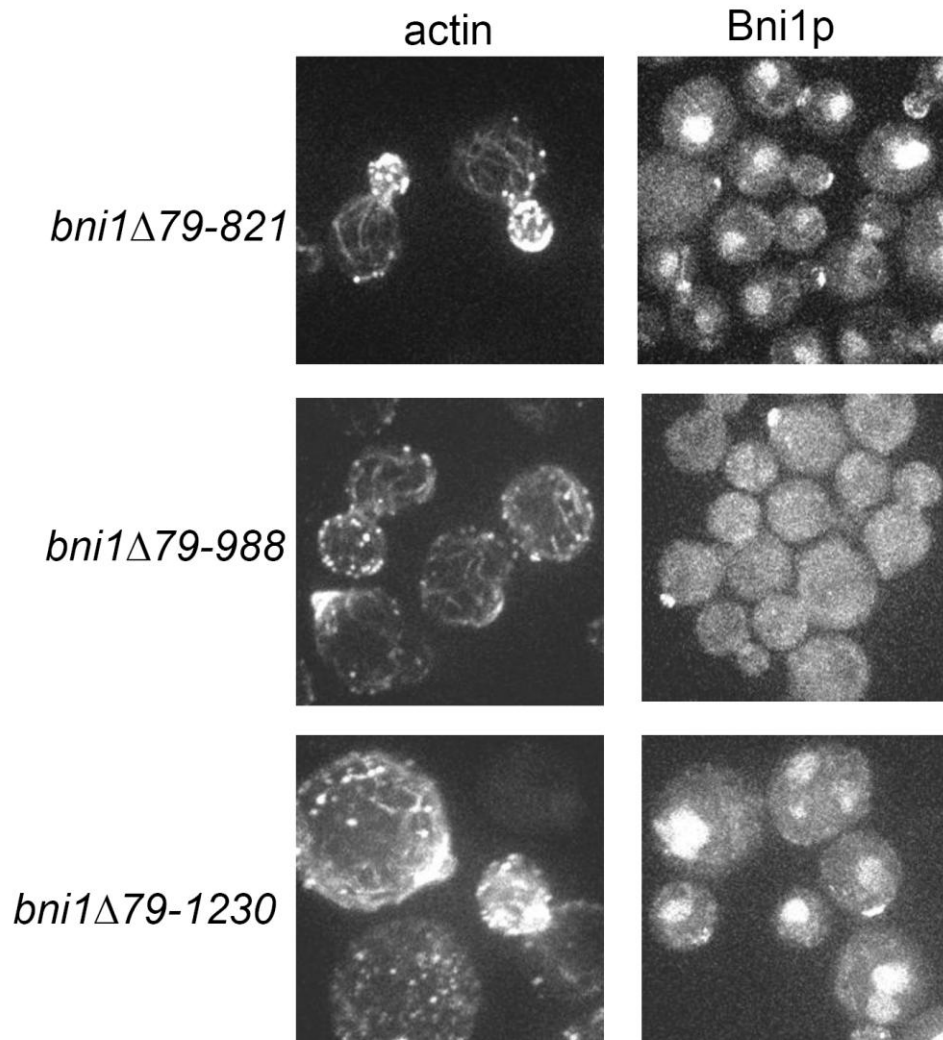
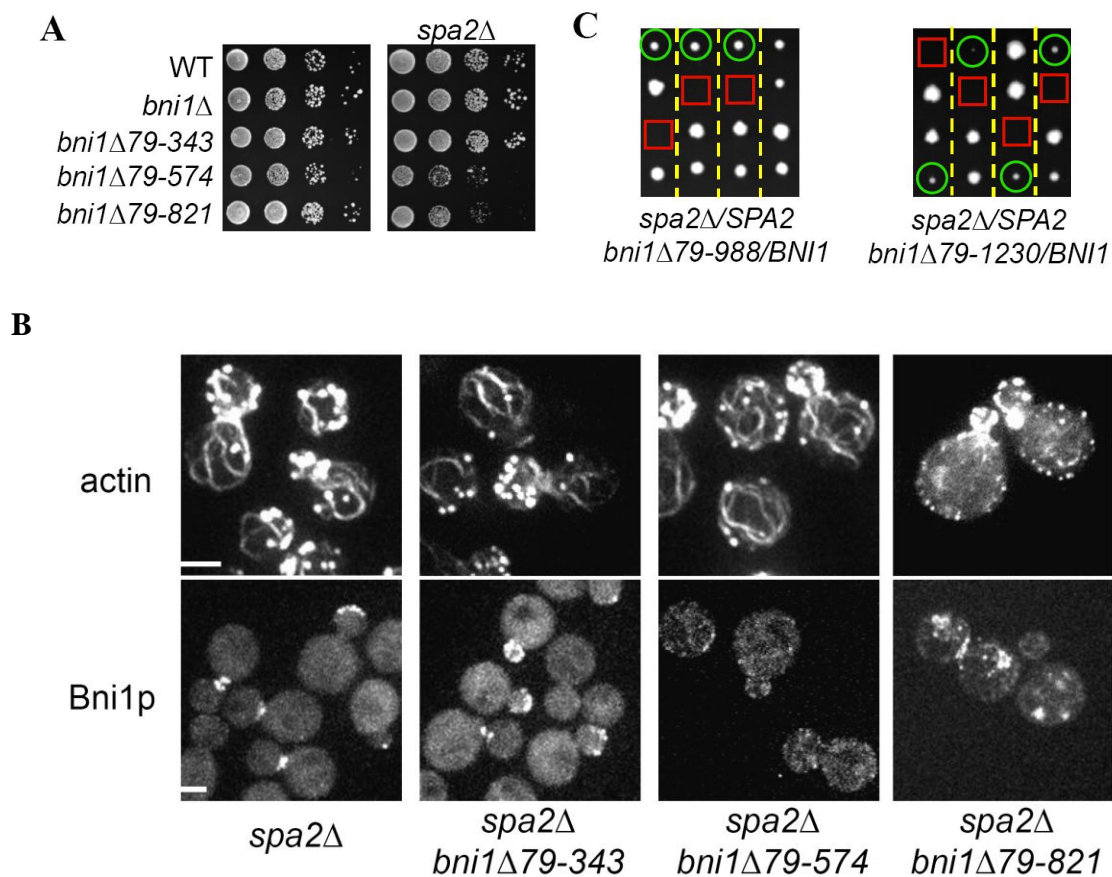


**Figure 3.4 Phenotypes of *bni1ΔN* in *spa2Δ* background**

(A) Growth assays of Class I Bni1p truncations with or without Spa2p at 26 °C on YPD plates. (B) Phalloidin staining and live GFP image of Class I Bni1p truncation in *spa2Δ* background. Scale bar: 5 μm. (C) Sporulation and dissection plate of heterozygous Class II *bni1Δ79-1230/BNI1 spa2Δ/SPA2* strains. Circle indicates *bni1Δ79-1230 SPA2* spores; rectangular indicates *bni1Δ79-1230 spa2Δ* spores. The spores from the same tetrad are shown in one column.



growth defects, I looked at actin structure and localization of the Bni1p-3GFP truncated proteins. When *spa2Δ* was combined with the Class I mutants, actin structures are more disrupted especially in *bni1Δ79-821 spa2Δ* cells, which had greatly reduced cables and depolarized actin patches. The localization of the Bni1p-deletion constructs was also affected, with the larger deletions being the most severe (Figure 3.4B).

I next examined the effect of combining *spa2Δ* with the Class II *BNI1* deletion mutants, which lack Bni1p's Spa2 binding domain, and found that they showed synthetic lethality (Figure 3.4C). Thus, although the SBD is not present in these Bni1p constructs, Spa2p is essential for the viability of these cells, indicating that Spa2p has an important function independent of its interaction with the SBD of Bni1p.

#### **The N-terminal region of Bni1p is essential for spindle orientation**

Bni1p has been suggested to function in the Kar9p/Myo2p/actin pathway for nuclear movement and spindle orientation, in parallel with the dynein and dynactin pathway. Disruption of either pathway is viable, but disruption of both pathways is lethal (Fujiwara et al., 1999; Miller et al., 1999; Tong et al., 2001). As Arp1p is a core component of the dynactin complex, disruption of *ARPI* will lead to the disassembly of the dynactin complex (Schroer, 2004), leaving actin cables as the only mechanism to direct spindle orientation and transport of one nucleus into the bud. I therefore set out to exploit the phenotypes of Bni1p truncations in *arp1Δ* cell that lacks a functional dynein/dynactin pathway, in the hope that this would be the more stringent condition for cell growth that will make the regulation of Bni1p essential.

When I combined *bni1Δ* with *arp1Δ* I was surprised to find that a *bni1Δ arp1Δ*

strain is viable, thereby in principle contradicts with the design of this study. However, this result is also observed by others (Lee et al., 1999; Yeh et al., 2000), suggesting this is due to strain background differences. Fortuitously, when I combined *arp1Δ* with the Class I and Class II series of internal truncations in Bni1p, there was a clear finding: Class I truncations are viable in conjunction with *arp1Δ*, and Class II are inviable in conjunction with *arp1Δ* (Figure 3.5).

To explore in more detail the potential role of the Bni1p localization determinants in spindle orientation and nuclear segregation, I examined the Class I mutants in more detail in both *ARPI* and *arp1Δ* cells. Since these processes require microtubules, which are less stable at low temperature, I examined the sensitivity of the strains for growth at 14 °C and in the presence of sub-lethal levels of the microtubule-destabilizing drug benomyl (Figure 3.6A). Class I mutants and *bni1Δ ARPI* cells showed no cold or benomyl sensitivity. However, in the *arp1Δ* background, *bni1Δ79-821* of Class I truncation is cold sensitive and benomyl sensitive, behaving similarly to *bni1Δ* (Figure 3.6A). This suggests that Class I truncations are defective in microtubule mediated spindle orientation. DAPI staining of Class I truncations to identify cells with more than one nucleus (Figure 3.6B) further confirmed that they have a deficiency in nuclear movement at 16 °C and this deficiency was exaggerated by *arp1Δ*.

Consistent with their synthetic lethality with *arp1Δ*, Class II truncations are cold sensitive and benomyl sensitive by themselves (Figure 3.7A), displaying more severe microtubule related defects. Heterozygous Class II mutants also exhibited cold sensitivity and benomyl sensitivity, suggesting that the truncation mutants are

**Figure 3.5 Growth assay of *bni1*ΔNp in an *arp1*Δ background with or without *ARP1* on a *CEN-URA3* plasmid**

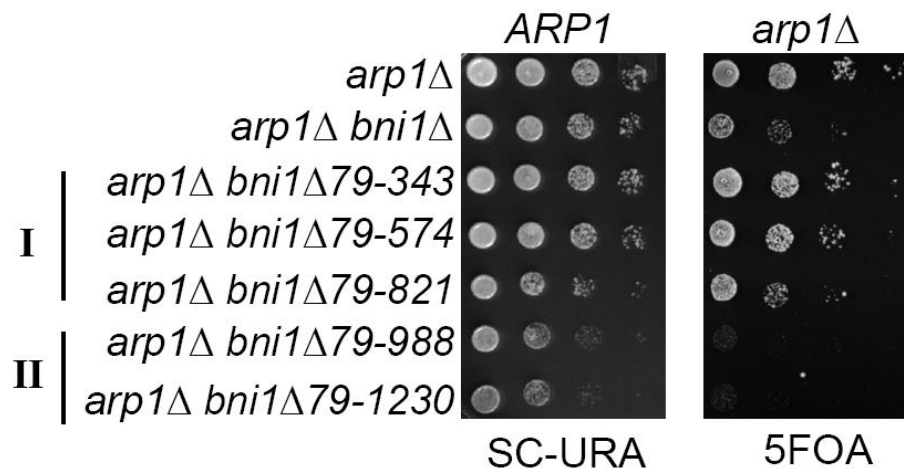


### **Table 3.3 Phenotypes of Bni1p truncations in different backgrounds**

\* Growth was tested using growth assays. WT: the growth is similar to wild type cells.  
c: cold sensitive, performed at 14 °C on YPD plates; t: temperature sensitive, performed at 37 °C on YPD plates; s: sick at 26 °C on YPD plates. The number of letter “c” “t” “s” shows how severe the phenotype is. # b: benomyl sensitive, performed on 10 µg/ml benomyl plates at 26 °C; The number of letter “b” shows how severe the sensitivity is.

Strain background	Bni1p	Growth*	Benomyl sensitivity #	Strain background	Bni1p	Growth	Benomyl sensitivity
Haploid WT	<i>BNI1::LEU2</i>	WT	WT	Haploid <i>arp1Δ</i>	<i>BNI1::LEU2</i>	WT	b
	<i>bni1Δ::LEU2</i>	WT	WT		<i>bni1Δ::LEU2</i>	cc;tt	bb
	<i>bni1Δ90-343</i>	WT	WT		<i>bni1Δ90-343</i>	cc;t	bb
	<i>bni1Δ90-574</i>	WT	WT		<i>bni1Δ90-574</i>	cc;tt	bb
	<i>bni1Δ90-821</i>	WT	WT		<i>bni1Δ90-821</i>	ccc;tt;ss	bb
	<i>bni1Δ90-988</i>	ccc;tt;ss	bb;ss		<i>bni1Δ90-988</i>	Dead	NA
	<i>bni1Δ90-1230</i>	ccc;tt;s	bb;ss		<i>bni1Δ90-1230</i>	Dead	NA
Haploid <i>bnr1Δ</i>	<i>BNI1::LEU2</i>	WT	WT	Haploid <i>arp1Δbnr1Δ</i>	<i>BNI1::LEU2</i>	WT	WT
	<i>bni1Δ::LEU2</i>	dead	NA		<i>bni1Δ::LEU2</i>	dead	NA
	<i>bni1Δ90-343</i>	WT	WT		<i>bni1Δ90-343</i>	WT	NA
	<i>bni1Δ90-574</i>	WT	WT		<i>bni1Δ90-574</i>	c;t	NA
	<i>bni1Δ90-821</i>	cc	bb		<i>bni1Δ90-821</i>	ccc;tt;ss	NA
	<i>bni1Δ90-988</i>	ccc;ttt	bbb		<i>bni1Δ90-988</i>	NA	NA
	<i>bni1Δ90-1230</i>	ccc;ttt	bbb		<i>bni1Δ90-1230</i>	NA	NA

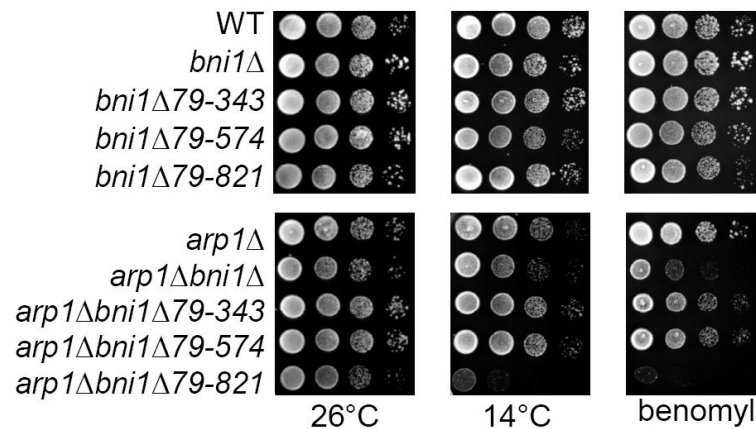
**Table 3.3 continued**

Strain background	Bni1p	Growth*	Benomyl sensitivity #	Strain background	Bni1p	Growth	Benomyl sensitivity
Diploid	<i>BNI1::LEU2/ BNI1::LEU2</i>	WT	WT	Diploid <i>arp1Δ</i> <i>/arp1Δ</i>	<i>BNI1::LEU2/ BNI1::LEU2</i>	WT	WT
	<i>bni1Δ::LEU2/ bni1Δ::LEU2</i>	WT	WT		<i>bni1Δ::LEU2/ bni1Δ::LEU2</i>	cc;t	bb
	<i>bni1Δ90-343/ bni1Δ90-343</i>	WT	WT		<i>bni1Δ90-343/ bni1Δ90-343</i>	WT	WT
	<i>bni1Δ90-574/ bni1Δ90-574</i>	WT	WT		<i>bni1Δ90-574/ bni1Δ90-574</i>	WT	WT
	<i>bni1Δ90-821/ bni1Δ90-821</i>	WT	b		<i>bni1Δ90-821/ bni1Δ90-821</i>	ccc	bbb
	<i>bni1Δ90-988/ bni1Δ90-988</i>	ccc	bbb		<i>bni1Δ90-988/ bni1Δ90-988</i>	Dead	NA
	<i>bni1Δ90-1230/ bni1Δ90-1230</i>	ccc	bbb		<i>bni1Δ90-1230/ bni1Δ90-1230</i>	Dead	NA
Diploid <i>arp1Δ</i> <i>/arp1Δ</i>	<i>BNI1::LEU2 /BNI1</i>	WT	WT				
	<i>bni1Δ::LEU2 /BNI1</i>	WT	b				
	<i>bni1Δ90-343 /BNI1</i>	WT	WT				
	<i>bni1Δ90-574 /BNI1</i>	WT	WT				
	<i>bni1Δ90-821 /BNI1</i>	c	b				
	<i>bni1Δ90-988 /BNI1</i>	cc	bb				
	<i>bni1Δ90-1230 /BNI1</i>	cc	bb				

**Figure 3.6 Phenotypes of Class I Bni1p truncations regarding spindle and nuclei orientation**

(A) Growth assay of Class I truncations with or without Arp1p at 26 °C, 14 °C on YPD plates and at 26 °C on 10 µg/ml benomyl plates. (B) Binucleated phenotype of Class I truncations with or without ARP1p. Cells were grown at room temperature till OD=0.2 then shifted to 16 °C for 8hrs. The numbers of nuclei in the mother cells were counted after DAPI staining. Cells>500.

(A)



(B)

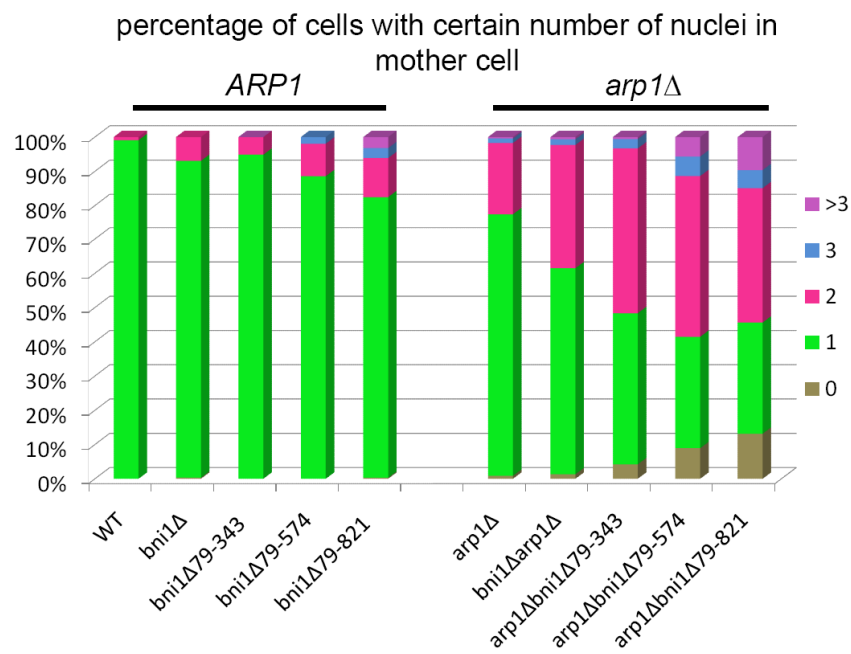
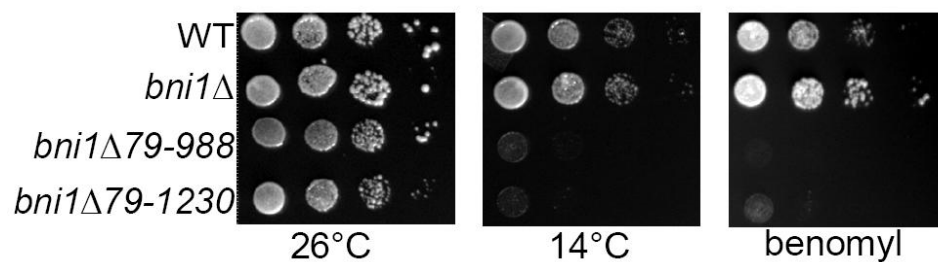


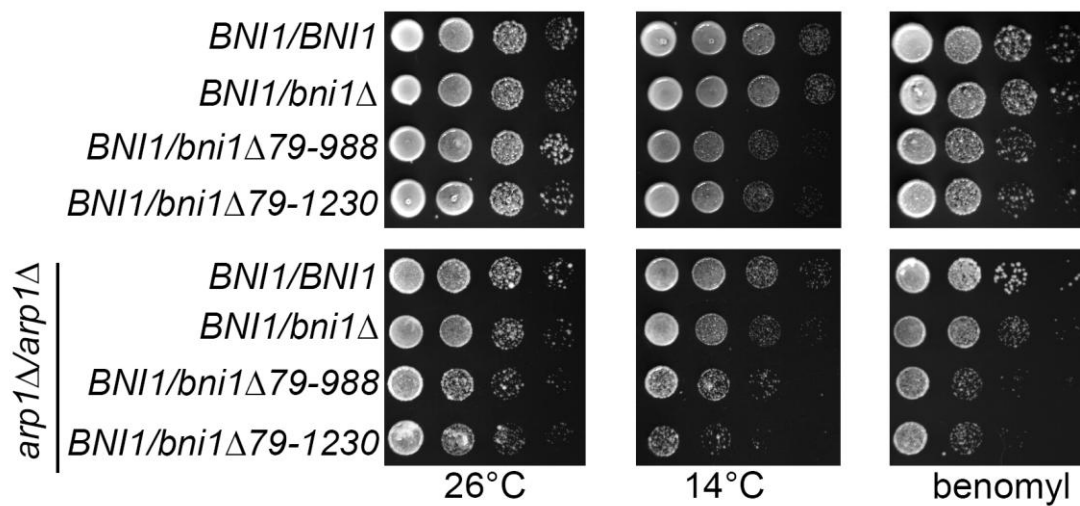
**Figure 3.7 Phenotypes of Class II Bni1p truncations**

Growth assays of Class II truncations at 26 °C, 14 °C on YPD plates and at 26 °C on 10 µg/ml benomyl plates. (A) Growth assays of Class II Bni1p haploids. (B) Growth assays of heterozygous Class II Bni1p in *ARPI*/*ARPI* or *arp1Δ*/*arp1Δ* background.

(A)



(B)



dominant negative (Figure 3.7B).

### **Actin assembly activity is essential for Bni1p class II phenotypes**

Since the major role of Bni1p in *S. cerevisiae* is to nucleate and assemble actin cables to serve as tracks for polarized growth, I asked whether the C-terminal actin assembly activity of the N-terminal truncation of Bni1p caused the phenotypes. I mutated the FH2 domain of Class II truncations using a single amino acid change that has been reported to almost completely abolish the actin assembly ability (Xu et al., 2004). This actin nucleation dead version of *bni1Δ79-988* is not synthetically lethal with *arp1Δ* (Figure 3.8A) and behaved similarly to *bni1Δ* (Figure 3.8B), suggesting that all the phenotypes caused by *bni1Δ79-988* are due to its actin assembly activity.

As *Bni1Δ79-988p-3GFP* is poorly localized (Figure 3.3), I wanted to know whether defects in spindle orientation/nuclear migration are due to mislocalized actin assembly. To test this, I tagged the Class II Bni1p truncations with the Cdc42-Rac Interactive binding (CRIB) domain of Gic2p, which binds Cdc42p and should localize the construct to the bud tip during bud growth and the bud neck during cytokinesis (Brown et al., 1997; Burbelo et al., 1995). The *CRIB-bni1Δ79-988* construct was able to restore Bni1p's normal localization and did not show cold sensitivity (Figure 3.9). In addition, phalloidin staining showed polarized actin patches and directed actin cables in *CRIB-bni1Δ79-988* cells (Figure 3.9B), suggesting that the phenotypes associated with expression of the Bni1p C-terminal region are mainly due to delocalized Bni1p during budding.

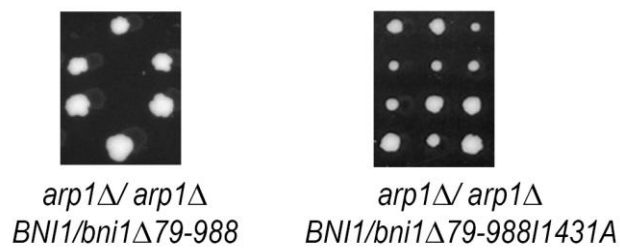
### ***Discussion and future direction***

In the previous chapter, I described the identification of three different localization

**Figure 3.8 Phenotypes of *bni1*ΔNp mutants are due to its actin assembly ability**

(A) Dissection of Class II mutant in *arp1*Δ indicates that mutating I1431A would rescue the synthetic lethality of *arp1*Δ*bni1*Δ79-988. (B) Growth assay of *arp1*Δ*bni1*Δ79-988 I1431 showed that it behaved similarly to *arp1*Δ*bni1*Δ.

(A)



(B)

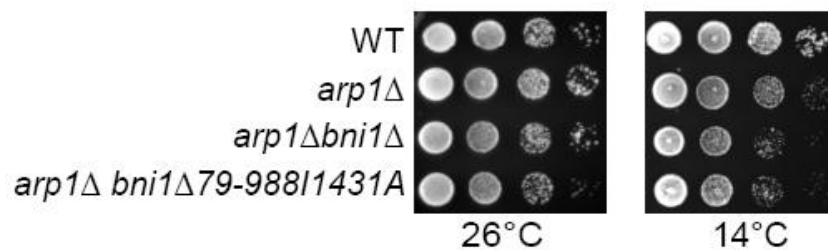
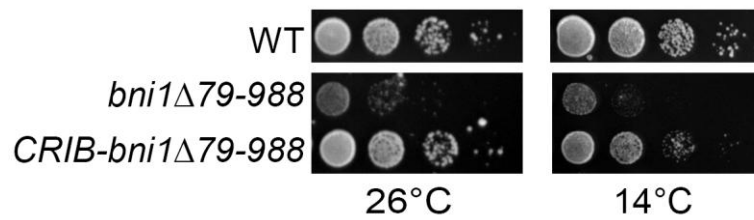


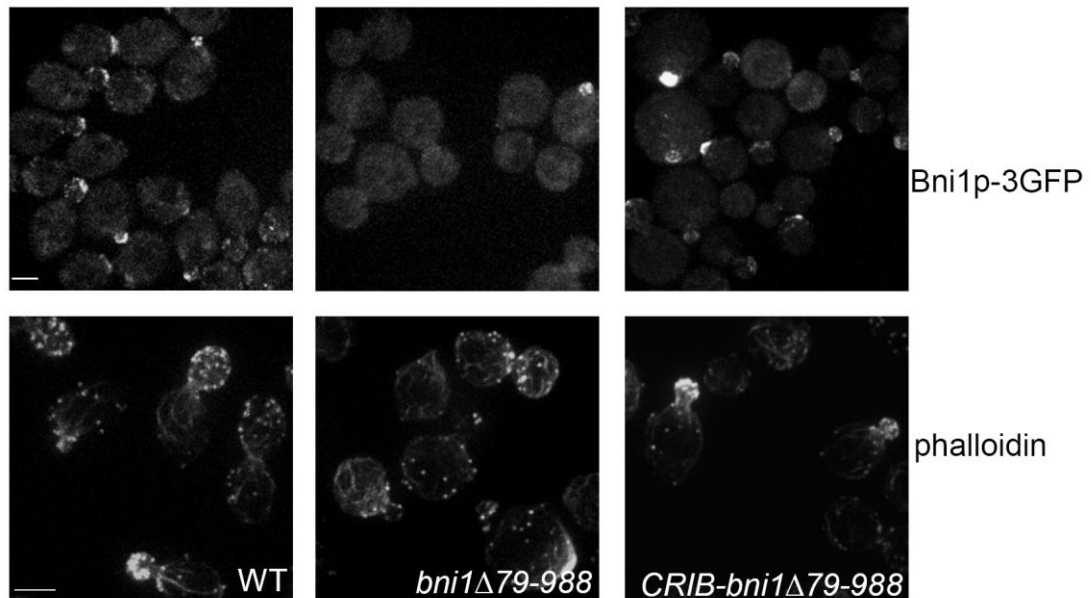
**Figure 3.9 Tagging *bni1*ΔN with CRIB domain rescues the cold sensitivity and actin disruption in *bni1*Δ79-988p**

(A) Growth assay of *CRIB* tagged *bni1*Δ 79-988 at 26 °C and 14 °C. (B) Phalloidin staining and live GFP image of *CRIB* tagged *bni1*Δ 79-988. Scale bar, 2 μm.

(A)



(B)



domains in the N-terminal region of Bni1p. In this chapter, I further studied the function of the N-terminal region by observing the phenotypes of cells with different deletions of the N-terminal domain. The five Bni1p truncations were divided into two classes according to their growth (Figure 3.2). Actin staining shows that Class I has minor defects in actin structures during bud growth and live cell images suggest that Bni1p localization was not much affected. However, Class II Bni1p leads to misoriented and short actin cables with depolarized actin patches. Class II Bni1p-3GFP surprisingly showed that Bni1p deleted of almost the entire N-terminal region before FH1 domain could still be localized, although only in unbudded or tiny-budded cells. This localization could be due to the Bud6p binding at the C-terminal end of Bni1p (Ozaki-Kuroda et al., 2001).

The major difference between class I and class II Bni1p constructs is the existence or absence of SBD, which has been shown to be a localization domain dependent on Spa2p (Chapter 2). To find out whether the loss of Spa2p binding caused the differences, I studied Bni1p truncations in *spa2Δ* cells. Class I truncations indeed showed more severe phenotypes in a *spa2Δ* background than in *SPA2* cells. However, Class II truncations were found to be synthetically lethal with *spa2Δ*, revealing that Spa2p contributes a function independent of binding Bni1p through SBD. One likely mechanism would be that Spa2p regulates Bni1p through another polarisome component Bud6p. Since Spa2p is the scaffolding protein of the polarisome complex, disruption of Spa2p would affect the function of Bud6p which has been shown to regulate Bni1p (Moseley and Goode, 2005; Moseley et al., 2004). Besides being the scaffolding protein of the polarisome, Spa2p has also been found to co-

immunoprecipitate with Myo1p, Myo2p, and Pan1p which are all proteins involved in cell polarity and actin function (Shih et al., 2005). Further studies are needed to determine what function Spa2p contributes and whether it has an additional direct or indirect function in the regulation of Bni1p.

The phenotypes of Bni1p truncations were also studied in cells defective in the dynein and dynactin pathway. Since Bni1p was suggested to function in the early stage of nuclear movement and dynein/dynactin pathway was shown to function at a later stage, disruption of the dynein/dynactin pathway leaves the Kar9p/Myo2p/actin pathway as the only mechanism for nuclear transport and spindle orientation (Fujiwara et al., 1999; Miller et al., 1999; Tong et al., 2001). However, in our background, *bni1Δ* is not synthetically lethal with *arp1Δ* or *dyn1Δ*. A third mechanism involving pushing force from astral microtubule elongation might be responsible for functioning in the double disruption strains to move nuclei (Yeh et al., 2000). On the other hand, Class II *bni1* truncations are synthetically lethal with *arp1Δ*. Further experiments suggested that *bni1* truncations have defects in spindle orientation and nuclear movement. Also, Class II *bni1* truncations that have no actin assembly ability are not synthetically lethal with *arp1Δ* anymore. Combining the actin staining and Bni1p localization of these *bni1* truncations, I suggest that *bni1* truncations, especially class II, are nucleating actin cables at the wrong places during budding, resulting in the misorientation of spindles and defects in nuclear movements. In *bni1Δ* cells, actin cables nucleated by Bnr1p from the bud neck could be acting with Myo2p to orient the spindle towards the bud neck. Alternatively, spindle orientation simply relies on the dynein/dynactin pathway and/or possibly pushing force from astral microtubules. To test our

hypothesis, a Class II *bni1* truncation was tagged with a CRIB domain to help localizing Bni1p. Indeed, this CRIB tagged Bni1p truncation could restore the mislocalization of Bni1p truncation and rescue its cold sensitivity.

As shown in Table 3.1, the deletion of Bnr1p does not affect the phenotypes of Bni1p truncations in terms of spindle orientation. This suggests that either Bnr1p does not function in the Kar9p/Myo2p/actin pathway or Bni1p truncation mutants are dominant negative which has been suggested in the heterozygous mutants (Figure 3.8).

## CHAPTER 4

### Discussion and future direction

I have demonstrated that yeast formin Bni1p is regulated by localization regions in the N-terminal region. However, exactly which protein(s) regulate Bni1p and how the regulation is adjusted during different stages in cell cycle and mating is not clear. The most obvious and critical challenge is to find those proteins. Yeast two hybrid screen would give some suggestions on how to pursue this question, which has been discussed in Chapter 2. Another sensitive and quantitative method, which is mass spectrometry coupled with Stable isotope labeling by amino acids in cell culture (SILAC), could also be used to identify binding partner. Strains with integrated Bni1 1-717aa tagged with 3HA under its own promoter will be labeled with heavy lysine and arginine, and strains with no tagged Bni1 1-717aa will be grown in normal media. Proteins that specifically bind to Bni1-717aa will be identified and quantified after running mass spectrometry. These results can be compared with the yeast two hybrid candidates. Double hits would be of high interests and reveal localization and activity regulation or new intriguing functions of N-terminal region of Bni1p. The mass spectrometry results would help to reveal new proteins that are missed by the yeast two hybrid assay. Since the likely candidates to localize Bni1p are membrane bound proteins which cannot be transported into the nucleus for the yeast two hybrid assays to work, the mass spectrometry might be especially informative. In addition, the yeast two hybrid library is a cDNA library which covers the whole length of a protein while the binding between Bni1p and candidates may only be through part of the protein masked in the full length molecule. Also, since the localization of Bni1p is cell cycle

dependent, it would be intriguing to use cells from different cell cycle stages to do this quantitative mass spectrometry which would tell us how Bni1p is regulated temporally.

The localization of dimerized G-domain in *rho1ts* and *cdc42ts* suggested that it could bind membrane independent of small GTPases. This could be through the basic residues binding to membrane, similar to Cdc42p effectors Ste20p, Gic1p, and Gic2p (Takahashi and Pryciak, 2007). This could be tested by mutating some of the basic residues in the G-domain. If the basic residues indeed have effects on G-domain's localization, it is possible that they interact with negatively charged phospholipids on the membrane. Lipid binding assays could be performed to explore this possibility.

The results presented in this study reveal that Bni1p has four localization domains and they contribute cumulatively to Bni1p's function in polarized growth and spindle orientation. It is surprising that so many independent localization domains exist in one protein. These findings could suggest that the cell needs very careful and intimate control of Bni1p localization to coordinate its localization, and hence cable assembly, with all the other events going on at sites of growth. Alternatively, the many localization domains may be used under other growth conditions, for example during shmooing, or during the highly polarized growth that occurs during filamentous growth. The finding of four distinct localization domains implies that four different mechanisms may be involved in localizing Bni1p. In addition to looking for different binding partners of Bni1p localization domains, the differences between the localization domains could shed light on the question. GFP tagged localization domains should be observed during shmoo formation and different cell stages after

cell cycle release or along with Tub1p, which indicates cell stage more accurately than simply looking at bud size. Double labeling of different localization domains in the same cell could give the differences of their precise localization temporally and spatially. FRAP of the different domains could also give information on how dynamic those domains are.

As shown in Chapter 3, Spa2p regulates the localization and function not only through the SBD. One obvious mechanism is that Spa2p regulates Bni1p indirectly through Bud6p, another component of polarisome which binds Bni1p C-terminal end. Since *bud6Δ* is already quite sick, to study the role of Bud6p on Bni1p, specific amino acids change could be made in the Bni1p C-terminal ends to abolish the binding of Bni1p to Bud6p (Moseley and Goode, 2005). The phenotypes of the Class I and Class II Bni1p truncations with Bud6p binding deficiency could reveal whether Spa2p is regulating Bni1p through Bud6p. In addition, Sph1p, a Spa2p homolog, and the other polarisome component Pea2p could also be interesting candidates in regulating Bni1p and their role in polarity has not been clearly studied.

## APPENDIX I

### Identification of Boi1/2p in *S. cerevisiae*

#### *Abstract*

Pob1p, the homolog of budding yeast Boi1p and Boi2p in fission yeast, has been shown to mediate the interaction between Cdc42p and the formin For3p (Rincon et al., 2009). An interaction between Boi1/2p and Cdc42p was shown previously (Bender et al., 1996) and here I show that Bni1p and Boi1/2p also interact. To study whether Boi1/2p is functionally similar to Pob1p, temperature sensitive strains of *boi1Δ boi2ts* were generated and revealed that Boi1/2p contribute to yeast polarity.

#### *Introduction*

In the fission yeast, *Schizosaccharomyces pombe*, a protein called Pob1p has been suggested to bind Cdc42p and the formin protein For3p through different domains and is required for For3p localization to the tips. It was proposed that Pob1p facilitates Cdc42-mediated relief of For3p autoinhibition to stimulate actin cable formation (Rincon et al., 2009). The Pob1p homolog AgBoi1/2p in *Ashbya gossypii* has also been implicated in regulating actin structure (Knechtle et al., 2006). In *Saccharomyces cerevisiae*, there are two Pob1p homologs, Boi1p and Boi2p. Analysis of the yeast genome suggests that *Saccharomyces cerevisiae* underwent a global genomic duplication, and *BOI1* and *BOI2* represent the duplication of a primordial *BOI* gene (Seoighe and Wolfe, 1999). Boi1p and Boi2p both contain a Src homology 3 (SH3) domain, a sterile alpha motif (SAM) domain, a poly-proline rich region and a pleckstrin homology (PH) domain. They were first discovered by binding polarity scaffold protein Bem1p through their poly-proline rich region (Bender et al., 1996).

Similar to many polarity proteins, they localize to growth sites during budding, at the bud tip in small to medium budded cells and at the bud neck during cytokinesis (Hallett et al., 2002). In some G1 cells, they were also found to be localized to the nucleus (Norden et al., 2006), suggesting they shuffle between the nucleus and cytoplasm. It has also been suggested that Cdc28p phosphorylates Boi1p and Boi2p directly in a cell cycle dependent manner (McCusker et al., 2007). No obvious mammalian homolog has been found for Boi1/2p, although anillin, a scaffolding protein that binds actin, RhoA and myosin at the cleavage furrow (Piekny and Glotzer, 2008), has been suggested to be the homolog mainly due to its PH domain and nucleus-cytoplasm shuffling ability. Since Boi1p has been shown to interact with active Cdc42p (Bender et al., 1996), it would be very interesting to know whether the Boi1p and Boi2p in *Saccharomyces cerevisiae* are also involved in the regulation of formins as in *Schizosaccharomyces pombe*.

### ***Materials and methods***

#### **Yeast Strains and General Molecular Biology Techniques**

Strains used in this study are listed in Table 5.1. All strains were generated in the S288C strain background coming from the deletion consortium (Brachmann et al., 1998). Standard media and techniques for growing and transforming yeast were used (Sherman, 1991). Dilution assays were performed at a ratio of 1:10.

#### **Yeast two hybrid assay**

Yeast 2 hybrid plasmids are shown in Table 5.2. Bait plasmids containing Gal4p binding domain (BD) were transformed into PJ69-4 $\alpha$  strains and prey plasmids containing Gal4p activation domain (AD) were transformed into PJ69-4a strains. The

**Figure 5.1 Domain organizations of Boi2p and construct scheme**

(A) Domain organizations of Boi2p. (B) Scheme of construct of the integration library used in the temperature sensitive screen. Numbers on the constructs represents nucleotides

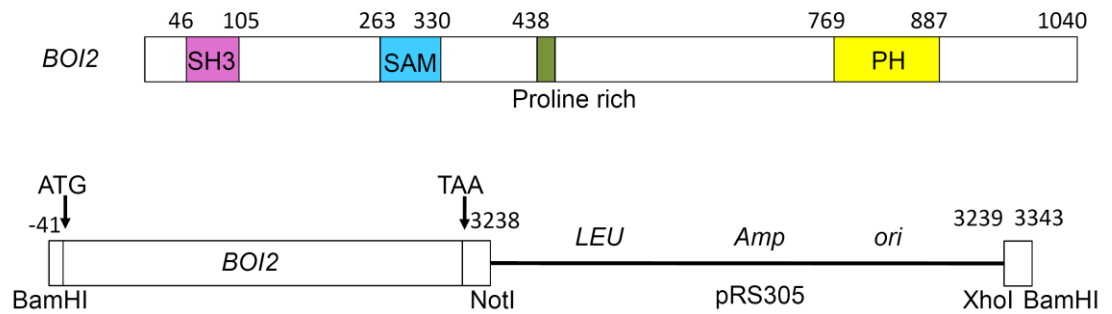


**Table 5.1 Yeast strains used in Appendix I**

Strain	Genotype	Source
ABY3097	MATa <i>his3Δ1 leu2Δ0 ura3Δ0 met15Δ0</i> <i>boi1Δ::Kan<sup>R</sup></i>	Invitrogen
ABY3208	MATa <i>his3Δ1 leu2Δ0 ura3Δ0 met15Δ0</i> <i>boi1Δ::Kan<sup>R</sup> boi2-1::Leu2</i>	This Study
ABY3211	MATa <i>his3Δ1 leu2Δ0 ura3Δ0 met15Δ0</i> <i>boi1Δ::Kan<sup>R</sup> boi2-4::Leu2</i>	This Study
ABY3212	MATa <i>his3Δ1 leu2Δ0 ura3Δ0 met15Δ0</i> <i>boi1Δ::Kan<sup>R</sup> boi2-5::Leu2</i>	This Study
ABY3213	MATa <i>his3Δ1 leu2Δ0 ura3Δ0 met15Δ0</i> <i>boi1Δ::Kan<sup>R</sup> boi2-6::Leu2</i>	This Study
ABY3214	MATa <i>his3Δ1 leu2Δ0 ura3Δ0 met15Δ0</i> <i>boi1Δ::Kan<sup>R</sup> boi2-7::Leu2</i>	This Study
pJ69-4a	MATa <i>trp1-901 leu2-3,112 ura3-52 his3-200</i> <i>gal4Δ gal80Δ LYS2::GAL1-HIS3 GAL2-ADE2</i> <i>met2::GAL7-lacZ</i>	(James et al., 1996)
pJ69-4a	MATa <i>trp1-901 leu2-3,112 ura3-52 his3-200</i> <i>gal4Δ gal80Δ LYS2::GAL1-HIS3 GAL2-ADE2</i> <i>met2::GAL7-lacZ</i>	(James et al., 1996)

**Table 5.2 Plasmids used in Appendix I**

\* The genotype was labeled in nucleotides.

Plasmid	Backbone	Genotype*
pWL105	pRS305	<i>BOI2</i> (3239-3343)
pWL106	TOPO2.1	<i>BOI2</i> (-41-3238)
pWL123	pRS316	$P_{BOI2}$ - <i>BOI2</i> (full length)
pRC651	Leu Cen	$P_{SEC4}$ - <i>GFP-SEC4</i>
pKD001	pRS306	$P_{MYO2}$ - <i>MYO2-3GFP</i>
pWL085	pRS306	<i>BNI1C-3GFP-BNI13'</i>
pWL088	pGBKT7	<i>BNI1 1-2172</i>
pWL089	pGBKT7	<i>BNI1 1-3717</i>
pWL090	pGBKT7	<i>BNR1 1-2274</i>
pWL091	pGADT7	<i>BOI1 541-981</i>
pWL095	pGADT7	<i>BOI1 1-2250</i>
pWL096	pGADT7	<i>BOI1 1-981</i>
pWL092	pGADT7	<i>BOI2 658-1125</i>
pWL097	pGADT7	<i>BOI2 1-2220</i>
pWL098	pGADT7	<i>BOI2 1-1125</i>

transformed PJ69-4a and PJ69-4 $\alpha$  were mated with different combinations and selected on SC-Trp-Leu plates. The resulting diploids were checked for interaction using dilution assays on SC-Trp-Leu-His or SC-Trp-Leu-His-Ade plates.

### **Isolation of conditional *boi1 $\Delta$ boi2-ts* mutants**

PCR-derived mutagenized DNA encoding the *BOI2* full length with short 5' and 3' ends (residues -41–3238) was amplified with primers (5'-GAGGATCCGAATCATACCAACTTCTCCG-3') and (5'-GTGCGGCCGCGATCATCGGCATCCTTTC-3'). The mutagenic PCR was performed using the PCR reaction mixture: 1 mM dCTP, 1 mM dTTP, 0.2 mM dATP, 0.2 mM dGTP, 75ng template DNA (pWL106), 5.5 mM MgCl<sub>2</sub>, 0.5 mM primers, 1X Taq buffer (Roche), 10  $\mu$ g BSA, and 0.05% Tween 20 per 100 $\mu$ l reaction; and after the mix had warmed up to 80  $^{\circ}$ C, 0.3 mM MnCl<sub>2</sub> and 5u *Taq* DNA polymerase were added. The mutagenic PCR reaction mixture was subjected to eight cycles of amplification and the BamHI-NotI fragment of the PCR product was subcloned into the corresponding region of pWL105 to make libraries of mutagenized *BOI2* (Schott et al., 1999). *boi1 $\Delta$*  strain (Invitrogen deletion consortium) was transformed with BamHI linearized mutagenized library to replace WT *BOI2* (Figure 5.1). Transformants were grown at the permissive temperature of 26  $^{\circ}$ C and replica-plate to 37  $^{\circ}$ C and 26  $^{\circ}$ C to identify temperature-sensitive isolates. Around 14,000 colonies were screened and 5 temperature sensitive alleles were recovered. They were named ABY3208 (*boi1 $\Delta$  boi2-1*), ABY3211 (*boi1 $\Delta$  boi2-4*), ABY3212 (*boi1 $\Delta$  boi2-5*), ABY3213 (*boi1 $\Delta$  boi2-6*), ABY3214 (*boi1 $\Delta$  boi2-7*) (Figure 5.2). All the five strains were able to grow at higher temperature after longer incubation. Thus an overexpression suppression screen

is not applicable for the five stains identified. The temperature sensitive strains contain one or multiple nucleotide changes.

The temperature sensitive strains can be suppressed by transformation with pWL123, a low copy plasmid with full length *BOI2*. Mating and sporulation confirmed that temperature sensitive phenotype always goes with *boi1Δ boi2ts* markers.

### **Microscopy and Imaging**

Live cells were placed under 2% agarose in synthetic medium, with appropriate amino acid. Images were acquired with a spinning disc confocal microscopy system (3I Corp) using a DMI 6000B microscope (Leica) and a digital camera (QuantEM; Photometrics). Images were then further analyzed and adjusted using Slidebook 5.

### **Results**

#### **Yeast two hybrid showed weak interaction between Boi1/2p with N-terminal region of Bni1p**

The Boi1/2p homolog in *S. pombe* Pob1p interacts with formin protein For3p through its SAM domain in the N-terminal region. The interactions of Boi1/2p with formin proteins were also examined using yeast two hybrid. As shown in Figure 5.2 and Table 5.3, the N-terminal region of Bni1p but not Bnr1p showed a weak interaction with the N-terminal region of both Boi1p and Boi2p.

#### **Isolation of temperature sensitive strains of *boi1Δ boi2ts***

Single disruption of either *boi1* or *boi2* does not cause obvious phenotype regarding polarity. Double disruption of *boi1Δ boi2Δ* is lethal or sick depending on the strain background (Bender et al., 1996; Matsui et al., 1996; Norden et al., 2006). In the

**Figure 5.2 Growth assay of the yeast two hybrid assays between formins and Boi1/2p**

Growth assays were performed on SC-Leu-Trp and SC-Leu-Trp-His plates.

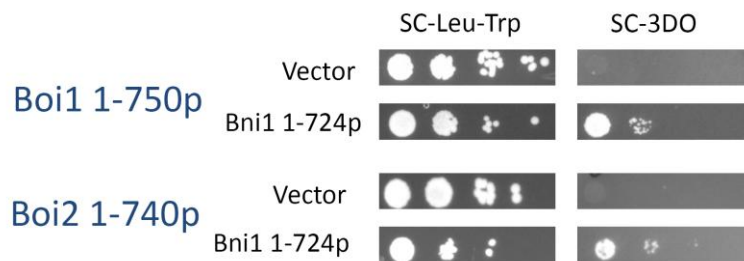


**Table 5.3 Summary of the yeast two hybrid assay between formins and Boi1/2p**

Yeast two hybrid (y2h) results on SC-Leu-Trp-His plates. “+” indicates there is an interactions while “-” indicates no interaction has been observed.

Y2h on 3DO	Bni1 1-724p	Bni1 1-1239p	Bnr1 1-758p
Boi1p	vector	-	-
	Boi1 181-327p	-	-
	Boi1 1-327p	-	-
	Boi1 1-750p	+	-
Boi2p	vector	-	-
	Boi2 220-375p	-	-
	Boi2 1-375p	-	-
	Boi2 1-740p	+	-

**Figure 5.3 Growth assay of *boi1Δ boi2ts* at 26 °C, 30 °C, 32 °C, 35 °C, and 37 °C**

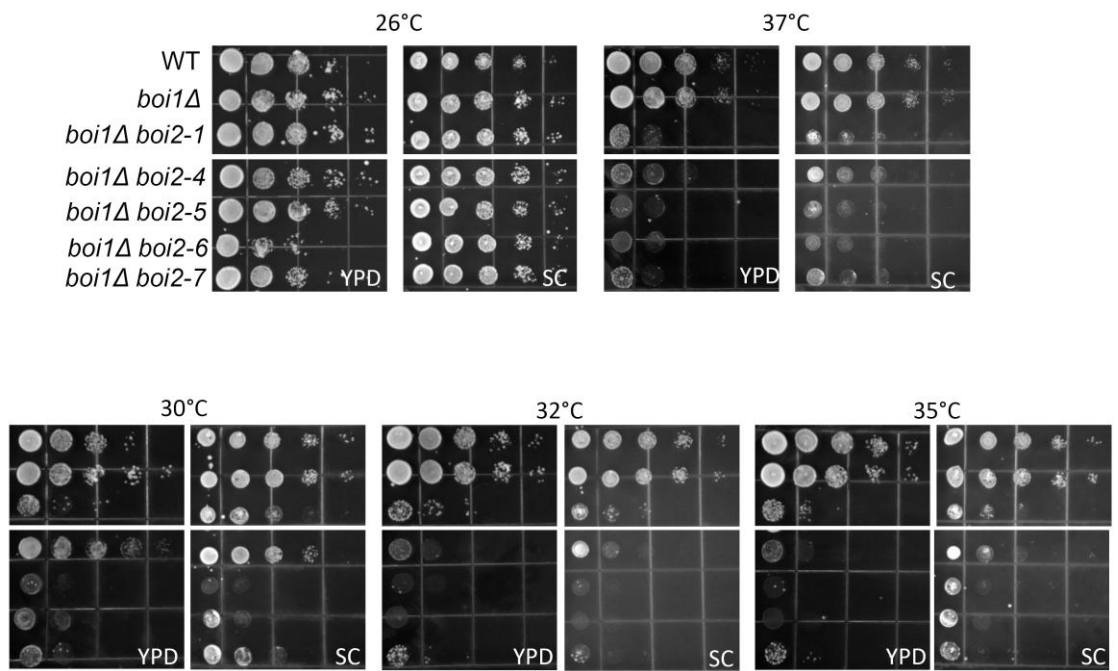


**Table 5.4 Nucleotide and amino acid change in *boi1Δboi2ts* mutant alleles**

Allele	Nucleotide change	Amino Acid change	old codon percentage‰	new codon percentage‰
<i>boi1Δboi2-1</i>	T745C	L249 silent	26.37	13.54
	T1293A	G431 silent	22.48	11.23
	A1934G	K645R	42.4	20.97
	T2371C	F791L	18.29	5.67
	A2967G	S989 silent	19.02	8.81
	T3020C	V1007A	10.92	6.29
	A3101C	K1034T	42.4	17.92
<i>boi1Δboi2-4</i>	A-36C	N/A	N/A	N/A
	C1012A	L338M	10.74	20.82
	T1993A	S665T	23.47	20.04
	A2120G	E767G	45.44	11.23
	G2263C	E755Q	45.44	26.65
	T2343C	G781 silent	22.48	9.82
	T2356A	W786R	10.45	9.55
<i>boi1Δboi2-5</i>	A2967G	S989 silent	19.02	8.81
	T2371A	F791A	18.29	16.9
	T2799A	D933 silent	37.73	45.44
<i>boi1Δboi2-6</i>	A2967G	S989 silent	19.02	8.81
	A814G	T272A	17.92	16.28
	C1637A	S579Y	23.47	19.03
	T2412C	S804 silent	20.04	12.45
	T2598C	Y866 silent	19.03	14.47
<i>boi1Δboi2-7</i>	A2967G	S989 silent	19.02	8.81
	A775G	N259D	24.49	20.07
	A1283G	E428G	45.44	11.23
	A1789T	S597C	14.56	8.13
	A2181G	K727 silent	42.4	30.4
	T2356C	W786R	10.45	1.88
	A2967G	S989 silent	19.02	8.81
A3109T	T1037S	12.45	14.15	

deletion consortium strain background, the deletion of both is lethal. Thus temperature sensitive alleles of *boi2ts* were generated in a *boi1Δ* background: *boi1Δ boi2-1*, *boi1Δ boi2-4*, *boi1Δ boi2-5*, *boi1Δ boi2-6*, *boi1Δ boi2-7* (Figure 5.3 and Table 5.4). The phenotypes will mainly be discussed for *boi1Δ boi2-5*, *boi1Δ boi2-6* because they have 1 and 2 missense mutations respectively and they will be referred collectively as *boi2ts* for simplification. No morphological changes were observed for these strains after incubating at the restrictive temperature for 5 hrs. After 20 hrs incubation at 37 °C, besides dead cells, multi-budded cells were observed in the *boi2ts* strains (data not shown).

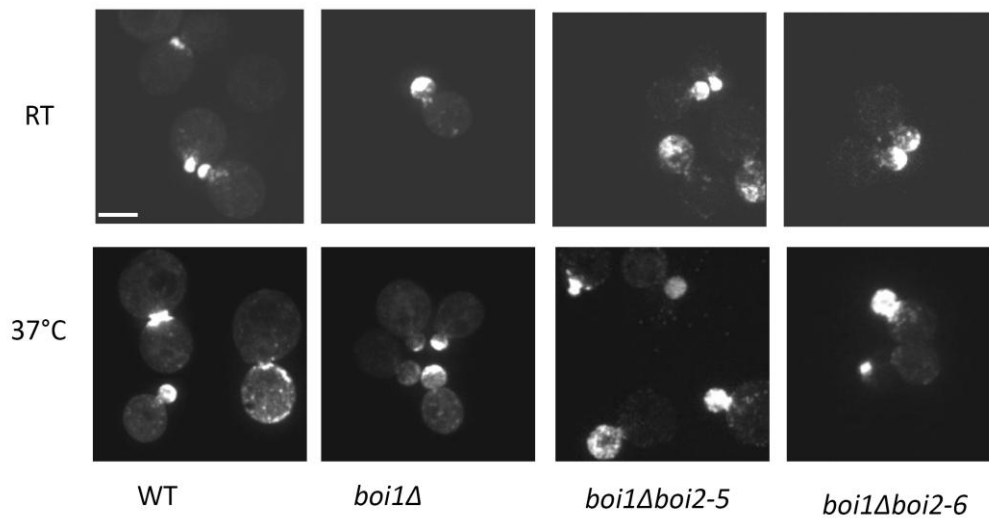
#### **Cell polarity is affected in *boi2ts* cells**

No obvious changes in the actin cytoskeleton were observed after *boi2ts* strains were shifted to the restrictive temperature for various amounts of time (from 1 hr to 5 hrs). However, since it is hard to see actin cables clearly in small to medium buds, the distributions of Myo2p and Sec4p, which always correlate with directed growth and are dependent on actin cable organization, were examined. Both Myo2p and Sec4p were found to have polarization defects in *boi2ts* strains after shifting to the restrictive temperature. In small and medium budded cells, Myo2p and Sec4p always concentrate at the bud tip in wildtype and *boi1Δ* cells. However in *boi2ts* strains, Myo2p and Sec4p are more dispersed in the bud and could also be observed at the bud neck region (Figure 5.4). This phenotype is similar to *bni1Δ* which lacks actin cables to serve as tracks for vesicle transport to the bud tip (Pruyne et al., 2004a). Thus, I examined the distribution of Bni1p in *boi2ts* strains at the restrictive temperature. Consistently,

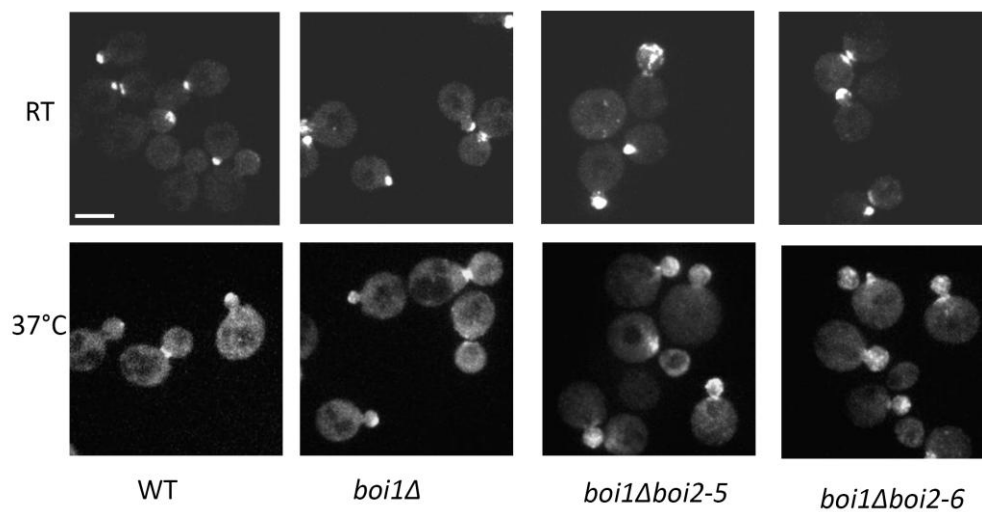
**Figure 5.4 Phenotypes of polarity marker Sec4p and Myo2p in *Boi2ts* strains at restrictive temperature**

(A) Live GFP image of Sec4p-GFP distribution in the strains either at room temperature (upper panel) or at 37 °C (lower panel) for 2hrs. (B) Live GFP image of Myo2p-3GFP distribution in the strains either at room temperature (upper panel) or at 37 °C (lower panel) for 2hrs. Scale bar, 2 μm.

(A) Sec4p-GFP



(B) Myo2p-3GFP



Bni1p-3GFP was seldom observed at bud tips at the restrictive temperature. Also interestingly, bud neck localization of Bni1p was frequently observed in medium budded cells, a phenotype never observed in wild type cells (Figure 5.5A). The same is also true for the localization of Bni1Np that contains the region interacted with Boi1p and Boi2p (Figure 5.5B). The localization of Bni1p and Bni1Np explain the distribution of Sec4p and Myo2p in the *boi2ts* strains at the restrictive temperature.

### ***Discussion and future directions***

Formins are critical regulators of the actin cytoskeleton, nucleating and elongating actin cables for polarized transport of organelles and secretory vesicles. How the formins are regulated so that they assemble actin cables at the right time and right place has been of great interest to us. Boi1p and Boi2p are good candidates to be formin regulators in *S. cerevisiae* as their homolog Pob1p in *S. pombe* has been proven to be so (Rincon et al., 2009). Boi1p and Boi2p have not been extensively studied in literature but their role in polarity has been suggested (Bender et al., 1996; Matsui et al., 1996; McCusker et al., 2007). Thus I started to study the possible function of Boi1/2p on formin localization.

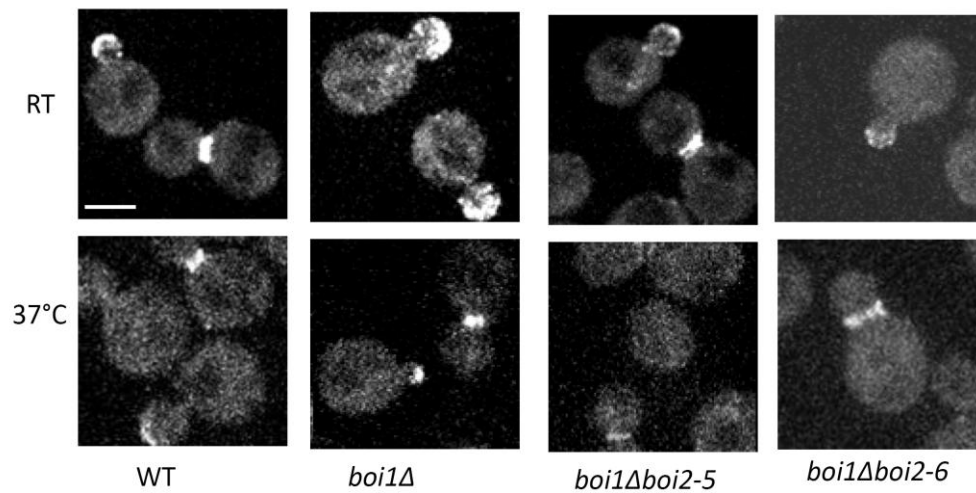
### **The interaction between Boi1/2p and formins**

The potential interaction between Boi1/2p and the formins was first studied using yeast two hybrid. Weak interactions were observed between Bni1p 1-724aa and Boi1p 1-750aa and Boi2p 1-740aa. However, the SAM domain did not show any interaction with the formins. This is different from the yeast two hybrid results with Pob1p in *S. pombe*, in which the SAM domain of Pob1p has been shown to interact with the For3p N-terminal region. This could be explained by the slow growth rate of yeast two

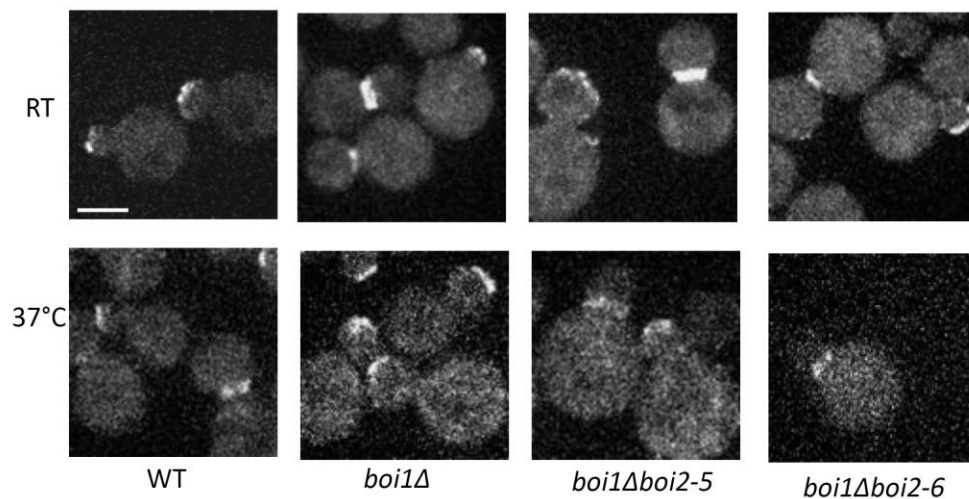
**Figure 5.5 Localization of Bni1p is affected in Boi2ts strains at restrictive temperature**

(A) Live GFP image of Bni1p-3GFP in the strains indicated either at room temperature (upper panel) or at 37 °C (lower panel) for 1 hrs. (B) Live GFP image of Bni1p 1-717aa-3GFP in the strains either at room temperature (upper panel) or at 37 °C (lower panel) for 1 hrs. Scale bar, 2 μm.

(A) Bni1p-3GFP



(B) Bni1p 1-717aa-3GFP



hybrid strains transformed with *Boi1/2p* SAM plasmids, suggesting that overexpressing the SAM domains could be detrimental to budding yeast. It is also possible that the poly-proline rich FH1 domain in the formins can mediate the interactions with *Boi1/2p* through their SH3 domain. Biochemical assays are needed to further confirm the interactions of *Bni1p* with *Boi1/2p*. Pull down systems in which strains with *Bni1p*-3GFP and overexpressed N-terminal *Boi2p* tagged with HA or myc have been established but the assays have not been performed due to lack of time.

### **The role of *boi1/2p* in polarized growth**

As shown in Figure 5.5, at restrictive temperature in *boi2ts* strains, *Myo2p* and *Sec4p*'s localization in the small to medium buds is more dispersed, whereas in wildtype cells *Myo2p* and *Sec4p* always concentrates at the very tip of the bud. As *Myo2p* transports vesicles marked by *Sec4p* along actin cables, this phenotypes indicates defects in actin structure in the bud in small to medium budded cells. The localization of full length *Bni1p* and *Bni1p* 1-717aa were studied and found that they both had a very low percentage of localization at the bud tip/cortex at restrictive temperature in *boi2ts* strains (Figure 5.5). In addition, their localizations were sometimes observed at the bud neck in medium budded cells which never occurs in wild type cells. No defects have been observed for polarity in large budded cells. I propose that *Boi1/2p* functions either to regulate the localization of *Bni1p* at the bud tip/cortex or during the transition of *Bni1p* from the bud tip/cortex to the bud neck.

## REFERENCES

- Adames, N. R., and Cooper, J. A. (2000). Microtubule interactions with the cell cortex causing nuclear movements in *Saccharomyces cerevisiae*. *J Cell Biol* *149*, 863-874.
- Alberts, A. S. (2001). Identification of a carboxyl-terminal diaphanous-related formin homology protein autoregulatory domain. *J Biol Chem* *276*, 2824-2830.
- Alberts, B. (2002). *Molecular biology of the cell*, 4th edn (New York: Garland Science).
- Altmann, K., Frank, M., Neumann, D., Jakobs, S., and Westermann, B. (2008). The class V myosin motor protein, Myo2, plays a major role in mitochondrial motility in *Saccharomyces cerevisiae*. *J Cell Biol* *181*, 119-130.
- Amberg, D. C., Basart, E., and Botstein, D. (1995). Defining protein interactions with yeast actin in vivo. *Nat Struct Biol* *2*, 28-35.
- Arai, S., Noda, Y., Kainuma, S., Wada, I., and Yoda, K. (2008). Ypt11 functions in bud-directed transport of the Golgi by linking Myo2 to the coatomer subunit Ret2. *Curr Biol* *18*, 987-991.
- Bardwell, L. (2004). A walk-through of the yeast mating pheromone response pathway. *Peptides* *25*, 1465-1476.
- Barral, Y., Mermall, V., Mooseker, M. S., and Snyder, M. (2000). Compartmentalization of the cell cortex by septins is required for maintenance of cell polarity in yeast. *Mol Cell* *5*, 841-851.
- Bartolini, F., Moseley, J. B., Schmoranzler, J., Cassimeris, L., Goode, B. L., and Gundersen, G. G. (2008). The formin mDia2 stabilizes microtubules independently of its actin nucleation activity. *J Cell Biol* *181*, 523-536.
- Beach, D. L., Thibodeaux, J., Maddox, P., Yeh, E., and Bloom, K. (2000). The role of the proteins Kar9 and Myo2 in orienting the mitotic spindle of budding yeast. *Curr Biol* *10*, 1497-1506.
- Bender, L., Lo, H. S., Lee, H., Kokojan, V., Peterson, V., and Bender, A. (1996).

Associations among PH and SH3 domain-containing proteins and Rho-type GTPases in Yeast. *J Cell Biol* *133*, 879-894.

Bi, E., Maddox, P., Lew, D. J., Salmon, E. D., McMillan, J. N., Yeh, E., and Pringle, J. R. (1998). Involvement of an actomyosin contractile ring in *Saccharomyces cerevisiae* cytokinesis. *J Cell Biol* *142*, 1301-1312.

Brachmann, C. B., Davies, A., Cost, G. J., Caputo, E., Li, J., Hieter, P., and Boeke, J. D. (1998). Designer deletion strains derived from *Saccharomyces cerevisiae* S288C: a useful set of strains and plasmids for PCR-mediated gene disruption and other applications. *Yeast* *14*, 115-132.

Brown, J. L., Jaquenoud, M., Gulli, M. P., Chant, J., and Peter, M. (1997). Novel Cdc42-binding proteins Gic1 and Gic2 control cell polarity in yeast. *Genes Dev* *11*, 2972-2982.

Burbelo, P. D., Drechsel, D., and Hall, A. (1995). A conserved binding motif defines numerous candidate target proteins for both Cdc42 and Rac GTPases. *J Biol Chem* *270*, 29071-29074.

Buttery, S. M., Yoshida, S., and Pellman, D. (2007). Yeast formins Bni1 and Bnr1 utilize different modes of cortical interaction during the assembly of actin cables. *Mol Biol Cell* *18*, 1826-1838.

Butty, A. C., Perrinjaquet, N., Petit, A., Jaquenoud, M., Segall, J. E., Hofmann, K., Zwahlen, C., and Peter, M. (2002). A positive feedback loop stabilizes the guanine-nucleotide exchange factor Cdc24 at sites of polarization. *EMBO J* *21*, 1565-1576.

Butty, A. C., Pryciak, P. M., Huang, L. S., Herskowitz, I., and Peter, M. (1998). The role of Far1p in linking the heterotrimeric G protein to polarity establishment proteins during yeast mating. *Science* *282*, 1511-1516.

Campellone, K. G., and Welch, M. D. (2010). A nucleator arms race: cellular control of actin assembly. *Nat Rev Mol Cell Biol* *11*, 237-251.

Chen, R. E., and Thorner, J. (2007). Function and regulation in MAPK signaling pathways: lessons learned from the yeast *Saccharomyces cerevisiae*. *Biochim Biophys Acta* *1773*, 1311-1340.

Chesarone, M., Gould, C. J., Moseley, J. B., and Goode, B. L. (2009). Displacement of formins from growing barbed ends by bud14 is critical for actin cable architecture and function. *Dev Cell* *16*, 292-302.

Chesarone, M. A., DuPage, A. G., and Goode, B. L. (2010). Unleashing formins to remodel the actin and microtubule cytoskeletons. *Nat Rev Mol Cell Biol* *11*, 62-74.

Chhabra, E. S., and Higgs, H. N. (2006). INF2 Is a WASP homology 2 motif-containing formin that severs actin filaments and accelerates both polymerization and depolymerization. *J Biol Chem* *281*, 26754-26767.

Copeland, J. W., Copeland, S. J., and Treisman, R. (2004). Homo-oligomerization is essential for F-actin assembly by the formin family FH2 domain. *J Biol Chem* *279*, 50250-50256.

Delgehyr, N., Lopes, C. S., Moir, C. A., Huisman, S. M., and Segal, M. (2008). Dissecting the involvement of formins in Bud6p-mediated cortical capture of microtubules in *S. cerevisiae*. *J Cell Sci* *121*, 3803-3814.

Dobbelaere, J., and Barral, Y. (2004). Spatial coordination of cytokinetic events by compartmentalization of the cell cortex. *Science* *305*, 393-396.

Dohlman, H. G. (2002). G proteins and pheromone signaling. *Annu Rev Physiol* *64*, 129-152.

Dong, Y., Pruyne, D., and Bretscher, A. (2003). Formin-dependent actin assembly is regulated by distinct modes of Rho signaling in yeast. *J Cell Biol* *161*, 1081-1092.

Drubin, D. G., and Nelson, W. J. (1996). Origins of cell polarity. *Cell* *84*, 335-344.

Duncan, M. C., Cope, M. J., Goode, B. L., Wendland, B., and Drubin, D. G. (2001). Yeast Eps15-like endocytic protein, Pan1p, activates the Arp2/3 complex. *Nat Cell Biol* *3*, 687-690.

Elion, E. A., Satterberg, B., and Kranz, J. E. (1993). FUS3 phosphorylates multiple components of the mating signal transduction cascade: evidence for STE12 and FAR1. *Mol Biol Cell* *4*, 495-510.

Esue, O., Harris, E. S., Higgs, H. N., and Wirtz, D. (2008). The filamentous actin cross-linking/bundling activity of mammalian formins. *J Mol Biol* 384, 324-334.

Evangelista, M., Blundell, K., Longtine, M. S., Chow, C. J., Adames, N., Pringle, J. R., Peter, M., and Boone, C. (1997). Bni1p, a yeast formin linking cdc42p and the actin cytoskeleton during polarized morphogenesis. *Science* 276, 118-122.

Evangelista, M., Pruyne, D., Amberg, D. C., Boone, C., and Bretscher, A. (2002). Formins direct Arp2/3-independent actin filament assembly to polarize cell growth in yeast. *Nat Cell Biol* 4, 260-269.

Fagarasanu, A., and Rachubinski, R. A. (2007). Orchestrating organelle inheritance in *Saccharomyces cerevisiae*. *Curr Opin Microbiol* 10, 528-538.

Fagarasanu, M., Fagarasanu, A., and Rachubinski, R. A. (2006). Sharing the wealth: peroxisome inheritance in budding yeast. *Biochim Biophys Acta* 1763, 1669-1677.

Finger, F. P., Hughes, T. E., and Novick, P. (1998). Sec3p is a spatial landmark for polarized secretion in budding yeast. *Cell* 92, 559-571.

Fujiwara, T., Tanaka, K., Inoue, E., Kikyo, M., and Takai, Y. (1999). Bni1p regulates microtubule-dependent nuclear migration through the actin cytoskeleton in *Saccharomyces cerevisiae*. *Mol Cell Biol* 19, 8016-8027.

Fujiwara, T., Tanaka, K., Mino, A., Kikyo, M., Takahashi, K., Shimizu, K., and Takai, Y. (1998). Rho1p-Bni1p-Spa2p interactions: implication in localization of Bni1p at the bud site and regulation of the actin cytoskeleton in *Saccharomyces cerevisiae*. *Mol Biol Cell* 9, 1221-1233.

Gao, L., and Bretscher, A. (2009). Polarized growth in budding yeast in the absence of a localized formin. *Mol Biol Cell* 20, 2540-2548.

Gao, L., Liu, W., and Bretscher, A. (2010). The yeast formin Bnr1p has two localization regions that show spatially and temporally distinct association with septin structures. *Mol Biol Cell* 21, 1253-1262.

Goehring, A. S., Mitchell, D. A., Tong, A. H., Keniry, M. E., Boone, C., and Sprague, G. F., Jr. (2003). Synthetic lethal analysis implicates Ste20p, a p21-activated protein

kinase, in polarisome activation. *Mol Biol Cell* *14*, 1501-1516.

Goldschmidt-Clermont, P. J., Machesky, L. M., Doberstein, S. K., and Pollard, T. D. (1991). Mechanism of the interaction of human platelet profilin with actin. *J Cell Biol* *113*, 1081-1089.

Goode, B. L., Rodal, A. A., Barnes, G., and Drubin, D. G. (2001). Activation of the Arp2/3 complex by the actin filament binding protein Abp1p. *J Cell Biol* *153*, 627-634.

Gould, C. J., Maiti, S., Michelot, A., Graziano, B. R., Blanchoin, L., and Goode, B. L. (2011). The Formin DAD Domain Plays Dual Roles in Autoinhibition and Actin Nucleation. *Curr Biol* *21*, 384-390.

Guo, W., Grant, A., and Novick, P. (1999a). Exo84p is an exocyst protein essential for secretion. *J Biol Chem* *274*, 23558-23564.

Guo, W., Roth, D., Walch-Solimena, C., and Novick, P. (1999b). The exocyst is an effector for Sec4p, targeting secretory vesicles to sites of exocytosis. *EMBO J* *18*, 1071-1080.

Guo, W., Tamanoi, F., and Novick, P. (2001). Spatial regulation of the exocyst complex by Rho1 GTPase. *Nat Cell Biol* *3*, 353-360.

Hallett, M. A., Lo, H. S., and Bender, A. (2002). Probing the importance and potential roles of the binding of the PH-domain protein Boi1 to acidic phospholipids. *BMC Cell Biol* *3*, 16.

Harris, E. S., Li, F., and Higgs, H. N. (2004). The mouse formin, FRLalpha, slows actin filament barbed end elongation, competes with capping protein, accelerates polymerization from monomers, and severs filaments. *J Biol Chem* *279*, 20076-20087.

Harris, E. S., Rouiller, I., Hanein, D., and Higgs, H. N. (2006). Mechanistic differences in actin bundling activity of two mammalian formins, FRL1 and mDia2. *J Biol Chem* *281*, 14383-14392.

Helliwell, S. B., Schmidt, A., Ohya, Y., and Hall, M. N. (1998). The Rho1 effector Pkc1, but not Bni1, mediates signalling from Tor2 to the actin cytoskeleton. *Curr Biol*

8, 1211-1214.

Higgs, H. N. (2005). Formin proteins: a domain-based approach. *Trends Biochem Sci* *30*, 342-353.

Higgs, H. N., and Peterson, K. J. (2005). Phylogenetic analysis of the formin homology 2 domain. *Mol Biol Cell* *16*, 1-13.

Higgs, H. N., and Pollard, T. D. (2001). Regulation of actin filament network formation through ARP2/3 complex: activation by a diverse array of proteins. *Annu Rev Biochem* *70*, 649-676.

Hoepfner, D., van den Berg, M., Philippsen, P., Tabak, H. F., and Hetteema, E. H. (2001). A role for Vps1p, actin, and the Myo2p motor in peroxisome abundance and inheritance in *Saccharomyces cerevisiae*. *J Cell Biol* *155*, 979-990.

Hofmann, C., Shepelev, M., and Chernoff, J. (2004). The genetics of Pak. *J Cell Sci* *117*, 4343-4354.

Howell, A. S., Savage, N. S., Johnson, S. A., Bose, I., Wagner, A. W., Zyla, T. R., Nijhout, H. F., Reed, M. C., Goryachev, A. B., and Lew, D. J. (2009). Singularity in polarization: rewiring yeast cells to make two buds. *Cell* *139*, 731-743.

Huckaba, T. M., Gay, A. C., Pantalena, L. F., Yang, H. C., and Pon, L. A. (2004). Live cell imaging of the assembly, disassembly, and actin cable-dependent movement of endosomes and actin patches in the budding yeast, *Saccharomyces cerevisiae*. *J Cell Biol* *167*, 519-530.

Hwang, E., Kusch, J., Barral, Y., and Huffaker, T. C. (2003). Spindle orientation in *Saccharomyces cerevisiae* depends on the transport of microtubule ends along polarized actin cables. *J Cell Biol* *161*, 483-488.

Imamura, H., Tanaka, K., Hihara, T., Umikawa, M., Kamei, T., Takahashi, K., Sasaki, T., and Takai, Y. (1997). Bni1p and Bnr1p: downstream targets of the Rho family small G-proteins which interact with profilin and regulate actin cytoskeleton in *Saccharomyces cerevisiae*. *EMBO J* *16*, 2745-2755.

Irazoqui, J. E., Gladfelter, A. S., and Lew, D. J. (2003). Scaffold-mediated symmetry

breaking by Cdc42p. *Nat Cell Biol* 5, 1062-1070.

Irazoqui, J. E., Howell, A. S., Theesfeld, C. L., and Lew, D. J. (2005). Opposing roles for actin in Cdc42p polarization. *Mol Biol Cell* 16, 1296-1304.

Ishikawa, K., Catlett, N. L., Novak, J. L., Tang, F., Nau, J. J., and Weisman, L. S. (2003). Identification of an organelle-specific myosin V receptor. *J Cell Biol* 160, 887-897.

Iwase, M., Luo, J., Nagaraj, S., Longtine, M., Kim, H. B., Haarer, B. K., Caruso, C., Tong, Z., Pringle, J. R., and Bi, E. (2006). Role of a Cdc42p effector pathway in recruitment of the yeast septins to the presumptive bud site. *Mol Biol Cell* 17, 1110-1125.

James, P., Halladay, J., and Craig, E. A. (1996). Genomic libraries and a host strain designed for highly efficient two-hybrid selection in yeast. *Genetics* 144, 1425-1436.

Jaquenoud, M., and Peter, M. (2000). Gic2p may link activated Cdc42p to components involved in actin polarization, including Bni1p and Bud6p (Aip3p). *Molecular and Cellular Biology* 20, 6244-6258.

Kamei, T., Tanaka, K., Hihara, T., Umikawa, M., Imamura, H., Kikyo, M., Ozaki, K., and Takai, Y. (1998). Interaction of Bnr1p with a novel Src homology 3 domain-containing Hof1p. Implication in cytokinesis in *Saccharomyces cerevisiae*. *J Biol Chem* 273, 28341-28345.

Kato, T., Watanabe, N., Morishima, Y., Fujita, A., Ishizaki, T., and Narumiya, S. (2001). Localization of a mammalian homolog of diaphanous, mDia1, to the mitotic spindle in HeLa cells. *J Cell Sci* 114, 775-784.

Kemper, M., Mohlzahn, L., Lickfeld, M., Lang, C., Wahlisch, S., and Schmitz, H. P. (2011). A Bnr-like formin links actin to the spindle pole body during sporulation in the filamentous fungus *Ashbya gossypii*. *Mol Microbiol* 80, 1276-1295.

Kitzing, T. M., Sahadevan, A. S., Brandt, D. T., Knieling, H., Hannemann, S., Fackler, O. T., Grosshans, J., and Grosse, R. (2007). Positive feedback between Dia1, LARG, and RhoA regulates cell morphology and invasion. *Genes Dev* 21, 1478-1483.

Knaus, M., Cameroni, E., Pedruzzi, I., Tatchell, K., De Virgilio, C., and Peter, M. (2005). The Bud14p-Glc7p complex functions as a cortical regulator of dynein in budding yeast. *EMBO J* *24*, 3000-3011.

Knechtle, P., Wendland, J., and Philippsen, P. (2006). The SH3/PH domain protein AgBoi1/2 collaborates with the Rho-type GTPase AgRho3 to prevent nonpolar growth at hyphal tips of *Ashbya gossypii*. *Eukaryot Cell* *5*, 1635-1647.

Kohno, H., Tanaka, K., Mino, A., Umikawa, M., Imamura, H., Fujiwara, T., Fujita, Y., Hotta, K., Qadota, H., Watanabe, T., *et al.* (1996). Bni1p implicated in cytoskeletal control is a putative target of Rho1p small GTP binding protein in *Saccharomyces cerevisiae*. *EMBO J* *15*, 6060-6068.

Korenbaum, E., Nordberg, P., Bjorkegren-Sjogren, C., Schutt, C. E., Lindberg, U., and Karlsson, R. (1998). The role of profilin in actin polymerization and nucleotide exchange. *Biochemistry* *37*, 9274-9283.

Kovar, D. R., Harris, E. S., Mahaffy, R., Higgs, H. N., and Pollard, T. D. (2006). Control of the assembly of ATP- and ADP-actin by formins and profilin. *Cell* *124*, 423-435.

Kovar, D. R., Kuhn, J. R., Tichy, A. L., and Pollard, T. D. (2003). The fission yeast cytokinesis formin Cdc12p is a barbed end actin filament capping protein gated by profilin. *J Cell Biol* *161*, 875-887.

Kovar, D. R., and Pollard, T. D. (2004). Progressing actin: Formin as a processive elongation machine. *Nat Cell Biol* *6*, 1158-1159.

Kozminski, K. G., Beven, L., Angerman, E., Tong, A. H., Boone, C., and Park, H. O. (2003). Interaction between a Ras and a Rho GTPase couples selection of a growth site to the development of cell polarity in yeast. *Mol Biol Cell* *14*, 4958-4970.

Kozminski, K. G., Chen, A. J., Rodal, A. A., and Drubin, D. G. (2000). Functions and functional domains of the GTPase Cdc42p. *Mol Biol Cell* *11*, 339-354.

Kozubowski, L., Saito, K., Johnson, J. M., Howell, A. S., Zyla, T. R., and Lew, D. J. (2008). Symmetry-breaking polarization driven by a Cdc42p GEF-PAK complex. *Curr Biol* *18*, 1719-1726.

Kusch, J., Meyer, A., Snyder, M. P., and Barral, Y. (2002). Microtubule capture by the cleavage apparatus is required for proper spindle positioning in yeast. *Genes Dev* *16*, 1627-1639.

Lammers, M., Rose, R., Scrima, A., and Wittinghofer, A. (2005). The regulation of mDia1 by autoinhibition and its release by Rho\*GTP. *EMBO J* *24*, 4176-4187.

Lee, L., Klee, S. K., Evangelista, M., Boone, C., and Pellman, D. (1999). Control of mitotic spindle position by the *Saccharomyces cerevisiae* formin Bni1p. *J Cell Biol* *144*, 947-961.

Lee, W. L., Bezanilla, M., and Pollard, T. D. (2000). Fission yeast myosin-I, Myo1p, stimulates actin assembly by Arp2/3 complex and shares functions with WASp. *J Cell Biol* *151*, 789-800.

Lewkowicz, E., Herit, F., Le Clainche, C., Bourdoncle, P., Perez, F., and Niedergang, F. (2008). The microtubule-binding protein CLIP-170 coordinates mDia1 and actin reorganization during CR3-mediated phagocytosis. *J Cell Biol* *183*, 1287-1298.

Li, F., and Higgs, H. N. (2003). The mouse Formin mDia1 is a potent actin nucleation factor regulated by autoinhibition. *Curr Biol* *13*, 1335-1340.

Li, F., and Higgs, H. N. (2005). Dissecting requirements for auto-inhibition of actin nucleation by the formin, mDia1. *J Biol Chem* *280*, 6986-6992.

Li, Y. Y., Yeh, E., Hays, T., and Bloom, K. (1993). Disruption of mitotic spindle orientation in a yeast dynein mutant. *Proc Natl Acad Sci U S A* *90*, 10096-10100.

Liakopoulos, D., Kusch, J., Grava, S., Vogel, J., and Barral, Y. (2003). Asymmetric loading of Kar9 onto spindle poles and microtubules ensures proper spindle alignment. *Cell* *112*, 561-574.

Liu, H., Krizek, J., and Bretscher, A. (1992). Construction of a GAL1-regulated yeast cDNA expression library and its application to the identification of genes whose overexpression causes lethality in yeast. *Genetics* *132*, 665-673.

Liu, H. P., and Bretscher, A. (1989). Purification of tropomyosin from *Saccharomyces cerevisiae* and identification of related proteins in *Schizosaccharomyces* and

Physarum. Proc Natl Acad Sci U S A 86, 90-93.

Lu, J., Meng, W., Poy, F., Maiti, S., Goode, B. L., and Eck, M. J. (2007). Structure of the FH2 domain of Daam1: implications for formin regulation of actin assembly. J Mol Biol 369, 1258-1269.

Marco, E., Wedlich-Soldner, R., Li, R., Altschuler, S. J., and Wu, L. F. (2007). Endocytosis optimizes the dynamic localization of membrane proteins that regulate cortical polarity. Cell 129, 411-422.

Martin, H., Mendoza, A., Rodriguez-Pachon, J. M., Molina, M., and Nombela, C. (1997). Characterization of SKM1, a Saccharomyces cerevisiae gene encoding a novel Ste20/PAK-like protein kinase. Mol Microbiol 23, 431-444.

Mass, R. L., Zeller, R., Woychik, R. P., Vogt, T. F., and Leder, P. (1990). Disruption of formin-encoding transcripts in two mutant limb deformity alleles. Nature 346, 853-855.

Matheos, D., Metodiev, M., Muller, E., Stone, D., and Rose, M. D. (2004). Pheromone-induced polarization is dependent on the Fus3p MAPK acting through the formin Bni1p. J Cell Biol 165, 99-109.

Matsui, Y., Matsui, R., Akada, R., and Toh-e, A. (1996). Yeast src homology region 3 domain-binding proteins involved in bud formation. J Cell Biol 133, 865-878.

McCusker, D., Denison, C., Anderson, S., Egelhofer, T. A., Yates, J. R., 3rd, Gygi, S. P., and Kellogg, D. R. (2007). Cdk1 coordinates cell-surface growth with the cell cycle. Nat Cell Biol 9, 506-515.

Miller, R. K., Matheos, D., and Rose, M. D. (1999). The cortical localization of the microtubule orientation protein, Kar9p, is dependent upon actin and proteins required for polarization. J Cell Biol 144, 963-975.

Mizuno, H., Higashida, C., Yuan, Y., Ishizaki, T., Narumiya, S., and Watanabe, N. (2011). Rotational movement of the formin mDia1 along the double helical strand of an actin filament. Science 331, 80-83.

Moore, J. K., and Miller, R. K. (2007). The cyclin-dependent kinase Cdc28p regulates

multiple aspects of Kar9p function in yeast. *Mol Biol Cell* *18*, 1187-1202.

Moseley, J. B., and Goode, B. L. (2005). Differential activities and regulation of *Saccharomyces cerevisiae* formin proteins Bni1 and Bnr1 by Bud6. *J Biol Chem* *280*, 28023-28033.

Moseley, J. B., and Goode, B. L. (2006). The yeast actin cytoskeleton: from cellular function to biochemical mechanism. *Microbiol Mol Biol Rev* *70*, 605-645.

Moseley, J. B., Sagot, I., Manning, A. L., Xu, Y., Eck, M. J., Pellman, D., and Goode, B. L. (2004). A conserved mechanism for Bni1- and mDia1-induced actin assembly and dual regulation of Bni1 by Bud6 and profilin. *Mol Biol Cell* *15*, 896-907.

Muhua, L., Karpova, T. S., and Cooper, J. A. (1994). A yeast actin-related protein homologous to that in vertebrate dynactin complex is important for spindle orientation and nuclear migration. *Cell* *78*, 669-679.

Nezami, A. G., Poy, F., and Eck, M. J. (2006). Structure of the autoinhibitory switch in formin mDia1. *Structure* *14*, 257-263.

Norden, C., Mendoza, M., Dobbelaere, J., Kotwaliwale, C. V., Biggins, S., and Barral, Y. (2006). The NoCut pathway links completion of cytokinesis to spindle midzone function to prevent chromosome breakage. *Cell* *125*, 85-98.

Otomo, T., Otomo, C., Tomchick, D. R., Machius, M., and Rosen, M. K. (2005a). Structural basis of Rho GTPase-mediated activation of the formin mDia1. *Mol Cell* *18*, 273-281.

Otomo, T., Tomchick, D. R., Otomo, C., Panchal, S. C., Machius, M., and Rosen, M. K. (2005b). Structural basis of actin filament nucleation and processive capping by a formin homology 2 domain. *Nature* *433*, 488-494.

Ozaki-Kuroda, K., Yamamoto, Y., Nohara, H., Kinoshita, M., Fujiwara, T., Irie, K., and Takai, Y. (2001). Dynamic localization and function of Bni1p at the sites of directed growth in *Saccharomyces cerevisiae*. *Mol Cell Biol* *21*, 827-839.

Park, H. O., and Bi, E. (2007). Central roles of small GTPases in the development of cell polarity in yeast and beyond. *Microbiol Mol Biol Rev* *71*, 48-96.

Perez, P., and Rincon, S. A. (2010). Rho GTPases: regulation of cell polarity and growth in yeasts. *Biochem J* 426, 243-253.

Petersen, J., Nielsen, O., Egel, R., and Hagan, I. M. (1998). FH3, a domain found in formins, targets the fission yeast formin Fus1 to the projection tip during conjugation. *J Cell Biol* 141, 1217-1228.

Piekny, A. J., and Glotzer, M. (2008). Anillin is a scaffold protein that links RhoA, actin, and myosin during cytokinesis. *Curr Biol* 18, 30-36.

Pollard, T. D., and Beltzner, C. C. (2002). Structure and function of the Arp2/3 complex. *Curr Opin Struct Biol* 12, 768-774.

Pollard, T. D., Blanchoin, L., and Mullins, R. D. (2000). Molecular mechanisms controlling actin filament dynamics in nonmuscle cells. *Annu Rev Biophys Biomol Struct* 29, 545-576.

Pring, M., Evangelista, M., Boone, C., Yang, C., and Zigmond, S. H. (2003). Mechanism of formin-induced nucleation of actin filaments. *Biochemistry* 42, 486-496.

Pruyne, D., Evangelista, M., Yang, C., Bi, E., Zigmond, S., Bretscher, A., and Boone, C. (2002). Role of formins in actin assembly: nucleation and barbed-end association. *Science* 297, 612-615.

Pruyne, D., Gao, L., Bi, E., and Bretscher, A. (2004a). Stable and dynamic axes of polarity use distinct formin isoforms in budding yeast. *Mol Biol Cell* 15, 4971-4989.

Pruyne, D., Legesse-Miller, A., Gao, L., Dong, Y., and Bretscher, A. (2004b). Mechanisms of polarized growth and organelle segregation in yeast. *Annu Rev Cell Dev Biol* 20, 559-591.

Pruyne, D. W., Schott, D. H., and Bretscher, A. (1998). Tropomyosin-containing actin cables direct the Myo2p-dependent polarized delivery of secretory vesicles in budding yeast. *J Cell Biol* 143, 1931-1945.

Qi, M., and Elion, E. A. (2005). Formin-induced actin cables are required for polarized recruitment of the Ste5 scaffold and high level activation of MAPK Fus3. *J*

Cell Sci 118, 2837-2848.

Richman, T. J., Sawyer, M. M., and Johnson, D. I. (1999). The Cdc42p GTPase is involved in a G2/M morphogenetic checkpoint regulating the apical-isotropic switch and nuclear division in yeast. *J Biol Chem* 274, 16861-16870.

Richman, T. J., Toenjes, K. A., Morales, S. E., Cole, K. C., Wasserman, B. T., Taylor, C. M., Koster, J. A., Whelihan, M. F., and Johnson, D. I. (2004). Analysis of cell-cycle specific localization of the Rdi1p RhoGDI and the structural determinants required for Cdc42p membrane localization and clustering at sites of polarized growth. *Curr Genet* 45, 339-349.

Rincon, S. A., Ye, Y., Villar-Tajadura, M. A., Santos, B., Martin, S. G., and Perez, P. (2009). Pob1 participates in the Cdc42 regulation of fission yeast actin cytoskeleton. *Mol Biol Cell* 20, 4390-4399.

Robinson, N. G., Guo, L., Imai, J., Toh, E. A., Matsui, Y., and Tamanoi, F. (1999). Rho3 of *Saccharomyces cerevisiae*, which regulates the actin cytoskeleton and exocytosis, is a GTPase which interacts with Myo2 and Exo70. *Mol Cell Biol* 19, 3580-3587.

Romero, S., Le Clainche, C., Didry, D., Egile, C., Pantaloni, D., and Carlier, M. F. (2004). Formin is a processive motor that requires profilin to accelerate actin assembly and associated ATP hydrolysis. *Cell* 119, 419-429.

Rose, R., Weyand, M., Lammers, M., Ishizaki, T., Ahmadian, M. R., and Wittinghofer, A. (2005). Structural and mechanistic insights into the interaction between Rho and mammalian Dia. *Nature* 435, 513-518.

Sagot, I., Klee, S. K., and Pellman, D. (2002a). Yeast formins regulate cell polarity by controlling the assembly of actin cables. *Nat Cell Biol* 4, 42-50.

Sagot, I., Rodal, A. A., Moseley, J., Goode, B. L., and Pellman, D. (2002b). An actin nucleation mechanism mediated by Bni1 and profilin. *Nat Cell Biol* 4, 626-631.

Santiago-Tirado, F. H., Legesse-Miller, A., Schott, D., and Bretscher, A. (2011). PI4P and Rab inputs collaborate in myosin-V-dependent transport of secretory compartments in yeast. *Dev Cell* 20, 47-59.

- Schmid, M., Jaedicke, A., Du, T. G., and Jansen, R. P. (2006). Coordination of endoplasmic reticulum and mRNA localization to the yeast bud. *Curr Biol* *16*, 1538-1543.
- Schmitz, H. P., Huppert, S., Lorberg, A., and Heinisch, J. J. (2002). Rho5p downregulates the yeast cell integrity pathway. *J Cell Sci* *115*, 3139-3148.
- Schott, D., Ho, J., Pruyne, D., and Bretscher, A. (1999). The COOH-terminal domain of Myo2p, a yeast myosin V, has a direct role in secretory vesicle targeting. *J Cell Biol* *147*, 791-808.
- Schroer, T. A. (2004). Dynactin. *Annu Rev Cell Dev Biol* *20*, 759-779.
- Schumacher, M. A., Goodman, R. H., and Brennan, R. G. (2000). The structure of a CREB bZIP.somatostatin CRE complex reveals the basis for selective dimerization and divalent cation-enhanced DNA binding. *J Biol Chem* *275*, 35242-35247.
- Segal, M., and Bloom, K. (2001). Control of spindle polarity and orientation in *Saccharomyces cerevisiae*. *Trends Cell Biol* *11*, 160-166.
- Selden, L. A., Kinosian, H. J., Estes, J. E., and Gershman, L. C. (1999). Impact of profilin on actin-bound nucleotide exchange and actin polymerization dynamics. *Biochemistry* *38*, 2769-2778.
- Seoighe, C., and Wolfe, K. H. (1999). Updated map of duplicated regions in the yeast genome. *Gene* *238*, 253-261.
- Sept, D., and McCammon, J. A. (2001). Thermodynamics and kinetics of actin filament nucleation. *Biophys J* *81*, 667-674.
- Seth, A., Otomo, C., and Rosen, M. K. (2006). Autoinhibition regulates cellular localization and actin assembly activity of the diaphanous-related formins FRLalpha and mDia1. *J Cell Biol* *174*, 701-713.
- Sherman, F. (1991). Getting started with yeast. *Methods Enzymol* *194*, 3-21.
- Sheu, Y. J., Santos, B., Fortin, N., Costigan, C., and Snyder, M. (1998). Spa2p

interacts with cell polarity proteins and signaling components involved in yeast cell morphogenesis. *Mol Cell Biol* 18, 4053-4069.

Shih, J. L., Reck-Peterson, S. L., Newitt, R., Mooseker, M. S., Aebersold, R., and Herskowitz, I. (2005). Cell polarity protein Spa2P associates with proteins involved in actin function in *Saccharomyces cerevisiae*. *Mol Biol Cell* 16, 4595-4608.

Shimada, A., Nyitrai, M., Vetter, I. R., Kuhlmann, D., Bugyi, B., Narumiya, S., Geeves, M. A., and Wittinghofer, A. (2004a). The core FH2 domain of diaphanous-related formins is an elongated actin binding protein that inhibits polymerization. *Mol Cell* 13, 511-522.

Shimada, Y., Gulli, M. P., and Peter, M. (2000). Nuclear sequestration of the exchange factor Cdc24 by Far1 regulates cell polarity during yeast mating. *Nat Cell Biol* 2, 117-124.

Shimada, Y., Wiget, P., Gulli, M. P., Bi, E., and Peter, M. (2004b). The nucleotide exchange factor Cdc24p may be regulated by auto-inhibition. *EMBO J* 23, 1051-1062.

Simon, V. R., Swayne, T. C., and Pon, L. A. (1995). Actin-dependent mitochondrial motility in mitotic yeast and cell-free systems: identification of a motor activity on the mitochondrial surface. *J Cell Biol* 130, 345-354.

Slaughter, B. D., Das, A., Schwartz, J. W., Rubinstein, B., and Li, R. (2009). Dual modes of cdc42 recycling fine-tune polarized morphogenesis. *Dev Cell* 17, 823-835.

Takahashi, S., and Pryciak, P. M. (2007). Identification of novel membrane-binding domains in multiple yeast Cdc42 effectors. *Mol Biol Cell* 18, 4945-4956.

Takizawa, P. A., DeRisi, J. L., Wilhelm, J. E., and Vale, R. D. (2000). Plasma membrane compartmentalization in yeast by messenger RNA transport and a septin diffusion barrier. *Science* 290, 341-344.

Takizawa, P. A., Sil, A., Swedlow, J. R., Herskowitz, I., and Vale, R. D. (1997). Actin-dependent localization of an RNA encoding a cell-fate determinant in yeast. *Nature* 389, 90-93.

Takizawa, P. A., and Vale, R. D. (2000). The myosin motor, Myo4p, binds Ash1

mRNA via the adapter protein, She3p. *Proc Natl Acad Sci U S A* *97*, 5273-5278.

Tcheperegine, S. E., Gao, X. D., and Bi, E. (2005). Regulation of cell polarity by interactions of Msb3 and Msb4 with Cdc42 and polarisome components. *Mol Cell Biol* *25*, 8567-8580.

TerBush, D. R., Maurice, T., Roth, D., and Novick, P. (1996). The Exocyst is a multiprotein complex required for exocytosis in *Saccharomyces cerevisiae*. *EMBO J* *15*, 6483-6494.

Theesfeld, C. L., Irazoqui, J. E., Bloom, K., and Lew, D. J. (1999). The role of actin in spindle orientation changes during the *Saccharomyces cerevisiae* cell cycle. *J Cell Biol* *146*, 1019-1032.

Tolliday, N., VerPlank, L., and Li, R. (2002). Rho1 directs formin-mediated actin ring assembly during budding yeast cytokinesis. *Curr Biol* *12*, 1864-1870.

Tong, A. H., Evangelista, M., Parsons, A. B., Xu, H., Bader, G. D., Page, N., Robinson, M., Raghibizadeh, S., Hogue, C. W., Bussey, H., *et al.* (2001). Systematic genetic analysis with ordered arrays of yeast deletion mutants. *Science* *294*, 2364-2368.

Toshima, J., Toshima, J. Y., Martin, A. C., and Drubin, D. G. (2005). Phosphoregulation of Arp2/3-dependent actin assembly during receptor-mediated endocytosis. *Nat Cell Biol* *7*, 246-254.

Uetz, P., Giot, L., Cagney, G., Mansfield, T. A., Judson, R. S., Knight, J. R., Lockshon, D., Narayan, V., Srinivasan, M., Pochart, P., *et al.* (2000). A comprehensive analysis of protein-protein interactions in *Saccharomyces cerevisiae*. *Nature* *403*, 623-627.

Vallen, E. A., Caviston, J., and Bi, E. (2000). Roles of Hof1p, Bni1p, Bnr1p, and myo1p in cytokinesis in *Saccharomyces cerevisiae*. *Mol Biol Cell* *11*, 593-611.

van Drogen, F., and Peter, M. (2002). Spa2p functions as a scaffold-like protein to recruit the Mpk1p MAP kinase module to sites of polarized growth. *Curr Biol* *12*, 1698-1703.

Versele, M., and Thorner, J. (2004). Septin collar formation in budding yeast requires GTP binding and direct phosphorylation by the PAK, Cla4. *J Cell Biol* 164, 701-715.

Wang, J., Neo, S. P., and Cai, M. (2009). Regulation of the yeast formin Bni1p by the actin-regulating kinase Prk1p. *Traffic* 10, 528-535.

Wedlich-Soldner, R., Wai, S. C., Schmidt, T., and Li, R. (2004). Robust cell polarity is a dynamic state established by coupling transport and GTPase signaling. *J Cell Biol* 166, 889-900.

Weisman, L. S. (2003). Yeast vacuole inheritance and dynamics. *Annu Rev Genet* 37, 435-460.

Wen, K. K., and Rubenstein, P. A. (2009). Differential regulation of actin polymerization and structure by yeast formin isoforms. *J Biol Chem* 284, 16776-16783.

Wen, Y., Eng, C. H., Schmoranzer, J., Cabrera-Poch, N., Morris, E. J., Chen, M., Wallar, B. J., Alberts, A. S., and Gundersen, G. G. (2004). EB1 and APC bind to mDia to stabilize microtubules downstream of Rho and promote cell migration. *Nat Cell Biol* 6, 820-830.

Winter, D., Lechler, T., and Li, R. (1999). Activation of the yeast Arp2/3 complex by Bee1p, a WASP-family protein. *Curr Biol* 9, 501-504.

Winter, D., Podtelejnikov, A. V., Mann, M., and Li, R. (1997). The complex containing actin-related proteins Arp2 and Arp3 is required for the motility and integrity of yeast actin patches. *Curr Biol* 7, 519-529.

Woychik, R. P., Maas, R. L., Zeller, R., Vogt, T. F., and Leder, P. (1990). 'Formins': proteins deduced from the alternative transcripts of the limb deformity gene. *Nature* 346, 850-853.

Wu, C., Lee, S. F., Furmaniak-Kazmierczak, E., Cote, G. P., Thomas, D. Y., and Leberer, E. (1996). Activation of myosin-I by members of the Ste20p protein kinase family. *J Biol Chem* 271, 31787-31790.

Wu, C., Lytvyn, V., Thomas, D. Y., and Leberer, E. (1997). The phosphorylation site

for Ste20p-like protein kinases is essential for the function of myosin-I in yeast. *J Biol Chem* *272*, 30623-30626.

Wu, H., Turner, C., Gardner, J., Temple, B., and Brennwald, P. (2010). The Exo70 subunit of the exocyst is an effector for both Cdc42 and Rho3 function in polarized exocytosis. *Mol Biol Cell* *21*, 430-442.

Xu, Y., Moseley, J. B., Sagot, I., Poy, F., Pellman, D., Goode, B. L., and Eck, M. J. (2004). Crystal structures of a Formin Homology-2 domain reveal a tethered dimer architecture. *Cell* *116*, 711-723.

Yang, H. C., and Pon, L. A. (2002). Actin cable dynamics in budding yeast. *Proc Natl Acad Sci U S A* *99*, 751-756.

Yeh, E., Yang, C., Chin, E., Maddox, P., Salmon, E. D., Lew, D. J., and Bloom, K. (2000). Dynamic positioning of mitotic spindles in yeast: role of microtubule motors and cortical determinants. *Mol Biol Cell* *11*, 3949-3961.

Yin, H., Pruyne, D., Huffaker, T. C., and Bretscher, A. (2000). Myosin V orientates the mitotic spindle in yeast. *Nature* *406*, 1013-1015.

Zhang, X., Bi, E., Novick, P., Du, L., Kozminski, K. G., Lipschutz, J. H., and Guo, W. (2001). Cdc42 interacts with the exocyst and regulates polarized secretion. *J Biol Chem* *276*, 46745-46750.